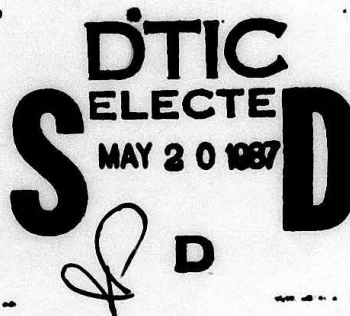②

AD-A180 276

THERMAL AND DYNAMICAL EFFECTS OF ELECTRODYNAMIC SPACE TETHERS

CPT John S. Prall Jr.
HQDA, MILPERCEN (DAPC-OPA-E)
200 Stovall Street
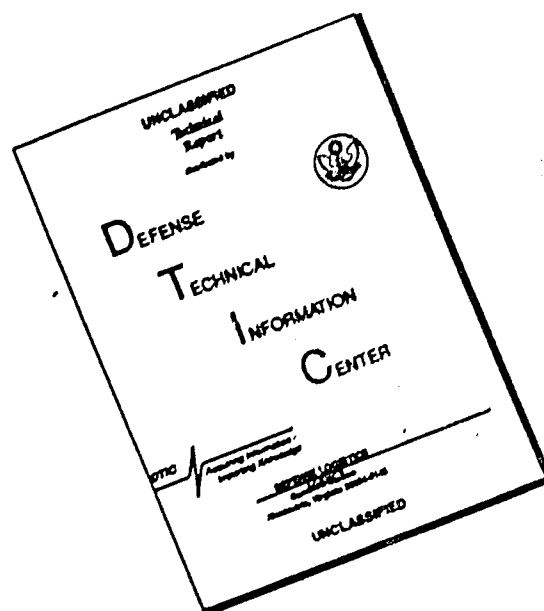Alexandria VA 22332.

Final Report 8 May 1987

DTIC
ELECTE
S MAY 2 0 1987
D
D

Approved for public release; distribution is unlimited

A thesis submitted to the Massachusetts Institute of Technology, Cambridge MA 02139, in partial fulfillment of the requirements for the degree of Master of Science in Aeronautics & Astronautics.

87 5 15 031

DISCLAIMER NOTICE

THIS DOCUMENT IS BEST QUALITY AVAILABLE. THE COPY FURNISHED TO DTIC CONTAINED A SIGNIFICANT NUMBER OF PAGES WHICH DO NOT REPRODUCE LEGIBLY.

REPORT DOCUMENTATION PAGE		READ INSTRUCTIONS BEFORE COMPLETING FORM
1. REPORT NUMBER	**2. GOVT ACCESSION NO.** AD A180 276	**3. RECIPIENT'S CATALOG NUMBER**
4. TITLE (and Subtitle) Thermal & Dynamical Effects on Electrodynamic Space Tethers		**5. TYPE OF REPORT & PERIOD COVERED** Final Report 8 May 1987
		6. PERFORMING ORG. REPORT NUMBER
7. AUTHOR(s) CPT John S. Prall Jr.		**8. CONTRACT OR GRANT NUMBER(s)**
9. PERFORMING ORGANIZATION NAME AND ADDRESS Student HQDA, MILPERCEN (DAPC-OPA-E) 200 Stovall St Alexandria VA 22332		**10. PROGRAM ELEMENT, PROJECT, TASK AREA & WORK UNIT NUMBERS**
11. CONTROLLING OFFICE NAME AND ADDRESS HQDA, MILPERCEN ATTN: DAPC-OPA-E 200 Stovall Street Alexandria VA 22332		**12. REPORT DATE** 8 May 1987
		13. NUMBER OF PAGES 135
14. MONITORING AGENCY NAME & ADDRESS(if different from Controlling Office)		**15. SECURITY CLASS. (of this report)** Unclassified
		15a. DECLASSIFICATION/DOWNGRADING SCHEDULE

16. DISTRIBUTION STATEMENT (of this Report)

Approved for public release; distribution unlimited

17. DISTRIBUTION STATEMENT (of the abstract entered in Block 20, if different from Report)

18. SUPPLEMENTARY NOTES

Document is a Master's Thesis from Massachusetts Institute of Technology

19. KEY WORDS (Continue on reverse side if necessary and identify by block number)

Electrodynamic Tethers
Space Power Generation Systems
Alfven Engines

20. ABSTRACT (Continue on reverse side if necessary and identify by block number)

Analytical & numerical evaluation of an electrodynamic tether system used as a space power generator and/or thruster. Examination includes determination of a comparative efficiency of an insulated versus an uninsulated tether; evaluation of the effects of system design parameters on system overall efficiency; and evaluation of effects of different operating modes on system orbital elements.

DD FORM 1 JAN 73 **1473** EDITION OF 1 NOV 65 IS OBSOLETE

THERMAL AND DYNAMICAL EFFECTS ON

ELECTRODYNAMIC SPACE TETHERS

by

JOHN SCOFIELD PRALL, JR.

B.S., United States Military Academy

(1977)

SUBMITTED IN PARTIAL FULFILLMENT
OF THE REQUIREMENTS FOR THE
DEGREE OF

MASTER OF SCIENCE
IN AERONAUTICS AND ASTRONAUTICS

at the

MASSACHUSETTS INSTITUTE OF TECHNOLOGY

JUNE 1987
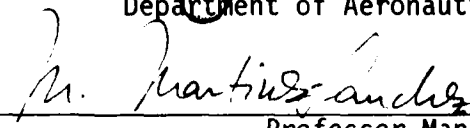
© John S. Prall, Jr. 1987

Signature of Author_____
Department of Aeronautics and Astronautics
8 May 1987

Certified by_____
Professor Manuel Martinez-Sanchez
Thesis Supervisor, Department of Aeronautics and Astronautics

Accepted by_____
Professor Harold Y. Wachman
Chairman, Department Graduate Committee

THERMAL AND DYNAMICAL EFFECTS ON

ELECTRODYNAMIC SPACE TETHERS

by

JOHN SCOFIELD PRALL, JR.

Submitted to the Department of Aeronautics and Astronautics
on 8 May 1987 in partial fulfillment of the
requirements for the Degree of Master of Science in
Aeronautics and Astronautics

ABSTRACT

An analytical and numerical analysis was carried out on the operation of an electrodynamic tether system used for power generation and/or thrusting in a space environment. Three problems were examined. First, the efficiency of an uninsulated tether of prescribed design, as determined by the magnitude of current leakage along its length due to positive ion capture and secondary electron emissions, was compared to that of a perfectly insulated tether of identical design. Second, the effects on system efficiency of variations in the design parameters of the tether and the orbit in which it operates were examined by means of a numerical analysis of the thermal balance of the system. Third, the effects which the mode of operation of the tether has on the classical elements of the orbit in which it operates were examined through a numerical analysis.

The results of the first examination indicated that the uninsulated tether can still operate as a power generator or thruster, although with an effective efficiency when compared to the perfectly insulated tether of about 90%. The second examination indicated that tethers operated more efficiently at lower temperatures, and that these temperatures were directly affected by the surface characteristics of the tether, specifically the absorptance and emittance. High emittance and low absorptance produced the lowest average operating temperatures, and hence the highest efficiencies. Fluctuations in the temperatures over an orbit were about ± 20 degrees. These variations were generally unaffected by the orientation of the tether's orbit, and by the position of the earth, with respect to the sun. The third examination indicated that the classical elements of the tether's orbit, with the desired exception of the semi-major axis which represents orbital energy, were generally unaffected when the tether was operated in a single mode, but dramatically increased the eccentricity of the orbit when operated in a mixed mode within an orbit, so much so that operation in this matter is prohibitive.

Thesis Supervisor: Dr. Manuel Martinez-Sanchez

Title: Associate Professor of Aeronautics & Astronautics

1

TABLE OF CONTENTS

TABLE OF CONTENTS Continued

4

LIST OF FIGURES

1. INTRODUCTION

Electrodynamic tethers are essentially long conducting wires which, when deployed from an orbiting satellite, can generate power by converting orbital mechanical energy into electrical energy for use on the satellite. They can accomplish this as a consequence of the electrodynamically induced voltage caused by the movement of the tether with respect to the earth's magnetic field; this acts to drive a current through the tether to an on-board load. Conversely, if current is forced through the tether from the satellite, the electrodynamic interaction will induce a force and allow the tether to perform as a so-called Alfven engine.

The concept of space tethers has been in existence for about a century, with the earliest reports attributed to the Russian Konstantin E. Tsiolkovsky in 1895. He discussed the construction of a tower to be built at the equator which would reach to geostationary heights, the purpose of which was to create an environment without terrestrial gravity. The next proposals came after a hiatus of about sixty-five years. The "heavenly funicular" of Y.N. Artsutanov and the "skyhook" of John D. Isaacs each envisioned the tether as a means to lift payloads into earth orbit. Additional investigations continued throughout the sixties and seventies which have considered the concept of a "space necklace," essentially an extension of the heavenly funicular in which equally-spaced funiculars about the equator serve as payload-carrying elevators from earth to GEO; and a "wheeled tether", in which long rotating tethers are placed into an orbit such that at specific times one end of the tether would just touch the earth's surface where, since it would briefly appear stationary relative to the rotating earth, payloads could be attached to be slung up into orbit as the tether rotated away.

Initial in-space experiments were conducted on Gemini XI and XII in 1966, which investigated the complex dynamics of tethers and of satellites attached by them. The first practical application of an orbiting tether in LEO was developed by Mario D. Grossi in 1972, who showed that the tether could be used as an antenna to generate ultra low frequency (ULF) emissions. This concept was further developed by Giuseppe Colombo et al in 1974 in a paper which proved the dynamic feasibility of a shuttle-borne

6

tether system, in addition to several other additional applications. Since that time, several other endeavors have explored the problems of tether dynamics, deployment and retrieval of long tethers from a free-flying vehicle, and the practicality of tethered constellations in space.

One of the first attempts to evaluate the electrodynamic interaction of long conducting tethers and the ionosphere was a paper by Dobrowolny, Colombo and Grossi in 1976. It developed computer models to analyze the distribution of the induced potential along the tether and the resulting current from this potential. Subsequently, NASA has conducted periodic seminars and sponsored a long series of projects to investigate the many and varied facets of this problem, which have led to the manifesting of the Tethered Satellite System (TSS) on a shuttle flight in 1991. This experimental package, sponsored by the U.S. and Italian space agencies, is designed to evaluate the feasibility of generating power with an electrodynamic tether.

The purpose of this thesis is three-fold: first, to evaluate the comparative operation of an electrodynamic tether which is perfectly insulated from the surrounding space plasma with one which is operated completely bare; second, to evaluate the effects which the design parameters of the tether itself and of the orbit in which it is placed have on the efficiency of the tether system; and third, to evaluate the effects which the operation of the tether in various modes have on the shape of its orbit. The first will be accomplished by performing an analytical evaluation of the magnitude of current lost along the length of an uninsulated tether as a result of captured positive ions and secondary electron emissions. The second will be accomplished as a numerical evaluation of the thermal balance of the tether system by computing the temperature of the tether as it moves through its orbit, then relating this to the system efficiency by means of the fluctuations in conductor resistance, which is a function of temperature. The third will be accomplished by calculating the external forces which act on the tether, particularly the induced electromotive force caused by the tether's operation, then numerically integrate the variational equations for the orbital elements with these forces present.

2. THEORETICAL BACKGROUND

2.1 INDUCED VOLTAGE

The Lorentz Relation specifies that the force on a charge q, moving at velocity $\underline{u}$ in an electric field $\underline{E}$ and magnetic field $\underline{B}$ is given by

$$\underline{F} = q \ (\underline{E} + \underline{u} \times \underline{B}) \qquad [N/m^2]$$

To evaluate this properly, since $\underline{F}$, $\underline{B}$ and q are all independent of motion for non-relativistic velocities, the field $\underline{E}$ must be viewed from different frames of reference. If $\underline{E}'$, then, is defined as the field when viewed in a rest frame, and $\underline{E}$ is defined as the field when viewed in a frame which is moving at $\underline{v}$ relative to the rest frame, this indicates

$$\underline{E}' + \underline{u} \times \underline{B} = \underline{E} + (\underline{u} - \underline{v}) \times \underline{B}$$

Thus,

$$\underline{E} = \underline{E}' + \underline{v} \times \underline{B}$$

If $\underline{v}$ is then defined as the mean mass velocity of the plasma surrounding a rigid wire, and since in the plasma frame $\underline{E}'$ must be small, the plasma will experience a potential across the length of the tether of $(\underline{v} \times \underline{B}) \cdot \underline{L}$. This may be expressed as

$$V_{oc} = (\underline{v} \times \underline{B}) \cdot \underline{L} \qquad [V]$$

where $\underline{L}$ represents the length of the wire and $\underline{v}$ is the velocity of the tether relative to the plasma. If no current flow is permitted due to the presence of a large impedance somewhere in the circuit, a potential of this magnitude will develop across that impedance due to the velocity and magnetic field interaction. This impedance could be at the points of plasma-wire contact, in the wire itself, or in a localized electrical load or open switch; any of these impedances, or a combination of them, will support the $\underline{v} \times \underline{B} \cdot \underline{L}$ voltage.

8

Additionally, the force induced by a current carrier moved through a purely magnetic field is

$$\underline{F} = (\underline{I} \times \underline{B}) \, L \qquad [N]$$

where L is the tether length, and the direction of $\underline{F}$ is dependent on the direction of $\underline{I}$. Thus, if current is allowed to pass through a conducting tether which is being moved through a magnetic field (e.g. the earth's) such that a force is induced which is opposite to the direction of motion, this force is termed electromagnetic drag; if the induced force is in the direction of motion, it is termed electromagnetic thrust. Its effect is to "steal" or "add" energy, respectively, from the satellite's orbit and alter its orbital altitude.

Power may be generated, or thrust produced, by capitalizing on these aspects of the Lorentz Relation, provided that current can be caused to flow through the tether. A current loop may be established by "clamping" the two ends of the tether to the plasma so that the voltage drop between each respective end and the plasma potential is minimized. As the plasma by its nature is highly conductive, the "clamping" will effectively create a current loop. Theoretical work indicates that this clamping is possible (although with varying degrees of resistivity) and that the ionosphere will pass this current with only negligible resistance. Once this loop has been established, the mechanical power added to the system may be expressed as

$$P = \underline{F} \cdot \underline{v} = L \, (\underline{I} \times \underline{B}) \cdot \underline{v}$$

$$= I \, (\underline{L} \times \underline{B}) \cdot \underline{v} = -I \, (\underline{v} \times \underline{B}) \cdot \underline{L}$$

which can be seen to be the product of the current and the open circuit voltage. This expression, integrated over time, represents the energy which can be extracted from, or injected into, the orbit of the tether. Of course, only a fraction of this can be delivered to a load; conversely, a driving power source would have to provide more than this amount.

2.2 EQUIVALENT CLOSURE CIRCUIT

In order to produce a current from the potential difference created by the electromotive force, the ends of the tether must make electrical contact with the earth's plasma environment. Once this contact is established, the current flows through a 'phantom' loop consisting of the tether itself and the ionospheric plasma. The medium in which the tether is orbiting may be modelled as a set of parallel transmission lines, the magnetic flux tubes, which are touched sequentially by the ends of the tether as it moves in its orbit. At this touch, electrons leave the positive end of the conducting tether and enter the ionospheric plasma where they produce charge packets which travel along these magnetic flux tubes as a plasma wave in a variety of modes, mostly as low-frequency Alfven waves. The charge packets from the opposite tether ends have, of course, opposite polarities, and they must eventually neutralize each other. However, this is of no concern to the spacecraft, since the distance travelled by the plasma wave down each magnetic tube in the time the tether contactor is in touch with it is on the order of the contactor size times the ratio of the wave speed to the contactor speed, and is no more than a few hundred meters in any case. The nature of the eventual "closure" in the E-layer of the ionosphere is mainly of interest in the sense of providing a diagnostic tool for ground observations of the phenomenon, and perhaps as a concern for its electromagnetic noise emission. The ends of the tether act as sliding contacts, so that this phenomenon in the ionosphere is fundamentally AC. However, since the ionosphere is a continuous medium, the ends of the tethers do not leave one line before touching the next one, so that the current in the tether itself is DC and nearly constant.

The basic equation of the circuit is

$$V_{oc} = IR + V_{load} + V_{anode} + V_{cathode} + V_{ion}$$

10

where V_{oc} = induced voltage across the tether = $\underline{v} \times \underline{B} \cdot \underline{L}$

I = tether current

R = resistance of the tether

V_{load} = voltage drop across the load

V_{anode} = voltage drop across the anodic contactor

$V_{cathode}$ = voltage drop across the cathodic contactor

V_{ion} = voltage drop through the ionosphere

Additionally, there are current leakage losses along the length of the tether which are dependent on the degree of effectiveness of the insulation of the conducting wire, and the inductance which would arise from the part of the current carrying tether which remains wound around a deployer reel. A schematic of this circuit path is shown in Figure 1. Obviously, if either the conducting wire, the ionosphere or the contact of the tether and plasma do not readily pass the current, i.e. if the effective impedance of any of these is high, then the efficiency of the system will plummet. It thus becomes essential to minimize those voltage drops in the system besides the load.

In performing the analysis of this system, the impedances of this circuit, with the exception of the impedance due to the reeled tether inductance, were modelled mathematically to produce a simplified equivalent circuit. It is assumed that the tether is completely deployed, so that the impedance due to inductance is zero. A discussion follows of the various models used and assumptions made to obtain this equivalent circuit.

2.2.1 Ionospheric Impedance

The power losses in the ionosphere can be properly called 'radiation losses', and have been evaluated in detail in References 15 and 18. These analyses made calculations of radiation resistance in the framework of linear cold plasma theory, referring in particular to low frequency Alfven waves and to waves in the vicinity of the ion cyclotron frequency. The conclusion of Reference 18 was that the effective radiation power loss for a tether of length 20 km would be minimal, and implied that a maximum total radiation resistance of approximately of 1.2 ohms was to be

11

expected. Reference 18 also provided, after a much more rigorous analysis based on antenna theory, an alternate means of determining the approximate radiation impedance in the Alfven regime. The author here showed that the impedance of an orbiting long wire is about $\frac{100}{n_a}$, where n_a is the Alfven refractive index. This index varies from day to night, typically falling in the range of 100 by night to 1000 by day, indicating an impedance of about 1 ohm by night and .1 ohm by day, and thus corroborating the first estimation.

Other analyses have been made to estimate the radiation impedance caused by resonance at higher frequencies in the Whistler range, notably References 4 and 22. Their conclusions are that impedances on the order of 1000 ohms should be expected in these regimes, and that the critical factor which determines the magnitude of the impedance is the smallest dimension of the wire. Reference 22 concludes that this is the diameter. Obviously, impedances of this magnitude would make the effectiveness of a tether system marginal at best. More recent work, as detailed in Reference 15, makes it clear that the critical dimension is that of the current interface, i.e., *the contactor. The authors of References 4 and 22 now concur on this point.* As will be discussed in the next section, the effective size of the plasma contactors is generally accepted as on the order of 50 meters, which would indicate an impedance of about 1 ohm.

The conclusion which may be drawn is that the wave impedance of the ionosphere for the electrodynamic tether will not present a major limiting factor to the current flow through the circuit. As the full implication of these results is not yet well understood and still the topic of some debate, this analysis will assume this conclusion to be accurate and presume that the total radiation impedance in the ionosphere is consistently less than 10 ohms.

2.2.2 Contactors

Several methods of 'bridging' the plasma sheath at the ends of the tether have been devised. The degree of success in effecting good contact between the tether and the plasma, i.e. their level of impedance, vary

markedly among the several methods. What follows is essentially a brief summary of these different plasma bridges.

Those contactors placed at the positive end of the tether, the anode, are essentially electron collectors (or ion emitters) and may be either passive or active. Conversely, the contactors at the negative end, the cathode, are all active electron emitters.

Cathodic contactors, as discussed in reference 10, pose little fundamental difficulty, since electrons can always be injected into the ionosphere with little energy loss, provided the emitter doses not charge up positively in the process. As long as the anodic contactor is doing its job of collecting electrons at an appropriate rate, this charging will not occur. The hollow cathode is the device almost universally recommended to serve as the plasma bridge at the cathodic end of the tether. This device injects a plasma, typically formed from a neutral gas such as mercury, xenon, or argon, into the ionosphere. This increases the density of ions in the immediate vicinity of the contactor, thus providing a sufficient thermal electron density to carry the full tether current in either direction at any distance from the tether and until it merges into the ambient ionospheric plasma currents. Being active plasma contactors, hollow cathodes require on-board electrical power and a gas supply to operate. Various estimates have been made for this voltage drop and the required mass consumption rate, notably in References 21 and 29. These indicate that sufficient current levels can be attained with voltage drops on the order of 100 volts. The attendant mass consumption rate can be estimated as

$$\dot{m} = \left(\frac{4\ m_i}{\alpha e}\right)\left(\frac{v_s}{c_e}\right) I$$

where

c_e = random thermal speed of electrons

v_s = ambipolar speed of sound

α = degree of ionization

m_i = ion mass

This yields a mass flow rate to current ratio on the order of 2 kg/A/year for 10% ionized argon.

The primary competitor of the hollow cathode device is the electron gun, which has the advantages of being an already existing technology which utilizes no mass flow and provides a ready control of current, but which has the disqualifying disadvantage of requiring large levels of on-board electrical power to draw sufficient levels of current, due to space charge limitations at the gun exit. These voltage levels have been estimated at from 1 to 10 kilovolts to draw 20 amps of current, which is on the order of the voltage potential induced across a moderately sized tether. In the hollow cathode, this space charge is neutralized by the plasma ions; thus, very low voltage drops are possible.

Anodic contactors may either collect electrons or emit ions. The former may also be either passive or active collectors. The passive type function essentially by placing a surface in the ionosphere, the size of which is large enough to collect the required magnitude of current from the ambient plasma. Obviously, if the ambient plasma density is low, the size of the surface area must be proportionally increased. As an example, if the ambient plasma density is 10^{11} m^{-3} then the random current density (given by $\frac{en_ec_e}{4}$) is .8 mA/m^2. If the required current level is 10 amps, this, then, dictates a surface area of 12500 m^2. Equivalently, a surface area of this magnitude represents a sphere of approximately 45 meters radius, or a flat screen 80 meters square. Diagrams of these configurations are shown in Figure 2. It is apparent that if a thin-skinned balloon is used as the sphere, it will be both heavy and draggy, since it will present a large surface area perpendicular to the direction of velocity. If a mesh of thin wires is used as the flat screen, its mass and drag can both be substantially decreased; it will still, however, present a dynamical monstrosity. As an alternative, the plasma cloud released by a hollow cathode device can be used as a substitute for this actual surface area. This would clearly improve things but does have its own limitations. Reference 29 presents calculations which indicate that a cloud radius of about 40 meters is necessary to collect 10 amps of current. This is further complicated by the fact that electrons must be able to diffuse across the magnetic field into the central plasma contactor, so the only useful portion of the plasma cloud is that in which

14

the collision frequency exceeds the gyro frequency, which occurs for
either high plasma densities ($\sim 3.5 \times 10^{17}$ m^{-3}) and/or high plasma
turbulence.

The primary deficiency in all of these types of electron collectors is
that they are totally dependent on the ambient electron density in order
to continually provide a sufficient current level. The Smithsonian
Astrophysical Observatory has conducted a study of electron density versus
orbital time, shown as Figure 3, calculated using a model based on the
three-dimensional maps constructed by Jones and Stewart (Reference 25).
This model is limited in that it is based on data from November 1966; as
this date is in the middle of the solar cycle, the model has no included
seasonal or solar activity variations. It also does not correctly model
the density variations at lower altitudes, but is accurate enough at 300
km to show the problem with electron collectors as anodic plasma bridges.
Specifically, the ambient electron density varies by as much as two orders
of magnitude, from 10^{12} m^{-3} to 10^{10} m^{-3}, between the sunlight and shadow
portions of the system's orbit. At the low points, the surface area
required to collect sufficient current, either physical surface or that of
a plasma cloud, becomes huge.

What seems to be a solution to this problem is to replace these
electron collectors at the anode with an ion emitter. The obvious
advantage of this device is its near independence from the ambient
electron density, in contrast with the discussion above. Such a device
would be essentially an ion engine minus the accelerator grid, which would
not be necessary as the ions would leave the device because of the
potential gradient. The mass consumption of this type device is somewhat
greater, though not significantly, than that of the hollow cathode; it has
been estimated in Reference 29 as approximately 2 kg/A/year with ammonia
as the working gas. The power requirements would likewise be somewhat
higher than the cathode, but still be on the order of 100 volts to
maintain adequate current levels.

For this analysis, the assumption will be made that the cathodic
plasma bridge is a hollow cathode device, and that the anodic bridge is a
pure ion emitter. Since mathematical models for the impedances of these

15

contactors are complex, nonlinear, and unknown functions of tether current, it will be assumed that the voltage drop across both the anode and cathode is a constant 100 volts apiece. Finally, it will be assumed that each device has sufficient mass in place for unlimited continuous operation so that the consideration of fuel consumption by the contactors may be neglected.

2.2.3 Insulation

In order to operate, the conducting material of the tether must pass a current, the magnitude of which is determined by the amount of power or thrust to be produced. If the conductor is covered with a dielectric material of sufficient thickness, then no current is lost to the surrounding plasma along the length of the tether. If, alternately, the tether is left bare, then the current is reduced by an amount which is a function of the tether's length and diameter, the potential bias, and the ambient ion density. The serious disadvantage of an insulated tether is that most dielectrics tend to differentially charge due to ion impacts, and then arc. This arcing typically occurs at potential levels well below the 4 kilovolt level which is to be anticipated for a 20 kilometer tether. Additionally, if pinholes are introduced into the dielectric, as is expected due to micrometeroid impacts, the magnitude of the current leakage through these pinholes is on the same order of the magnitude of current lost by a bare tether. Thus it appears that unless a dielectric can be chosen which is resistant to this arcing and which is durable enough to withstand most debris impacts, for all intents and purposes the insulated tether will act electrically like a bare tether, but have a greater mass.

Reference 18 indicates that the necessary thickness of polyethylene to prevent surface discharge is .38 mm. This was evidently determined in a quick and dirty way by dividing the maximum potential which the tether would encounter by the dielectric strength of the insulating material to obtain the required thickness, then multiplying by an arbitrary safety factor. The thickness indicated may be obtained using values of 4750 volts for the maximum potential, 5×10^5 V/cm for the dielectric strength

16

of polyethylene, and a safety factor of 4. Reference 34 presents a similar analysis to determine the required dielectric thickness to insulate a satellite from the Jovian flux.

Obviously, insulation of this thickness will prevent current from leaking directly through the dielectric. The cost of this is primarily in additional mass and in the manufacturing complexities involved in producing such a tether. For an aluminum tether, 2 mm in diameter and 20 km in length, using polyethylene as the insulator will add approximately 52.3 kg to each tether mass; the insulator to conductor mass ratio is thus .297. Comparatively, anodized aluminum, with a dielectric strength of 5 x 10^6 V/cm, would require a thickness of only 38 microns to insulate the conductor, and consequently an insulator to conductor mass ratio of .041. These mass ratios may be improved somewhat by tapering the insulation so that it is thickest at those points on the tether where the largest potential gradient is expected to occur. However, as stated above, although the current leakage along the length of the tether would be prevented by this insulation, the major problems still to be faced would be arcing and pinhole leakage.

Arcing is defined in Reference 17 as the rapid rearrangement of charge by punch-through (internal breakdown of dielectrics), by flash-over (dielectric breakdown) between surfaces, or between surfaces and space. The mechanisms leading to arcing are not well understood. They fall into three general categories: ungrounded insulators; buried or trapped charge layers; and differential voltage distributions. Typically, the charge build-up associated with ungrounded insulators can be prevented by proper design of the insulating jacket. Buried charges are caused by mid energy electrons, on the order of 50 KeV, which penetrate the insulating jacket and deposit their charge in the dielectric. Electron energies of this order are not typically encountered in LEO, the operating regime of the tether. Differential voltage distributions occur either when the surface of the dielectric is at a lower potential than the conductor beneath it, and small gaps or cracks exist in the dielectric which expose the conductor and allow charge to escape locally, or through charge deposition on the surface of the dielectric due to the ambient plasma and due to

17

secondary emissions from surface impacts. Protecting the tether from this phenomenon requires production techniques which encase the tether without any gaps, cracks, or crevices in the dielectric, in addition to the selection of a dielectric which has a high dielectric strength and is durable enough to resist erosion and penetration.

The consequences of a bare tether will be discussed in a subsequent section, as will the use of anodized aluminum as a dielectric which appears to have the desired characteristics of high dielectric strength and durability, in addition to values of absorptance and emittance which will cause the tether to operate in a favorable temperature range. For the remainder to this analysis, it will be assumed that the tether is perfectly insulated by a jacket of anodized aluminum, and that arcing and pinhole damage do not cause any difficulties in system operation.

2.2.4 Reduced Circuit

With these simplifying models, the equivalent circuit to be analyzed is as shown in Figure 4. Here, the constant voltage drops across the anode and cathode have been subtracted from the variable emf, V_{oc}. The low impedance of the ionosphere has been assumed negligible, and therefore omitted. The tether is assumed to be perfectly insulated so that there are no leakage losses, and is assumed to be completely deployed so that there exists no reeled inductance. The electromotive force remains variable because of the magnetic field variations. The tether resistance also is variable because of temperature variations throughout the orbit.

2.3 MODEL FOR INDUCED VOLTAGE

Essential to the evaluation of various tether configurations is the accurate calculation of the fluctuations in the electromotive force (emf), defined as $(\underline{v} \times \underline{B}) \cdot \underline{L}$. If it is assumed that the orbit of the tether is circular, v becomes a constant fixed by the orbital altitude. Further, if variations in L are computed as a consequence of temperature changes, the single variable to be evaluated becomes B.

18

The magnetic field data used in the analyses of the thermal variations which the tether experiences, which were all conducted for an invariant circular orbit, were produced by the SAO using the NEWMAG software code. This is a spherical harmonic model of the earth's magnetic field which starts with the assumption that the predominant portion of the earth's magnetic field $\underline{B}$ can be expressed as the gradient of a scalar potential function V as

$$\underline{B} = -\nabla V$$

and that the expression of the potential V of the internal field can be written as a series of spherical harmonics:

$$V = a \sum_{n=1}^{\infty} \left(\frac{a}{r}\right)^{n+1} \sum_{m=0}^{n} \left(g_n^m \cos m\phi + h_n^m \sin m\phi\right) P_n^m(\theta)$$

where a is the equatorial radius of the earth; g and h are Gaussian coefficients; r, θ, and ϕ are the geocentric distance, coelevation, and east longitude from Greenwich, respectively, which define a point in space; and $P_n^m(\theta)$ are the associated Legendre functions. The Gaussian coefficients are determined empirically by a least squares fit of measurements of the magnetic field. Together with the associated Legendre functions, it is thus possible to calculate the magnetic field at any point in space.

From V, three orthogonal components of the magnetic field may be derived as:

$$B_\theta = \frac{-1}{r} \frac{\partial V}{\partial \theta} = -\sum_{n=1}^{\infty} \left(\frac{a}{r}\right)^{n+2} \sum_{m=0}^{n} \left(g^{n,m} \cos m\phi + h^{n,m} \sin m\phi\right) \frac{\partial P^{n,m}(\theta)}{\partial \theta}$$

$$B_\phi = \frac{-1}{r \sin\theta} \frac{\partial V}{\partial \phi} = \frac{-1}{\sin\theta} \sum_{n=1}^{\infty} \left(\frac{a}{r}\right)^{n+2} \sum_{m=0}^{n} m\left(-g^{n,m} \sin m\phi + h^{n,m} \cos m\phi\right) P^{n,m}(\theta)$$

$$B_r = \frac{-\partial V}{\partial r} = \sum_{n=1}^{\infty} \left(\frac{a}{r}\right)^{n+2} (n+1) \sum_{m=0}^{n} \left(g^{n,m} \cos m\phi + h^{n,m} \sin m\phi\right) P^{n,m}(\theta)$$

and

$$B = \sqrt{B_r^2 + B_\theta^2 + B_\phi^2}$$

The data produced by SAO with this code utilized the set of coefficients of the International Geomagnetic Reference Field (IGRF) for epoch 1975.0.

In addition to the determination of the Gaussian coefficients as mentioned above, the coefficients of the IGRF assume that the associated Legendre functions are Schmidt normalized, i.e.:

$$\int_0^{\Pi} \left[P_n^m(\theta) \right]^2 \sin\theta \; d\theta = \frac{2\left(2 - \delta_m^0\right)}{2n + 1}$$

where δ_m^0 is the Kronecker delta. These coefficients together with the geocentric system of reference (coelevation θ, east longitude ϕ, and geocentric distance r) then provide the vectorial components B_θ, B_ϕ, and B_r at the specified point where the electrodynamic tether is located in space.

It should be noted that this model approximates the various magnetic anomalies observable in LEO which would not be accounted for had a pure tilted dipole model been used. The tilted dipole is essentially the spherical harmonic field model expanded to the first degree (n = 1) and all orders (m = 0,1). As can be seen from the plots of $(\underline{v} \times \underline{B}) \cdot \underline{L}$ versus time for a 24 hour period in Figures 5A and 6, the output using the tilted dipole model is simply a sinusoidal oscillation specified by the cross product of $\underline{v}$ and $\underline{B}$ (assuming the tether is perfectly rigid along the radial line), where

$$\underline{B} = - \left(\frac{r_e}{r}\right)^3 \left[g^{0,1} \sin\theta - \left(g^{1,1} \cos\phi + h^{1,1} \sin\phi\right) \cos\theta \right]$$

Here r_e is the equatorial radius of the earth, r is the orbital radius, g and h are the IGRF coefficients for the first degree and orders 0 and 1, $\theta = \sin^{-1} (\sin i \sin nt)$, and $\phi = \sin^{-1} (\cot i \tan nt)$, where i is the tether's orbital inclination to the magnetic polar axis, which varies during the course of a day, and nt is the true anomaly of the tether in its orbit. This sinusoidal variation is due to the rotation of the dipole axis about the earth's geographic axis during the course of a day; if the earth's rotation were neglected, the induced voltage potential would remain constant throughout the orbit. By comparison, the output from the NEWMAG code shows this same daily sinusoid due to the earth's rotation, but additionally very large intra-orbital fluctuations superimposed on

this sinusoid as a result of flying over or near the actual magnetic anomalies in the earth's field, notably the great negative South Atlantic anomaly and the positive Australian and Asian anomalies. For the analyses conducted to determine the variation in the orbital elements, an expansion to the third order, the so-called octopole model, was used. It can be seen from Figure 5B that this represents a reasonably close approximation of the fully expanded model, while requiring less computational time and permitting deviations from a circular orbit.

The inputs for NEWMAG were generated by the Smithsonian Astrophysical Observatory (SAO) using their SKYHOOK computer program. This software package is designed to model the electrodynamic interactions of a tethered satellite system, and includes models for the earth's magnetic field as described above, electron density, and charge collection by the wire and various contactors. It functions in three steps. The first is the establishment of initial conditions for the computer run. The second is the analytical calculation of orbital motion to obtain the behavior of the tether as a function of time. The third is the analysis of the output using various post-processors. For this analysis, a rigid tether was assumed and its mass modeled by two end points. The initial conditions for the position and velocity of each of these mass points were obtained using a pre-processor called DUMBEL, which takes orbital parameters and computes a set of initial conditions which allow the formulation to be started in tension equilibrium so that there are no initial oscillations in the radial, in-plane, or out-of-plane directions. The computations by SKYHOOK produce the state vector of the system at each time step, which includes the position and velocity of each mass point in geocentric coordinates; this state vector is the input for NEWMAG.

A post-processor written by SAO then took the SKYHOOK values for the state vector produced by the integration to calculate the vector product V_{oc}, and the NEWMAG values for the magnetic field components, as described above, to calculate the magnitude of the magnetic field strength, at 50 second time intervals. These two data were the basis for the thermal analysis conducted for varying tether surface conditions and operating modes.

21

3. METHODS OF ANALYSIS

In this examination of thermal and certain dynamical effects on the operation of an electrodynamic tether system, three areas in particular will be discussed.

First, an analysis of the consequences of leaving the conducting material of the tether bare, instead of insulated as is generally presumed in most analyses, will be made. This will be done to a first approximation by calculating the magnitude of the current which could be expected to be lost along the length of an uninsulated tether due to the capture of ions from the surrounding plasma and additionally to the emission of secondary electrons as a result of these captures. The ratio of this current loss to the system current without losses will provide an effective efficiency for an uninsulated tether.

Second, using the reduced closure circuit described in Section 2.4 above as the basis for the analysis, an examination of the effects of the variation of the operational temperature on tether performance, as defined by its efficiency, as a result of the revolution of the tether about the earth, will be made by numerically integrating the temperature equation forward in time from an arbitrarily selected set of initial conditions. The orbital elements of the tether's orbit will be varied to determine their individual effects, as will the design parameters of the tether itself. This analysis will be restricted by the assumptions of a rigid tether moving in a perfectly circular, invariant orbit. Additionally, the tether will be simulated to be operating as a power generator, a thruster, and various combinations of the two.

Third, the dynamical effects of the various modes of tether operation on the orbit of the tether will be examined by computing those external forces which act on the tether and serve as perturbations to the orbital elements. Again, these perturbation equations will be numerically integrated forward in time to determine if any particular method of operation is physically prohibitive.

22

3.1 INSULATION

As discussed in Section 2.2.3 above, the conducting material of the tether may be insulated from the surrounding plasma to eliminate any current leaking along its length by coating it with a sufficient thickness of some type of dielectric. However, a tether insulated in this manner experiences the disadvantages of arcing due to differential charging of the dielectric, and large leakage currents through pinholes in the dielectric. An alternative to this problem is to actually leave the tether bare if the amount of current which leaks along its length is of a small enough magnitude to constitute an acceptable loss. The following is an analysis to estimate the magnitude of this current leakage loss.

An upwardly deployed tether moving in a prograde orbit will charge negatively with respect to the surrounding plasma. Thus, the current loss which the tether will experience along its length will be the result of positive ions from the plasma which are captured by the negatively biased tether, plus the secondary electrons emitted by the wire upon ion impact. The number of ions which are captured is a function of the ion density at the operational altitude, the bias of the tether, the ion mass and velocity, and the thickness of the tether.

There are several mathematical models which may be used to estimate the magnitude of the current collected by the tether as it moves through the surrounding plasma. The most appropriate for our case is the so-called inertia limited current collection model, in which current collection is due only to those ions whose trajectories under the attraction of the wire intercept the wire itself. It acts as an upper limit for the amount of current which can be collected, because the presence of earth's magnetic field restricts somewhat the number of ions which can actually strike the tether. It is also less than that of a space-charge limited collection model, in which a positive ion sheath is formed around the tether such that the only current collected is due to those ions which randomly "walk" across the sheath boundary. As detailed in Reference 17, this type of mode is generally more applicable to structures which have larger relative dimensions than a tether.

23

If sheath effects about the tether are ignored, which may exaggerate the estimate of ions captured as described above, this number of ions may be calculated by balancing the momentum of the ion far from the tether with the momentum of one which just grazes the tether's surface. As shown in Figure 7, if x is the distance from a line passing through the tether's center which is parallel to the velocity direction, and the velocity of the ion far from the tether is represented as v_0, then

$$x v_0 = r v_i$$

where r is the radius of the tether and v_i is the velocity of the ion as it grazes the tether. The momentum balance then yields

$$m_i v_0^2 = m_i v_i^2 - 2 e V$$

where V represents the magnitude of the tether bias. Substituting the first equation into the second and solving for x shows the distance from the tether greater than which the ions will not impact, and hence not cause a current loss, when they are attracted by the negative bias. Thus

$$x = r \sqrt{1 + \frac{2ev}{m_i v_0^2}}$$

Obviously, this analysis assumes that the plasma potential far from the tether is zero. This is a reasonably good assumption so that the estimate for x should also be good. Having determined this distance, the current loss due to ion capture is estimated as

$$I_{LOSS} = 2 \times L \, n_i \, v_0 \, e$$

where L is the length of the tether and n_i is the ion density at the operational altitude. Having assumed a completely neutral plasma, i.e. $n_i = n_e$, then

$$I_{LOSS} = 2 \, e \, r \, L \, n_e \, v_0 \sqrt{1 + \frac{2ev}{m_i^2 v_0^2}}$$

24

Finally, since $\dfrac{2eV}{m_i^2 v_o^2} >> 1$, then

$$I_{LOSS} = e\, n_e\, d\, L \sqrt{\dfrac{2ev}{m_i}} \qquad (1)$$

where d is the tether diameter. Using typical values of $n_e = 10^{11}$ m^{-3}, d = 3 mm, L = 20 km, V = 4 kV, and m_i = .016 kg/mol, this would indicate a current leakage of approximately .21 amps if the tether potential with respect to the surrounding plasma were constant along its length. For a tether operating to generate 10 kw of power, this represents an approximately 7.5% loss above any other system losses. However, since the tether potential with respect to the plasma really varies along its length, a better estimate for the loss can be obtained by defining this variation for a specified system.

For the case of a tether which is being operated to generate power, the current in the system is positive upward, as shown in Figure 9, where 9A shows the generator mode and 9B the thruster mode. From 9A it can be seen that the voltage induced across the length of the tether, V_{oc}, is equal to the sum of the potential drops across the contactors at the anode and cathode, the load and the tether itself. This assumes, of course, that these are the only system losses as discussed in the formulation of the equivalent circuit above. If it is assumed that the potential of the tether, ϕ_T, is linear with z, then

$$\phi_T = Az + B$$

Solving for the integration constants, we note from Figure 9A that the boundary conditions may be written as

at z = 0: $\qquad\qquad \phi_T = \phi_{Po} - V_a - V_L = B$

and

at z = L: $\qquad\qquad \phi_T = \phi_{Po} - V_{oc} + V_c = Az + B$

25

which yields

$$A = (V_L + V_a + V_c - V_{oc}) / L$$

Therefore

$$\phi_T(z) = \left(V_L + V_a + V_c - V_{oc}\right)\left(\frac{z}{L}\right) + \phi_T - V_a - V_L$$

Using this, and defining the plasma potential as function of z as

$$\phi_P = \phi_{Po} - v_c B\, z$$

where ϕ_{Po} is the plasma potential at $z = 0$, v_c is the orbital velocity, and B is the magnetic flux, we can then write an equation for the potential of the tether with respect to the plasma at any point as

$$\phi_P - \phi_T = V = V_L + V_a - \left(V_L + V_a + V_c\right)\left(\frac{z}{L}\right) \qquad (2)$$

Rewriting Equation 1 for an arbitrary value of z, we get a current per unit length as

$$\frac{dI}{dz} = e\, n_e\, d\, \sqrt{\frac{2e}{m_i}\left(\phi_P - \phi_T\right)}$$

If the voltage drop due to the tether's resistance is written as

$$\phi_T' = -IR = -I\left(\frac{z}{\sigma A}\right),\; \text{therefore}$$

$$\frac{d\phi_T'}{dz} = -\left(\frac{4}{\sigma\pi\, d^2}\right) I$$

and

$$\frac{d^2\phi_T'}{dz^2} = -\left(\frac{4}{\sigma\pi\, d^2}\right)\frac{dI}{dz} = -\left(\frac{4}{\sigma\pi\, d^2}\right)en_e d\, \sqrt{\frac{2e}{m_i}\left(\phi_P - \phi_T\right)}$$

Integrating this twice yields

$$\phi_T' = -\left(\frac{16\, e\, n_e\, L^2}{15\, \sigma\pi\, d}\right)\sqrt{\frac{2e}{m_i}}\left(\frac{1}{V_L + V_a + V_c}\right)^2 \sqrt{V_L + V_a - \left(V_L + V_a + V_c\right)\frac{z}{L}} + Az + B$$

26

Applying the boundary conditions as before defines the constants of integration as

$$A = \frac{1}{L}\left[-V_{oc} + V_L + V_a + V_c - \left[\frac{16\,e\,n_e\,L^2}{15\,\sigma\pi\,d\left(V_L + V_a + V_c\right)^2}\right]\sqrt{\frac{2e}{m_i}}\left(\left(V_L + V_a\right)^{\frac{5}{2}} - \left(-V_c\right)^{\frac{5}{2}}\right)\right]$$

and

$$B = \phi_{Po} - V_L - V_a + \left[\frac{16\,en_e L^2}{15\sigma\pi d\left(V_L + V_a + V_c\right)2}\right]\sqrt{\frac{2e}{m_i}}\left(V_L + V_a\right)^{\frac{5}{2}}$$

The current at the load may now be determined by solving $I = \left[\frac{\sigma\pi d^2}{4}\right]\frac{d\phi_T'}{dz}$ at at $z = 0$. Thus

$$I_L = \left[\frac{\sigma\pi d^2}{4L}\right]\left[\left(-V_{oc} + V_L + V_a + V_c\right) + \left(\frac{8en_e L^2}{3\sigma\pi d\left(V_L + V_a + V_c\right)}\right)\sqrt{\frac{2e}{m_i}}\left[\frac{-2\left(\left(V_L + V_a\right)^{\frac{5}{2}} - \left(-V_c\right)^{\frac{5}{2}}\right)}{5\left(V_L + V_a + V_c\right)}\right.\right.$$

$$\left.\left. + \left(V_L + V_a\right)^{\frac{3}{2}}\right]\right]$$

or

$$I_L = \left[\frac{\sigma\pi d^2}{4L}\right]V_L\left(1 + \delta_a + \delta_c - \frac{1}{\eta}\right) + \left(\frac{2en_e\,d\,L}{3\left(1+\delta_a+\delta_c\right)}\right)\sqrt{\frac{2eV_L}{m_i}}\left[\frac{-2\left(\left(1+\delta_a\right)^{\frac{5}{2}} - \left(-\delta_c\right)^{\frac{5}{2}}\right)}{5\left(1+\delta_a+\delta_c\right)} + \left(1+\delta_a\right)^{\frac{3}{2}}\right]$$

Here, $\eta = \frac{V_{oc}}{V_L}$, $\delta_a = \frac{V_a}{V_L}$, and $\delta_c = \frac{V_c}{V_L}$.

Examining the two terms of this equation, it can be seen that the first is equivalent to that of the current flow due to the voltage drop across the tether itself, $I = \frac{E}{R}$, while the second is equivalent to that of the current flow due to the ion capture. The difference in sign between the two terms indicates that the ion capture is effectively a current loss.

The ratio of these two terms is essentially an efficiency for the bare tether. A good approximation for this is made by expanding the second term as a binomial series and neglecting all factors of order greater than one and the products of all factors. This neglect is reasonable as $\delta_a \sim \delta_c \ll 1$. This expansion yields a ratio expressed as

27

$$\text{Loss} \sim \frac{8\sqrt{2}}{5} \left[\frac{n_e e^{3/2}}{\sigma \pi \sqrt{m_i}} \right] \left(\frac{L^2}{d\sqrt{V_L}} \right) \left[\frac{\left(1 + \frac{1}{2}\delta_a - \frac{1}{3}\delta_c\right)}{\left(1 + \delta_a + \delta_c - \frac{1}{\eta}\right)} \right]$$

Calculating this loss using the typical values stated previously, and assuming a system efficiency of 90%, a value of 3.24% is attained. This represents the effective current loss due solely to ion capture along the length of the bare tether, and is about half of what was calculated previously for a tether of uniform potential along its length.

The loss calculated above represents only that current which is due to ion collection. The total current loss is the sum of several additional components, specifically secondary electron emission due to ion impacts, photoelectric emission, backscattering, and thermal-induced currents. In a low earth orbit, such as that in which the tether would operate, these components are typically negligible with the exception of secondary electron emission. So, to complete this estimate for current leakage from an uninsulated tether, the additional current losses resulting from secondary electron emission due to ion impacts must be accounted for.

Since the emission of an electron is the equivalent of the capture of a position ion, these secondary electrons also represent an effective leakage loss. References 11 and 17 both discuss this and present graphs of electron emission from nickel and aluminum targets. For ion impacts at the 4 kV energy level, the ratio of the electron emission current to the positive ion current is approximately 60% from the nickel target, and 240% from the aluminum target. Additionally, as corroboration, it is indicated that the number of secondary electrons emitted per primary impact from an aluminum target is about 4 times the number emitted from a nickel target. Hence, the total current leakage loss would be 3.4 times the loss indicated previously. Together with the ion current calculated above, a total current leakage loss due to positive ion capture and secondary electron emissions amounts to approximately 11.0%.

Finally, before deciding if a loss of this magnitude is acceptable with respect to the mass savings, an estimate should be made to determine

the degree of conductor loss over time due to the ion impacts. The rate of mass loss may be expressed as

$$\frac{dm}{dt} = K \left[\frac{m_i \, I_i}{e} \right]$$

where I_i is the leakage current as determined above, and K is a constant, characteristic to the conductor, representing the number of conductor atoms ejected per ion impact. Data from Reference 11 may be extrapolated to make an estimate for K for an aluminum target as approximately .44 Al atoms / O^+ ions. This is probably a pessimistic estimate as an oxide coating has been found to develop on bare aluminum in the presence of atomic oxygen, such as in the ionosphere, which sputters very little. Thus, the degree of mass loss over the expected operational life of the tether is about 2 kg in 10 years. Hence, conductor mass loss, or sputtering, does not appear to pose a problem for an uninsulated tether.

A consistent analysis may be made for a tether operated in the thruster mode by referring to the potential diagram in Figure 9B. The result of this process is an estimate for the leakage loss due to positive ion capture as

$$\text{Loss} \sim \frac{8\sqrt{2}}{5} \left[\frac{n_e e^{3/2}}{\sigma \pi \sqrt{m_i}} \right] \left(\frac{L^2}{d\sqrt{V_s}} \right) \left[\frac{\left(1 - \frac{1}{2} \delta_a + \frac{1}{3} \delta_c \right)}{\left(1 - \delta_a - \delta_c - \eta \right)} \right]$$

where now V_s represents the voltage drop across the source, $\delta_a = \frac{V_a}{V_s}$, $\delta_c = \frac{V_c}{V_s}$, $\eta = \frac{V_{oc}}{V_s}$. The percent loss when operated in this mode, including losses for secondary electron emissions, amounts to approximately 13.6%.

Similarly, an analysis can be made for a downwardly deployed, and hence positively biased, tether. The expressions for the leakage losses are similar to those derived above. Now, however, the capture of the negative electrons in the surrounding plasma are the cause of the leakage, and so the mass of the electron must be substituted into the expressions in place of the ion mass. Since the ratio of the mass of atomic oxygen to that of an electron is approximately 30000, this drives the loss ratio to 100%. A positively biased, uninsulated tether is thus prohibitive.

29

As a consequence of this analysis, an effective efficiency for the uninsulated tether may be defined as

$$\eta_{Loss} = 1 - 3.4 \, Loss$$

where Loss is the ratio calculated above to estimate the current loss due to ion capture along the length of the tether compared to the current flow without losses, and the 3.4 accounts for the additional losses due to secondary electron emission. As previously stated, however, for the remainder of this analysis it will be assumed that the tether is perfectly insulated so that no current leakage losses occur.

3.2 METHOD OF THERMAL ANALYSIS

Given the reduced circuit as discussed in Section 2.4 above so that the equation of the circuit is written as

$$IR = V_{OC} - 200 - \frac{P_L}{I} \quad [V]$$

and conducting the system analysis for a constant load power, P_L, the only remaining variables to be determined are the tether resistance, R, and the system current, I. The resistance of the tether is primarily a function of the temperature of the conductor; hence, a thermal analysis will be done to calculate the temperature, and subsequently the resistance, electromotive force, and efficiency, as a function of orbital time. The current will be determined such that a constant load power is maintained at an arbitrarily specified level when the tether is operating as a power generator. When the tether is operated as a thruster, the current will be determined by the thrusting mode, i.e., to maintain a constant current level while thrusting, to maintain a constant force level while thrusting, or to maintain a constant voltage level while thrusting.

In the analysis, the parameters of the tether itself, i.e., the length, diameter, type of conductor material, and surface characteristics, will be examined to determine their relative effects on the system operation. Likewise, the orbital parameters, i.e., the altitude, inclination, distance from the sun, and orientation to the sun, will be examined to determine their relative effects.

30

3.2.1 Thermal Balance

As in any system, the thermal balance of the tether may be expressed as

$$q_{in} + q_{gen} - q_{out} = \dot{q}$$

Formally, q_{out} consists of radiation to free space, radiation to other objects, and conduction losses; q_{gen} is the ohmic heat generated as current passes through the tether; and q_{in} consists of solar irradiation, earth irradiation, earth albedo, self-irradiation, and aerodynamic heating. For this analysis it will be assumed that q_{out} consists only of radiation to free space, and that self-irradiation is a negligible portion of q_{in}. These assumptions are fairly well justified. The neglect of self-irradiation follows from the assumption, made previously, of a perfectly rigid tether. Radiation from the tether to free space dominates that to other nearby objects, primarily the base station, again as a consequence of the rigid tether assumption; thus, only considering radiation to free space seems reasonable. Neglecting conduction losses is not as easily justified. However, the ends of the tethers must be electrically insulated to prevent current from discharging through the base supports. As electrical insulators are generally also good thermal insulators, conduction between the tether and supports should not occur.

Given these assumptions, the components of the thermal balance are as follow:

$$\dot{q} = m\, C\, \frac{dT}{dt}$$

$$q_{out} = \epsilon\sigma_B\, A\, T^4 = \epsilon\sigma_B\, \pi\, d\, L\, T^4$$

$$q_{gen} = I^2\, R = I^2 \left(\frac{4\rho L}{\pi\, d^2}\right)$$

31

where $q_{solar} = S \alpha_s\ d\ L\ Z$

$$q_{aero} = \frac{1}{2} \rho_a\ d\ L\ V_{rel}^3$$

$$q_{albedo} = .28\ S\ \alpha_s\ \pi\ d\ L\ F\ |\cos \hat{\tau}|$$

$$q_{earth} = 237\ \epsilon\ \pi\ d\ L\ F$$

These equations use variables defined as:

d = tether diameter

L = tether length

T = temperature

σ_B = Boltzman's constant

I = current

α_s = solar absorptivity

ϵ = emissivity

Z = sun factor

F = earth view factor

V_{rel} = relative velocity

ρ_a = atmospheric density at altitude

$\hat{\tau}$ = biased true anamoly

ρ = resistivity

t = time

m = conductor mass

C = specific heat

S = solar constant $\simeq 1368$ W/m^2

More detailed explanations of the selections of values for these parameters will be discussed in Section 3.2.2.

The thermal capacitance of the system must be examined to determine how quickly the tether will reach thermal equilibrium, and thus to decide whether the equilibrated state can be used as a point for evaluation. Writing the equation above for the thermal balance strictly in terms of temperature, we have

$$\frac{dT}{dt} = \frac{-A'\ T^4 + B'}{m\ C}$$

32

where $A' = \epsilon \sigma_B \pi d L$, and $B' = q_{in} + q_{gen}$. Assuming that B' is a constant with respect to temperature, this implies that the time constant for the system is

$$\tau = \frac{m C}{4 \epsilon \sigma_B \pi d L T_0^3}$$

where T_0 is the equilibrium temperature. Using typical values for these parameters, as follow:

$$m = 400 \text{ kg}$$
$$C = 875 \text{ J/kg/}^{o}\text{K}$$
$$d = 3 \text{ mm}$$
$$L = 20 \text{ km}$$
$$T_0 = 240 \text{ }^{o}\text{K}$$
$$\epsilon = .85$$

this yields a time constant of $\tau = 700$ seconds, or about 11.6 minutes. Compared to an approximately 90 minute orbit, this indicates that a state of equilibrium would be inappropriate for evaluation, and that the thermal transients caused by the capacitance of the tether must be taken into account.

Despite this transience throughout the orbit, at any given time the tether may be assumed to be at a uniform temperature. Since in our case, the length of the tether will always be much longer than the radius, the tether may be considered a cylinder with a uniformly distributed heat source (the current). Thus, it will be assumed throughout this analysis that all portions of the tether are simultaneously at the same temperature when performing computations.

3.2.2 Calculation of Components of Thermal Balance

Having made these assumptions, an examination of the separate components of the thermal balance can be conducted.

Radiation from the tether to free space is solely a function of the temperature of the conductor, as specified by the Stefan-Boltzmann law, presuming that the other variables in the equation may be expressed in

33

terms of T. While this is indeed the case, the variations of the emissivity and the diameter are so slight over the range of temperature variations which the tether will undergo that they may be considered as constants. The length, on the other hand, may vary significantly over an orbit depending on the magnitude of the temperature variation and must be taken into account. This variation in length may be expressed as

$$\frac{dL}{L} = \alpha_e \left(T_2 - T_1\right)$$

where α_e is the coefficient of expansion, typically about 12.9×10^{-6} m/m/$^{\circ}$K for aluminum.

Solar irradiation of the tether is a function of the intensity of the solar flux and the magnitude of the tether's surface area presented normally to the incident radiation. The solar flux is a parameter which is typically considered to be a constant; it does, however, vary somewhat within the 11-year solar cycle and routinely is affected by solar storms. The average value of the solar flux outside of the earth's atmosphere over the past several years has been about 1368 W/m^2. Since the solar flux varies as the inverse square to the distance from the sun, there is a variation of $\pm 3\%$ due to the eccentricity of the earth's orbit throughout the year. The maximum occurs at the perihelion of the earth's orbit (about 3 January, 1399 W/m^2); the minimum at aphelion (about 4 July, 1309 W/m^2). The absorptance of the material is, like the emittance, relatively invariant with such temperature variations as the tether will experience, and will also be a considered a constant. What here has been called the sun factor is obtained by a series of rotation angles to calculate the tether area perpendicular to the incoming solar rays at a given point in the orbit. The angles, as shown in Figure 10, represent the inclination of the orbit, i, relative to the equatorial plane; the obliquity of the equatorial plane, β, relative to the ecliptic plane; the longitude of the line of notes, Ω, relative to the normal to the earth-sun line; and the true anomaly of the tether in its orbit, f, measured from the line of nodes.

Both the inputs due to earth irradiation and albedo involve the earth view factor for the tether. This view factor is a function of the altitude of the tether in its orbit, and its orientation with respect to the earth-tether radial line. Formulae for various orientations are given in Reference 10. Assuming that the tether remains perfectly aligned with this radial line, the view factor may be calculated as

$$F = \frac{\theta - \sin \theta \cos \theta}{\pi}$$

where

$$\theta = \sin^{-1}\left(\frac{r_e}{r}\right).$$

At an altitude of 300 km, this yields an earth view factor of F=.31413.

The earth albedo flux is essentially that fraction of the solar irradiation reflected back onto the tether as a result of scattering in the atmosphere and reflection from clouds and earth surfaces. This fraction is, much like the solar flux itself, basically a constant, although variations do occur as a result of changes in cloud cover and snow and ice covered regions. Typical values in the low latitudes are 30% ±2%. The primary difference between the two is that instead of only the normal area being irradiated, here the entire surface area of the tether receives the incident albedo, mitigated by the earth view factor and the proximity of the tether to the terminator. This proximity is included as the cosine of the biased anomaly, such that the albedo is a maximum when directly facing the sun and decreasing to zero at the point in the orbit where the earth's shadow is entered.

Irradiation by the earth itself involves essentially an "earth flux", caused by solar radiation which has been absorbed by the earth and atmosphere being reemitted as thermal radiation. Again, this remains approximately constant at 237 ±7 W/m^2, with the earth view factor mitigating the total surface area. Now, however, the emissivity of the tether surface determines the energy input instead of the absorptance as in the solar irradiation and albedo calculations. This is because the earth's radiation is not at the wavelengths of the solar radiation; hence, the solar absorptance cannot be used in this calculation.

35

Aerodynamic heating is a function of the density of the atmosphere at the operational altitude (which in turn is a function of atmospheric temperature and the solar cycle); and the velocity of the atmosphere relative to the tether. Each of these tend to vary as the satellite moves in its orbit. In performing the calculation for drag the maximum values which presented themselves were used in order to produce a conservative estimate.

Empirical formulas have been developed for the calculation of density. For an orbital altitude of 300 km this is:

$$\rho_a = \frac{\left(1.47 \times 10^{-16}\right) T_{ex} \left(3000 - T_{ex}\right)}{\left[1 + \frac{2.9 \left(Alt - 200\right)}{T_{ex}}\right]^{10}}$$

For this evaluation, the exosphere temperature was selected to be 1600° K, the maximum for the solar cycle. Thereafter, in subsequent calculations

$$\rho_a = 6.225 \times 10^{-11} \text{ kg/m}^3$$

was used.

Atmospheric velocity varies according to latitude and altitude as

$$v_{air} = 465 \cos L \left[\frac{r}{r_e}\right]$$

$$= 465 \left[\frac{r}{r_e}\right] \cos (28.5° \cos f)$$

where f is the true anomaly and the 28.5° is the assumed orbital inclination used in this analysis. The velocity of the tether relative to the surrounding air is then a vector difference, which may be expressed as

$$v_{rel}^2 = v_{orb}^2 + v_{air}^2 - 2v_{orb} v_{air} \cos\phi$$

where ϕ may be expressed as 28.5° sin f. For our purposes then, the maximum relative velocity at an orbital altitude of 300 km is

$$v_{rel} = 7300 \frac{m}{s}$$

36

Using these values for ρ_a and v_{rel}, the maximum energy input from aerodynamic heating is given by

$$q_{aero} = 12.108 \; d \; L \; [W]$$

Obviously, when calculated in this manner, the value for aerodynamic heating will vary throughout the orbit.

The ohmic heat generated by the current passing through the tether varies with both temperature and with the magnitude of the open circuit voltage, $(\underline{v} \times \underline{B}) \cdot \underline{L}$ or V_{OC}. Since the electrical resistance may be expressed as

$$R = \frac{4\rho L}{\pi \; d^2}$$

where both ρ and L are functions of temperature, the resistivity as

$$\rho = \rho_0 \left[1 - \alpha_T \left(T - 293.15° \right) \right]$$

and L as described previously, and since I varies throughout the orbit proportionally with V_{OC}, this Joule heating will be a constantly varying source of energy for the tether. The magnitude of the current will further depend on the amount of power which is required to be delivered to the load.

Using these equations and substituting into the equation for the thermal balance, the temperature transients that would occur for tethers of various diameters as the system orbits the earth and the changes in those parameters, such as resistance, efficiency, and current, which are functions of temperature can be evaluated. In this analysis, the efficiency of the tether itself, not including other system losses, may be expressed as

$$\eta = 1 - \frac{I^2 R}{(\underline{v} \times \underline{B}) \cdot \underline{L}}$$

37

As can be seen from Figures 11, which represent the variations in the properties of a tether operating as a pure generator, temperature variations of up to 40 degrees can be expected throughout the orbit, depending on the diameter of the tether under consideration. Similarly, the efficiency can fluctuate by about 30 points. Efficiency improves when the tether is operated at lower temperatures (an expected result as resistivity increases with temperature), and when the current levels are low so that the ohmic losses are minimized.

3.2.3 Conductor Material

The choice of the conducting material of the tether must be made on the basis of the material's conductivity and density. A lighter tether is preferable to a heavier one from the standpoint of the cost of energy to place the tether into orbit; however, a light tether which is highly resistive will have to be made thicker in order to pass a specified level of current. Conversely, a more conductive tether will decrease the ohmic losses in the system, hence improving the system's overall efficiency; however, if it is an extremely dense material the improvement in efficiency will not compensate for the increased energy costs.

To this end, the parameter to evaluate is the ratio of conductivity and density, $\frac{\sigma}{\rho}$, such that the determination of merit is for a large value. Examinations of this parameter were made for various materials, as indicated in the table below, which were selected on the basis of either high conductivity, low density, or both. Both density and conductivity were allowed to vary over the range of temperatures in which the tether would most probably operate, although the variations in density of any of the materials examined over the small range of probable temperatures was negligible. The characteristics of the material evaluated are also listed in the table. The variations in the parameter are shown graphically for the several materials in Figure 12.

Conductor Characteristics

Type	Ref Resistivity	Coeff Resistivity	Ref Density	Coeff Density
Aluminum	2.857×10^{-8}	.00424	2707	-6.912×10^{-5}
Copper	1.724×10^{-8}	.0068	8910	0
Silver	1.629×10^{-8}	.0061	7148	0
Nickel	7.8×10^{-8}	.0069	8890	0
Platinum	$10. \times 10^{-8}$	.00393	2145	0

It can be seen from Figure 12 that the parameter for aluminum is significantly better (higher) than those of the other materials evaluated. Thus, aluminum will be the conducting material used in this analysis of a tether system.

3.3 ORBITAL VARIATIONS

When an external set of accelerations, in addition to the primary acceleration due to the main gravitational field, acts on an orbiting satellite the parameters which define the orbit vary with time. Appendix C details the theoretical development which leads up to the variational equations of Lagrange and Gauss which may be used to calculate the rate of change of the orbital elements. If the external forces acting on the satellite, in this case the tether, can be calculated, then the vector components of that total force will specify how the orbit will be altered in the presence of that force.

3.3.1 Disturbing Acceleration Vector

The disturbing acceleration is essentially the sum of all external forces which act on the tether system throughout its orbit. The components which were included for this analysis were the induced electromagnetic force, aerodynamic forces, solar radiation forces, tether libration-induced forces, and the effects of the earth's oblateness. Additionally, there are external forces caused by induced eddy currents in the system which may interact with the earth's magnetic field, and by the solar wind and cosmic dust; however, these are negligible by comparison with the other forces listed here and will not be included.

39

For this analysis, an earth-centered coordinate system was used with the first coordinate axis parallel with the eccentricity vector, the third parallel to the angular momentum vector, or normal to the orbital plane, and the second such that it formed a right-hand set with the other two, and consequently is parallel to the parameter of the orbit. Although this is apparently a rotating coordinate frame with respect to inertial space, the calculation of the variational equations as described in Appendix C is made instantaneously along an osculating orbit, so that the Coriolis, Euler, and centripetal accelerations are not present. This coordinate system is depicted in Figure 13. Thus, we can write

$$\underline{r} = r \begin{vmatrix} \cos f \\ \sin f \\ 0 \end{vmatrix} \quad \text{and} \quad \underline{v} = \begin{vmatrix} v_r \cos f - v_t \sin f \\ v_r \sin f + v_t \cos f \\ 0 \end{vmatrix}$$

with v_r representing the radial component of velocity, equal to $\frac{\mu\, e\, \sin f}{h}$, and v_t representing the component normal to v_r in the orbital plane, equal to $\frac{\mu(1 + e\, \cos f)}{h}$.

The disturbing acceleration due to the induced electromagnetic force may be expressed as

$$\underline{a}_d = \frac{(\underline{I} \times \underline{B})L}{m}$$

where L is the tether length, m the system mass, $\underline{I}$ the vector representation of the current, and $\underline{B}$ the magnetic field strength. For this analysis, it was assumed that the system could be modeled as a point mass; hence, the tether is rigid and oscillates only in the orbital plane. Further, it was assumed that a positive I represents current flowing up the tether, i.e. the generator mode. The oscillation of the tether was modelled in accordance with Reference 26, assuming that the length of the tether remains constant and that the moment of inertia of the tether about the longitudinal axis is negligible compared to the moments of inertia about the two transverse axes. Assuming that e $\ll$ 1, as would be the case for the orbit of the tether, Equation 5.102b of this reference becomes

$$\frac{d^2\alpha}{dt^2} + 3 n^2 \alpha = 2 n^2 e \sin nt$$

where α represents the in-plane libration angle; the particular solution of this equation is $\alpha = e \sin nt$. Hence, approximating $f = nt$, we can define the current vector as

$$\underline{I} = I \begin{vmatrix} \cos \alpha \cos f - \sin \alpha \sin f \\ \cos \alpha \sin f + \sin \alpha \cos f \\ 0 \end{vmatrix}$$

in terms of the e, p, h coordinate system. The magnetic field, $\underline{B}$, was modeled for this analysis by an octopole model, in which the field model is expanded to the third degree and all orders, with the vector components again referred to the e, p, h coordinate system described above. This is essentially as described in Section 2.3; a representation of the field strength computed by this model appears as Figure 5B. A comparison with Figure 5A, the simple tilted dipole model, and Figure 6, the fully expanded model, shows that the octopole is significantly better approximation than the dipole which does not require the computational effort of the expanded model.

Typically, the magnitude of the electromagnetic acceleration, for a current level of approximately 1 amp and a tether length of 20 km, is on the order of 1 N/kg.

The component of the disturbing acceleration due to aerodynamic forces was calculated as a function of the density of the atmosphere at the operational altitude (which in turn is a function of atmospheric temperature and the solar cycle); the velocity of the atmosphere relative to the tether; and the drag coefficient for the system. Values for aerodynamic heating were calculated in the formulation of the thermal balance; values for aerodynamic drag may be made using the same parameters, as follows.

Like electromagnetic drag, the aerodynamic drag is a force which is distributed evenly along the tether's length. It may be calculated by the integral

41

$$\underline{F}_d = \frac{1}{2} \int \rho_a \, C_D \, \underline{v}^2_{rel} \; d \, L \, \delta r$$

Assuming, as we have, that all of the variables in the integral remain constant over the length of the tether, the drag force may be expressed as

$$\underline{F}_d = \frac{1}{2} \, C_D \, \rho_a \, \underline{v}^2_{rel} \; d \, L$$

where d is again the tether diameter in meters, and F_d represents the drag on the tether acting opposite the direction of the relative velocity. For a tether diameter of three millimeters, the magnitude of this force is on the order of .02 Nt.

Vectorially, Reference 10 defines the relative velocity as

$$\underline{v}_{rel} = \underline{v} - \underline{v}_{air}$$

where $\underline{v}$ is the tether's orbital velocity, as defined above, and $\underline{v}_{air}$ is the local air velocity. This local air velocity is, in turn, defined as

$$\underline{v}_{air} = \left(\frac{r}{r_e}\right) \underline{v}_e \cos \lambda$$

where λ is the local latitude, and $\underline{v}_e$ is the rotational velocity of the earth at the equator. These calculations are made in the program attached as Appendix B, referring the vector components again to the e, p, h system. The air density is calculated as a function of both altitude, H, and exosphere temperature, T_{ex}, from formulae listed in Reference 10. These are

$$\rho_a = 11 \, e^{-\left(\frac{H}{6}\right)} \qquad \text{for } 70 < H < 118$$

$$\rho_a = \frac{(H - 95)^{-3}}{2600} \qquad \text{for } 118 < H < 200$$

$$\rho_a = \frac{\left(1.47 \times 10^{-16}\right) T_{ex} \left(3000 - T_{ex}\right)}{\left[1 + \frac{2.9 \, (H - 200)}{T_{ex}}\right] 10} \qquad \text{for } H > 200$$

42

with T_{ex} varying in relation to the tether's position with respect to the sun as T_{exo} (1 + .12 sin f). With the exception of H, λ, T_{exo}, $\underline{v}_{orb}$, and r, all other variables were assumed constant for this calculation. Those not specified by the dimensions of the tether were chosen as C_D = 2.2; and T_{ex} = 1100 K.

The component of the disturbing acceleration due to the solar radiation force is given by

$$\underline{F}_r = -K \, A \, P \, \underline{i}_y$$

where K is a dimensionless constant which indicates the reflectivity of the material; A is the satellite's area perpendicular to the sun; and P is the solar momentum flux, approximately 4.4 x 10^{-6} kg/m/s^2. As indicated, the force acts opposite the direction of the sun. Typically, K varies between 0 and 2, with a value of 0 indicating a translucent material, and 2 indicating a totally reflective material. Using a dark coating, such as anodized aluminum as will be discussed in Section 4.1.1, would set K at about 1.25. As before, A would equal d L and must be referred to the x, y, z coordinate frame to be consistent. Thus, the greatest magnitude of this force becomes F_r = .0005 N.

To evaluate the effect of the earth's oblateness and transform it into a disturbing acceleration, it is necessary to express it first as a disturbing function, then find its gradient. If the distribution of mass in the earth is assumed to be symmetric about the polar axis, so that all tesseral harmonics are neglected, and only the effects of the first three zonal harmonics of the earth's gravitational potential are included, then the disturbing function is

$$R = -\left(\frac{\mu}{r}\right) \sum_{n=2}^{4} J_n \left(\frac{r_e}{r}\right)^n P_n(\cos \phi)$$

where

$$\cos \phi = \underline{i}_r \cdot \underline{i}_z$$

The assumption of axial symmetry is reasonably good for the earth and is routinely used; likewise, the approximation of the earth's oblateness by

only the J_2, J_3, and J_4 terms is also routinely used and is good since the coefficients for the earth become progressively smaller (J_3 is approximately 500 times smaller than J_2).

The calculation of the gradient of R with respect to $\underline{r}$, and hence the disturbing acceleration, is detailed in Appendix B. The magnitude of this acceleration is typically about .01 N/kg.

Due to the gravity gradient which occurs in extended bodies, such as a tether, small net forces are produced as the body librates during its orbit. As detailed in Reference 26, and assuming for this analysis that the tether is represented as a simple system of two equal masses, these forces may be written as a radial force

$$F_r = \frac{-1.5\mu\, m\, L^2}{r^4} \left(1 - 1.5 \sin^2 a\right)$$

and an azimuthal force

$$F_t = \frac{1.5\mu\, m\, L^2}{r^4} \sin a \cos a$$

where a is the libration angle in the plane of the orbit, equal to e sin nt as described above. To first order, then, the disturbing acceleration due to tether libration may be written as

$$\underline{a}_1 = \frac{-1.5\mu\, L^2}{r^4} \begin{vmatrix} \cos f + e \sin^2 f \\ \sin f\, (1_0 - e \cos f) \end{vmatrix}$$

in the e, p, h frame. The magnitude of this acceleration is thus typically on the order of 10^{-4} N/kg.

The sum of these individual disturbances is the disturbing acceleration vector to be used in the calculation of the variation of the orbital parameters.

3.3.2 Variation Equations

The equations which were used to analyze the effects of the disturbing acceleration on the orbit of the tether were the variational equations in vector form, as are described in Appendix C. These are

$$\frac{da}{dt} = \frac{2a^2}{\mu} \; \underline{v} \cdot \underline{a}_d$$

$$\frac{d\Omega}{dt} = \frac{r \sin \theta}{h \sin i} \; \underline{i}_h \cdot \underline{a}_d$$

$$\frac{di}{dt} = \frac{r \cos \theta}{h} \; \underline{i}_h \cdot \underline{a}_d$$

$$\frac{d\omega}{dt} = - \frac{\partial f}{\partial \underline{v}} \; \underline{a}_d - \cos i \; \frac{d\Omega}{dt}$$

$$\frac{df}{dt} = \frac{h}{r^2} + \frac{\partial f}{\partial \underline{v}} \; \underline{a}_d$$

$$\frac{de}{dt} = \frac{1}{\mu} \left[2 \left(\underline{v} \cdot \underline{a}_d \right) \underline{r} - \left(\underline{r} \cdot \underline{a}_d \right) \underline{v} - \left(\underline{r} \cdot \underline{v} \right) \underline{a}_d \right]$$

where the perturbative derivative of the true anomaly is

$$\frac{\partial f}{\partial \underline{v}} = \left(\frac{r}{eh^2} \right) \left[\left(\frac{h \left(\cos f + e \right)}{p} + \frac{h}{r} \right) \underline{r}^T - (p + r) \sin f \; \underline{v}^T \right]$$

and the scalar derivative of the eccentricity is

$$\frac{de}{dt} = \frac{\left(\underline{r} \cdot \underline{v} \right) \left(\underline{r} \cdot \underline{a}_d \right) + \left(pa - r^2 \right) \left(\underline{v} \cdot \underline{a}_d \right)}{\mu \; a \; e}$$

Although these equations are valid for any coordinate frame, as long as $\underline{r}$, $\underline{v}$, and $\underline{a}_d$ are consistent, it is obvious that a numerical solution using them will blow up when applied to orbits characterized by very low inclination and/or eccentricity. Of course this is because the line of nodes, and hence Ω, is undefined for zero inclination, or equatorial, orbits; similarly, ω is undefined for zero eccentricity, or circular, orbits.

4. APPLICATION OF METHODS & INTERPRETATION OF RESULTS

Each of the methods of analysis described in Section 3 were applied to a tether system using the basic computer programs included in Appendices A and B with parameters varied to achieve desired conditions of operation. The system was modelled to maintain a constant power to the load in all modes of operation. The reactions of the tether, as evidenced by variations in operating temperature and in orbital elements, when operated under varying conditions were then examined to determine if any of these operating conditions posed a problem which would make the operation of the tether, with that condition present, prohibitive.

4.1 THERMAL EFFECTS

Using the method of thermal analysis described in Section 3.2, the relative effects of certain design parameters of the tether system may be examined to determine the degree of their influence on the system's operation. Generally, these design parameters fall into two groups: first, those related to the physical tether itself, such as the surface characteristics, conductor material, diameter and length; and second, those related to the type of orbit in which the tether is operating, such as the altitude, inclination, longitude of the line of nodes, and relative position with regard to the sun.

This examination will briefly describe the relative effects of these parameters on the average operating temperature of the system, and graphically present the variations in system temperature, current level, tether resistance, magnitude of induced electromagnetic force, and system efficiency.

Prior to this, however, it is useful to examine how the properties of a typical tether vary throughout several orbits. As described in Section 3.2.1, far from being in a state of equilibrium the tether's temperature is continually changing as it orbits the earth. In a typical orbit, the variation in its operating temperature will be as depicted in Figure 15A. As can be seen, the peak temperatures occur when the greatest surface area

46

is exposed to the sun. This occurs in two places, just before and just after 'noon'. Also, as shown in Figure 15B, tether resistance follows this temperature variation. Thus, it is expected that if current is held constant, the system's efficiency will also follow this variational pattern. This can be seen in Figure 15C. If current is allowed to fluctuate, as in the case of operation as a pure generator which is required to maintain a constant load power, this fluctuation will basically follow the fluctuations in the induced voltage, shown previously in Figure 6. In this case, the efficiency tends to follow the current fluctuations.

4.1.1 Effects of Tether Parameters

Absorptance & Emittance

As can be seen from the equation listed in Section 3.2.2, the characteristics of the surface of the tether will primarily determine the operating temperature of the system.

Of the external flux which impinges on the tether, only aerodynamic heating is not a function of either absorptance or emittance. Thus, we would expect that if the tether surface was characterized by high emittance and high absorptance, then a large amount of the incoming flux would be absorbed and the tether would heat up. Conversely, the tether sheds energy by radiating it to free space; as shown before, this radiation is proportional to the surface emittance. Thus, a tether characterized by a high emittance would rid itself of heat more easily than one with low emittance. We would thus expect that the greatest operating temperatures would appear for tethers which possess a high absorptance, to absorb energy, but low emittance, to ineffectively emit energy. Similarly, the lowest average operating temperatures should occur for tethers characterized by high emittance and low absorptance.

Figure 16A shows the average operating temperatures for identical tethers with varying surface characteristics. As expected, those tethers which operate at the lowest temperatures are characterized by values of low absorptance and high emittance, while those operating at the highest

47

temperatures are those characterized by high absorptance and low emittance. The operating temperature levels are most influenced by the absorptance of the material.

It is convenient to use the trends of Figure 16A to require the tether to operate in a specific temperature range by choosing a surface material which possesses the correct characteristics to achieve the desired temperature level. As stated previously, the tether will operate more and more efficiently as the ohmic losses are reduced. Since the system power is a function of the current level, which thus cannot be reduced without also reducing this power, this is accomplished by minimizing the resistance of the conductor. The lowest resistances will occur at low temperatures, as resistivity is linearly proportional with temperature. Thus, it is desirable to cause the tether to operate at as low a temperature as possible. Choosing a surface material characterized by high emittance and low absorptance will accomplish this. Figure 16B graphically shows the characteristics of some typical dielectrics as determined by their values of absorptance and emittance. As can be seen, a good choice for the tether surface would be anodized aluminum; this will be the assumed surface in the remainder of the analysis.

Conductor Material

As discussed in Section 3.2.3, the selection of the conductor material for the tether is determined primarily by a conductance to mass comparison. Figure 12 shows this parameter for some typical conducting materials. Figure 17 compares the average operating temperature of similarly dimensioned tether made of copper. As stated before, aluminum represents the best choice for the anticipated range of tether operating temperatures, in addition to causing the tether to operate at a low temperature.

Tether Diameter

With the exception of the ohmic heat generated internally by the tether, the variation in the average operating temperature of the tether is basically independent of the tether diameter. If no current is passed

through a tether system characterized by equal parameters of absorptance and emittance, the magnitude of the temperature fluctuations will thus remain essentially constant as the diameter increases. This can be seen by rewriting the equation for the thermal balance in an abbreviated steady state form, as

$$T^4 = \frac{S}{\pi \sigma_B} + \frac{\frac{1}{2} S}{\sigma_B} + \frac{\frac{1}{2} \rho_a v^2}{a \pi \sigma_B}$$

where the solar constant is represented as S.

The temperature fluctuations due to ohmic heat generation may be evaluated by looking at the same equation and adding the term for Joule heating. If the open circuit equation listed above is defined as a constant K, then

$$T^4 = K + \frac{4 I^2 \rho}{a \sigma_B \pi^2 d^3}$$

When a constant current is allowed to pass through tethers of increasing diameters, the average temperature would be expected to decrease slowly because the Joule heating decreases as the diameter cubed.

If the tether is required to generate a constant power to the load for all diameters, then the current level must be expressed as

$$I = \frac{1}{2} \frac{V_{oc}}{R} - \sqrt{\left(\frac{1}{2} \frac{V_{oc}}{R}\right)^2 - \frac{P}{R}}$$

Consequently, the analogous expression for the temperature becomes

$$T^4 = K + Q d \left[1 - \left(1 - \frac{16 P \rho}{\pi v^2 B^2 d^2 L} \right)^{\frac{1}{2}} \right] - \frac{P}{a \sigma_B \pi d L}$$

Here

$$Q = \frac{v^2 B^2}{8 \rho a \sigma_B}$$

49

and the open circuit voltage V_{OC} has been approximated as v B L. Thus, for tethers of increasing diameters required to maintain a constant level of power to a load, the average temperature will again begin to decrease as the diameter increases.

Figures 18A and 18B show these two phenomena graphically by portraying the variation in average operating temperature versus increasing tether diameter for the cases of constant current and current required to maintain constant load power, respectively. As expected, the average temperature in both cases decreases with increasing diameter when current is passed through the tether.

Tether Length

Similar to the diameter, the length of the tether affects the amount of energy which is absorbed, the amount which is radiated away, and the magnitude of the electromagnetic force which is induced across the tether, and hence the amount of energy generated as ohmic heat. In each case, the outcome is linearly proportional to this length. By referring to the equations discussed in the previous section, it can be seen that a tether of arbitrary length would be expected to experience basically the same changes in temperature as a tether of different length, which moves in an identical orbit, for the same level of current. The overall average operating temperature is independent of variations in length, as the increased amount of energy absorbed and generated internally will be offset by the increased amount radiated away. Thus, the average operating temperature versus length for a tether with all other variables remaining constant is itself a constant.

Obviously, as the induced voltage across the tether grows in magnitude with increasing length, more ohmic heat will be generated (providing that the current level is not inhibited from increase and that all other variables, in particular the load impedance, are held constant) and the operating temperature will rise. It must be noted that the tether power increases approximately as L^2 under these conditions, however. Figure 19 illustrates the converse of this by comparing the variation in operating

50

temperature versus increasing length for a tether required to maintain a constant power level to the load for all lengths; when operated in this manner, only progressively decreasing levels of current are allowed to pass through the system, driving the average operating temperature lower.

4.1.2 Effects of Orbital Parameters

Altitude

Variation in the operational altitude of the tether system will affect both the orbital velocity, as $v = \sqrt{\frac{\mu}{r}}$ for a circular orbit, and the magnetic field strength, which is inversely proportional to the cube of the orbital radius. Thus, the total effect on the induced voltage across the tether will go as $r^{-3.5}$. As the ohmic heat generated by passing current is proportional to the square of the induced voltage, an increase in altitude from a 300 km to a 500 km orbit will correspond to an approximately 19% decrease in internally generated heat.

Increasing altitude will also affect the incoming flux which the tether receives. The effect on solar radiation is basically negligible, as the tether remains in the sunlight for only a slightly longer period of time, approximately .01%, for a 300 km versus a 500 km orbit, and the magnitude of the solar constant is unchanged for such a slight altitude variation. The other incoming fluxes are more severely affected, however. The albedo flux and earth radiation flux are both dependent on the earth view factor, as previously defined in Section 3.2.2. This factor decreases by approximately 15% from a 300 km to a 500 km orbit. The aerodynamic heating is dependent on the atmospheric density and the relative velocity at the operational altitude; the density decreases by approximately 97%, and the relative velocity decreases by approximately 2%, from a 300 km to a 500 km orbit. Thus, the overall affect on aerodynamic heating is a decrease of approximately 97%. Radiation from the tether, on the other hand, is independent of the altitude of the orbit (assuming that the background temperature at both 300 km and 500 km is the same).

51

The net effect then is that the tether will operate at lower temperatures as the orbital altitude is increased. This is graphically portrayed in Figure 20, showing the average operating temperature versus altitude. While it was stated previously that it is desirable to cause the tether to operate at low temperatures in order to minimize ohmic losses in the system, this is correct only for a constant altitude. It must be remembered that the magnitude of the power which the tether is capable of generating is also inversely proportional to the orbital radius raised to the seventh power.

Orbital Inclination

The most significant effect of the orbital inclination is on the magnitude of the induced voltage across the tether. At 0° inclination, the velocity vector of the tether is perpendicular to the magnetic field, thus maximizing the induced voltage. Similarly, in a polar orbit, or an inclination of 90°, the velocity is parallel to the magnetic field and no voltage is induced. Because the induced voltage is calculated as the cross product of $\underline{v}$ and $\underline{B}$, the magnitude of the induced voltage varies as cos i (assuming a rigid tether aligned with the vertical).

The operating temperature of the tether is relatively insensitive to changes in the orbital inclination, with none of the energy inputs being significantly affected. With regard to solar radiation, the orbital inclination primarily changes the amount of surface area of the tether which is exposed to the incoming flux, and hence how much energy is instantaneously absorbed; however, the average over the course of an orbit is independent of the inclination. With regard to earth radiation and albedo, it primarily changes the amount of incoming energy because of variations in cloud cover, surface conditions of snow and ice, and water covered areas. In low inclination orbits, which are the only feasible ones for a tether system because of the decrease in induced voltage at high inclinations, typical variations between 0° and 28.5° are approximately a 6% increase for earth radiation and albedo flux, and a 3% increase for aerodynamic heating.

52

Longitude of the Line of Nodes

It would be expected that the longitude of the line of nodes of the orbit would have little effect on the temperature of the tether. The only variable which it affects is the flux due to solar radiation by varying the magnitude of the surface area of the tether which is exposed to the incoming flux. Typically, shifting the line of nodes by 90°, from a line perpendicular to the earth-sun radius to a line parallel to this radius, will cause a decrease of approximately 68% in the solar radiation absorbed.

It can be seen from Figure 22 that even this decrease in the solar flux has little effect on the operating temperature, acting only to slightly decrease the average temperature and limiting the amplitude of modulation. Both cases shown here are with the ecliptic and equatorial planes aligned. Figure 21A represents the tether in a circular orbit with the line of nodes oriented perpendicular to the earth-sun line; it is this orientation which exposes the tether to the largest incoming flux during the course of its orbit. The average temperature in this orientation is approximately 215° K, with temperature ranges over 35°. Figure 21B represents an orbit with the line of nodes shifted by 90° so that it is aligned to the earth-sun line. Now the average temperature is slightly lower, as expected, at approximately 205° K with a temperature range of 20°.

Seasonal Variations

Seasonal variations, meaning fluctuations due to the position of the earth in its orbit about the sun, are generally of two types. First, the magnitude of the solar flux, as measured at the earth, varies because of the eccentricity of the earth's orbit. Second, the tilt of the earth's rotational axis to the ecliptic causes the angle between the earth-sun line and the equator to vary between ± 23.5°. The first of these affects all of the external fluxes except for aerodynamic heating, while the second affects only the solar radiation flux. However, the magnitude of the variations is small enough so that it would be expected that the operating temperature of the tether will not be altered significantly.

53

Typically, the solar flux varies by approximately 3% throughout the year, while the sun angle causes variations in the solar radiation flux of approximately 9%.

Since the variations in the solar flux are much less than they were for changes in the line of nodes, it is anticipated that the operating temperature of the tether would be affected very little by seasonal changes. Figures 22 show this to be the case. The three figures presented represent the tether at the summer solstice (approximately aphelion), at the winter solstice (approximately perihelion), and at the vernal equinox. Only very small variations in the average temperature and the range of temperatures are discernible between the three graphs.

4.2 VARIATIONS OF ORBITAL ELEMENTS

The manner in which the tether is operated, i.e. as a power generator, thruster, or a combination of the two, may affect the elements of the orbit in which it begins its operation. This is because the production of the induced electromagnetic drag and/or thrust force may not always be constant throughout the orbit, nor may it always lie in the orbital plane. Indeed, it is typical that neither of these two conditions will be true.

This examination will use the method described in Section 3.3 to analyze the variation of the orbital elements for the cases of the tether orbiting but not passing any current, for the pure generator mode, for the pure thruster mode, and finally for the case of the tether generating power when in the earth's shadow and thrusting when in sunlight.

The orbital elements which are looked at are the semi-major axis, which corresponds to the energy in the orbit, the eccentricity, the longitude of the line of nodes, the orbital inclination, and the argument of pericenter. These are calculated as described in Section 3.3.2. Thus, the variation of the semi-major axis and the eccentricity are affected only by the components of the disturbing acceleration in the orbital plane, the variation of the longitude of the line of nodes and the orbital

54

inclination are affected only by the out-of-plane component, while the argument of pericenter varies with both in and out-of-plane forces. These may be conveniently illustrated by writing these variational equations as

$$\frac{da}{dt} = \frac{2a^2}{\mu} \, \underline{v} \cdot \underline{a}_d$$

$$\frac{d\Omega}{dt} = \frac{r \sin \theta}{h \sin i} \, \underline{i}_h \cdot \underline{a}_d$$

$$\frac{de}{dt} = \frac{1}{\mu ae} \left[\left(\underline{r} \cdot \underline{v} \right) \left(\underline{r} \cdot \underline{a}_d \right) + \left(pa - r^2 \right) \left(\underline{v} \cdot \underline{a}_d \right) \right]$$

$$\frac{di}{dt} = \frac{r \cos \theta}{h} \, \underline{i}_h \cdot \underline{a}_d$$

$$\frac{d\omega}{dt} = \frac{-r}{eh^2} \left[\left(\frac{h \, (\cos f + e)}{p} + \frac{h}{r} \right) \underline{r}^T - (p + r) \sin f \, \underline{v}^T \right] \underline{a}_d - \cos i \, \frac{d\Omega}{dt}$$

For this analysis, initial conditions were arbitrarily selected for a 400 km orbit of 28.5° inclination, with the line of nodes perpendicular to, and the line of apsides parallel to, the earth-sun line. The orbit was specified as near-circular, with a finite eccentricity of .01. The tether itself was specified as an aluminum conductor, 3 mm in diameter and 20 km long. The total mass of the system, tether and sub-satellite, was specified as 25000 kg.

4.2.1 Open Circuit Operation

In the open circuit operation, no current is allowed to pass through the tether; hence, no electromagnetic force is produced. Therefore, the disturbing acceleration acting on the tether is composed only of aerodynamic, gravitational, libration, and solar radiation specific forces, and the tether system is effectively just another earth-orbiting satellite. Each element of the disturbing acceleration has both in and out-of-plane components, with the exception of the libration specific forces which act only in-plane because of our first order approximation. As described in Section 3.3.1, the dominant element of these is the contribution due to the earth's oblateness. The other components cause intra-orbital fluctuations in the orbital elements, and can have definite long-term effects on the orbit, but in the short-term generally do not appreciably perturb the shape of the orbit.

55

To make an initial estimate of the effect of this disturbing acceleration on the orbital elements, it is convenient to use Gauss' planetary equations (the derivation of which is included in Appendix C, for a coordinate frame with radial, tangential, and normal components) and linearize them by assuming that the eccentricity of the orbit is small. When this done, Gauss' variational equations become

$$\frac{d\Omega}{dt} = \frac{h}{\mu \sin i} \left[(\sin \omega \cos f + \cos \omega \sin f)(1 - e \cos f) \right] a_n$$

$$\frac{di}{dt} = \frac{h}{\mu} \left[(\cos \omega \cos f - \sin \omega \sin f)(1 - e \cos f) \right] a_n$$

$$\frac{d\omega}{dt} = \frac{h}{\mu} \left[-\frac{\cos f}{e} a_r + \left(\frac{2 \sin f}{e} - \frac{\sin 2f}{2} \right) a_t - \cot i \left(\sin \omega \left(\cos f - \frac{e}{2} - \frac{e \cos f}{2} \right) + \cos \omega \left(\sin f - \frac{e \sin 2f}{2} \right) \right) a_n \right]$$

$$\frac{da}{dt} = \frac{2a^2}{h} \left[e \sin f \, a_r + (1 + e \cos f) \, a_t \right]$$

$$\frac{de}{dt} = \frac{h}{\mu} \left[\sin f \, a_r + \left(2 \cos f + \frac{e}{2} - \frac{e \cos 2f}{2} \right) a_t \right]$$

The representation of the disturbing acceleration due to the earth's oblateness is indicated in *Appendix B. The vector components for this* axially symmetric representation may be written as

$$a_r = A \left(3 \sin^2 i \sin^2 \theta - 1 \right)$$

$$a_t = - A \sin 2i \sin 2\theta$$

$$a_n = - A \sin 2i \sin \theta$$

where $A = \dfrac{3\mu \, J_2 \, r_e^2}{2 \, r^4} = .01247 \dfrac{m}{s^2}$ (for a 400 km earth orbit)

When these are substituted into the variational equations, the mean variational rates of the orbital elements may be calculated. Doing this, with values for the orbit of our system, indicates that the inclination, semi-major axis, and eccentricity remain essentially constant throughout an orbit, while the longitude of the line of nodes and the argument of pericenter vary as

$$\left\langle \frac{d\Omega}{dt} \right\rangle = -7.1 \text{ degrees/day}$$

and

$$\left\langle \frac{d\omega}{dt} \right\rangle = 11.5 \text{ degrees/day}$$

These average secular variations in Ω and ω are classically referred to as the regression of the node, and the precession of the argument of perigee, respectively. For an earth orbiting satellite, the magnitudes of these average variations may also be calculated directly from the disturbing function associated with the earth's gravitational field and expressed as

$$\left\langle \frac{d\Omega}{dt} \right\rangle = -9.96 \frac{\left(\frac{r_e}{a}\right)^{3.5} \cos i}{\left(1 - e^2\right)^2}$$

and

$$\left\langle \frac{d\omega}{dt} \right\rangle = 5 \frac{\left(\frac{r_e}{a}\right)^{3.5} (5 \cos^2 i - 1)}{\left(1 - e^2\right)^2}$$

which corroborate the estimates calculated previously.

Figures 23 depict the variations of the orbital elements over an 8 day period. As can be seen, the mean variations are essentially as anticipated above, with intra-orbital fluctuations superimposed onto the mean. The slight decrease in the eccentricity and in the semi-major axis with time may be attributed to the effects of aerodynamic drag as it takes energy from and begins to circularize the orbit. All satellites in orbits identical to the tether system will experience variations in their orbit exactly as the tether in the absence of the electromagnetic force. When current is permitted to flow through the tether, the variations caused by it will be superimposed on the base variations.

4.2.2 Pure Mode Operation

As stated above, the only difference between pure mode operation and open circuit operation is the addition of the induced electromagnetic force to the disturbing acceleration. When operated in only a single mode, the components of the electromagnetic force are cyclic with the true anomaly. Assuming that the tether remains vertical, these may be approximated as

$$a_r = 0$$
$$a_t = B (C + \cos 2f)$$
$$a_n = D \sin f$$

where $B = \pm 3.635 \times 10^{-6} \frac{m}{s^2}$ (positive for thrusting)

$C = 15.504$

$D = 1.735 \times 10^{-6} \frac{m}{s^2}$

It can be seen that the electromagnetic force dominates in the tangential direction, while the oblateness effects continue to dominate in the radial and normal directions. When these accelerations are added to those which are present before the current is passed, and the sum is substituted into the variational equations as before, the mean variational rates which are to be expected when the tether is operated in a single mode are

$$\left\langle \frac{di}{dt} \right\rangle = \pm .01 \text{ degrees/day} \quad \text{(negative for thrusting)}$$

$$\left\langle \frac{d\Omega}{dt} \right\rangle = -7.1 \text{ degrees/day}$$

$$\left\langle \frac{da}{dt} \right\rangle = \pm 5.2 \text{ km/day} \quad \text{(positive for thrusting)}$$

$$\left\langle \frac{de}{dt} \right\rangle = 0$$

$$\left\langle \frac{d\omega}{dt} \right\rangle = 11.5 \text{ degrees/day}$$

Not surprisingly, the elements all essentially vary as they do for an ordinary satellite with the exception of the semi-major axis, which increases as energy is added when the tether is operated as a thruster and decreases when it is operated as a generator, and the orbital inclination, which varies in the opposite manner. The eccentricity also actually varies slightly, but not to noticeable magnitudes.

Figures 24 and 25 verify these expectations. Reviewing the graphs of the variations of the orbital elements for a pure generator operation as depicted in Figures 24, and a pure thrusting operation as depicted in Figures 25, it can be seen that the orbital inclination does display a finite change with time, and the semi-major axis and perigee altitude

58

change dramatically in response to the operational mode. As before, there are intra-orbital fluctuations superimposed onto the mean variations; the magnitude of the amplitudes of these fluctuations does not appear significantly different from those calculated before the emf was added. No significant variations, beyond those which were anticipated, are apparent in the other orbital elements over the 8 day period.

4.2.3 Mixed Mode Operation

Mixed mode operation is characterized by alternately causing the tether to generate and thrust throughout the course of its orbit, the purpose of which is to maintain the average energy of the orbit, and thus the semi-major axis, at an approximately constant level. The result of this is a continual variation in the direction of the disturbing acceleration. This acts to intensify the variations in the orbital elements as the tether completes an orbit.

Since the disturbing acceleration due to the induced electromagnetic force varies throughout the orbit, and not as a function of the true anomaly, an analytical approach via Gauss' equations as before does not seem appropriate. Although the induced forces may be generally considered as being continually applied throughout the orbit, it is convenient for a simple analysis to consider them as impulsive forces applied at the perigee and apogee of the orbit. Thus, if the operating mode being considered is one in which the energy of the orbit is being held constant by generating power, or extracting energy from the orbit, in the earth's shadow, and injecting an equal amount of energy into the orbit by thrusting when in sunlight, then we can consider this as a finite force applied in the direction of velocity on the sunlight side of the orbit, and an equal but opposite force applied on the shadow side. If the orbit is initially specified as being characterized by a small, finite eccentricity vector pointing toward the sun and parallel to the earth-sun line, then this operating mode is similar to that of applying an impulsive Δv in the direction of the orbital velocity at perigee, and applying a second, but equal, one opposite the orbital velocity at apogee. The maneuver at perigee would be expected to add energy to the orbit, and consequently increase the semi-major axis and apogee height, while the

59

apogee maneuver would subtract energy, and consequently decrease the semi-major axis and the perigee height. The cumulative effect of this alternately thrusting and generating is to increase the eccentricity of the orbit as the altitude of perigee decreases and the altitude of apogee increases. The other orbital elements are unaffected by this type of operation, except as they are influenced by the remainder of the components of the disturbing acceleration, just as was described in the previous two sections.

Figures 26 graphically illustrate this phenomenon by portraying the variations of each of the orbital elements over an 8 day period when operated in the mixed mode described above. As can be seen the variations in the argument of perigee and in the longitude of the line of nodes remain essentially as was determined for the open circuit mode of operation. The variation in the semi-major axis may be attributed to an imbalance between the amount of time that the tether is caused to generate power versus the amount that is caused to thrust. Generally, it may be observed that it experiences no significant change since the energy of the orbit remains essentially constant. The eccentricity, and unexpectedly the orbital inclination, however, increase relatively rapidly over the time period considered. If the rate of eccentricity change is extrapolated form this 8 day period, it indicates that after approximately 85 days the tether will descend to a level at which the perigee will be low enough to cause the tether to re-enter the atmosphere. Fortunately, this does not appear to be precisely the case, as will be shown shortly; however, this type of operation will still be prohibitive in and of itself.

Using the type of simple analytical approach as before to develop a solution to this problem erroneously leads one to a mode of operation in which the tether, initially inserted into an orbit which has its perigee opposite the sun, still generates power throughout the shadow period, but thrusts to make up the orbital energy loss only in the vicinity of the line of nodes. While it would appear that the effect of this operating technique is to continually lower the apogee height while maintaining the

semi-major axis constant over the course of each orbit, when this technique is simulated the eccentricity of the orbit still displays a rapid increase, as before, and the system rapidly gets low enough to re-enter the atmosphere. In fact, this increase in eccentricity was evident in every other scheme which could be devised for operating the tether in mixed mode. This is evidently a problem for which there is no intrinsic solution; if the tether is to be operated in this manner, compensation for the eccentricity increase will have to be externally provided.

If the power to mass ratio of the system is increased, by increasing the current level and/or decreasing the system mass, the saturating effects of the eccentricity variation may be observed. When this is done with the system current and mass specified at different levels, it can be seen in Figure 27 that the increase in the eccentricity is actually more sinusoidal than linear, with a maximum amplitude of .08 and a period of approximately 165 days when referred back to the original system specifications. The cause of this saturating effect is due to the simultaneous variations in the longitude of the line of nodes and the argument of perigee, caused by the earth's oblateness. However, as an eccentricity in excess of approximately .04 insures that the system will re-enter the atmosphere before the orbit re-circularizes, the magnitude of this amplitude still makes the use of the mixed mode of operation prohibitive for a tether system which utilizes a constant current without an external system dedicated to compensate for the eccentricity increase.

5. CONCLUSION

5.1 SUMMARY

Within the constraints of the assumptions which were made to conduct this analysis, several conclusions may be drawn. Some of them are perfectly obvious, while others are somewhat unexpected.

First, the tether may be operated in an uninsulated fashion as well as an insulated one. The insulated mode must face the problems of arcing and dielectric degradation due to the tether's operational environment, in addition to leakage losses of comparatively large magnitudes through any holes which are present in the insulating jacket. The uninsulated mode must face current leakages along the tether's length on the order of 10% plus some minor degradation of the conductor itself due to sputtering. The surprising result is that the tether need not actually be fully insulated against the surrounding plasma in order to operate; however, this type of operation would be done at the expense of the current leakage as described in Section 3.1, and over wider operating temperature ranges because of the relatively shiny conductor surface as described in Section 4.1.1. The use of anodized aluminum as the dielectric coating for the conducting material of the tether appears to be an attractive solution to both types of problems. It is characterized by high dielectric strength, durability, high emittance and low absorptance. Its use as an insulator certainly merits further theoretical and experimental analysis.

The operating temperature of the tether is determined primarily by its values of absorptance and emittance. It is not significantly affected by tether length, nor by tether diameter once a certain minimum is reached. To operate at low temperatures, and hence at low tether resistances and higher efficiencies, higher ratios of emittance to absorptance must be achieved by properly selecting the surface material of the tether. In general, the operating temperatures range by ± 20 degrees about the average, determined by the surface characteristics, over the course of each orbit. Changes in the orbital elements, for near circular orbits, and seasonal variations, as the earth orbits the sun, do not generally

change the average operating temperature, but only modulate the intra-orbital temperature range. As would be expected, tether resistance basically follows temperature variations, while current flow and induced force basically follow the magnitude of the induced potential across the tether. Efficiency is affected by both temperature and current, generally being inversely proportional to current.

The type of operation in which the tether system is employed can affect the variation of the orbital elements over time. The open circuit mode, generator mode, and thruster mode present no surprises. As anticipated, the only variations present when no current flow is permitted are those due primarily to the earth's oblateness, causing precession of the argument of pericenter and regression of the line of nodes, but only negligibly small effects on the other orbital elements. Also as anticipated, the generator mode, in addition to the variations present in the open circuit mode, causes the semi-major axis to dramatically decrease as the orbital energy of the tether is transformed into on-board power. Similarly, the semi-major axis increases rapidly in the thruster mode as energy is added to the orbit by the tether's operation. Surprisingly, in both modes the orbital inclination make small but detectable changes, increasing in the generator mode and decreasing when thrusting. Beyond this, the other orbital elements show no other significant variations beyond those evident in the open circuit mode. In mixed mode, however, while the semi-major axis, and hence the orbital energy, can be held constant when averaged over an orbit, it appears impossible when operating with a constant current to preclude an increase in orbital eccentricity to the extent that perigee is soon low enough for the tether to re-enter the atmosphere. This effect may be mitigated by operating with a low system power-to-mass ratio, which slows the rate of this increase to what are probably tolerable levels.

5.2 RECOMMENDATIONS

All of this analysis has been on the basis of several simplifying assumptions. Essentially, two types were made: those assumed because it is known that the assumption is a good one, either because parameters neglected are small, linearization was desired for simplicity, or models

used have been shown to be accurate representations; and those assumed because to date there is no definitive information available which can be used to produce a more accurate model for the analysis. The former group includes, among others, the assumptions of the tether modelled as a rigid body composed of point masses, and the mathematical models of the earth's magnetic field, mass distribution, ionospheric composition, and air density. The latter group primarily includes those made to produce the simplified electrical circuit to model the tether system, and to neglect any dynamic effects of the tether's operation, such as oscillations and deployment. Because of the lack of any actual experimental or flight data, most of what is available in these areas is theory; its accuracy is the subject of significant debate. It is on these subjects that more extensive research, coupled with actual flight testing, should be dedicated to determine if the model which as been used here is adequate or must be modified to produce accurate results.

The main assumptions which have been made regarding the system's circuit path are the following: the impedance of the ionosphere is negligible; the potential drop across each contactor which is required to permit sufficient current to flow through the circuit is relatively small, on the order of 100 volts as assumed here, compared to the total induced potential across the tether; and the properties of anodized aluminum are such that the tether would be essentially impervious to sputtering and current leakage, while possessing the required characteristics of absorptance and emittance. Those made regarding dynamics are that the deployment of the tether from the base satellite may be accomplished with little difficulty, and the tether will remain deployed permanently; and that the dynamics of the tether motion, particularly resonance with the out-of-plane oscillation frequency, do not pose a problem to the system's operation. If the impedance of the ionosphere is much more than the few ohms which were assumed in the discussion of Section 2.2.1, then the efficiency of the system, and hence its ability to compete with other power generation systems, will drop below what may be considered an acceptable level. Similarly, if the potential drops across the anode and/or cathode, which must be developed in order to pass sufficient

64

current through the tether to reach the desired levels of power generation, become so large that they also drive the overall efficiency of the system below acceptable levels, then the system will not be competitive. Obviously, if the tether itself cannot be deployed because of dynamical difficulties, or cannot be kept in operation without excessive oscillations, then the system will be physically impossible to employ. Finally, if a suitable dielectric cannot be found which possesses the necessary qualities of high emittance, low absorptance, high dielectric strength, and resistance to the operational environment, then it will be necessary to accept the additional losses incumbent on operating as an uninsulated conductor.

Manifesting an experiment on a shuttle flight, as is currently scheduled in the form of the TSS, should provide answers to most of these questions. On smaller scales, the magnitude of the impedance of the ionosphere and contactors could be determined, as well as the motions of the tether once it is deployed and in operation. Deployment schemes would have to be exercised, as well as the additional, and probably greater, problems involved in retrieval. Prior to actual flight testing, further research, both experimental and theoretical, should be devoted to the feasibility of using anodized aluminum as a dielectric coating for the conductor, and to the development and testing of newer and more efficient contactor configurations.

FIGURE 1

EQUIVALENT CIRCUIT
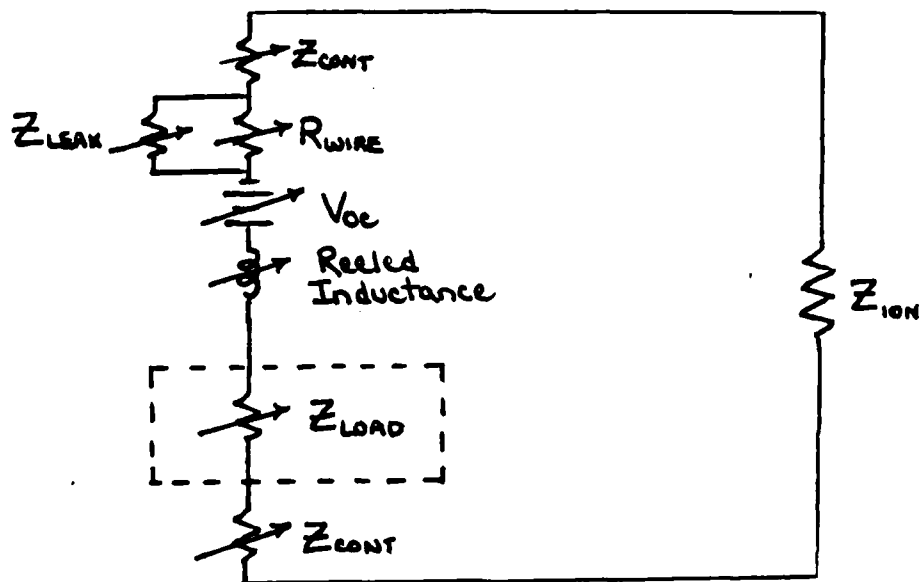
** Generally, 4 Groups of Impedances **

1) Load
2) Wire
3) Contactors
4) Ionospheric Plasma

FIGURE 2

— ELECTRON COLLECTOR (OR ION EMITTER) CAN BE

PASSIVE LARGE SURFACE (BALLOON)

- NEED 20,000$^+$ m^2
- HEAVY
- LARGE DRAG

PASSIVE GRID

- THIN INDIVIDUAL WIRES
- LIGHT
- LOW DRAG
- ΔV_A CAN BE LOW

HOLLOW CATHODE (AS ANODIC PLASMA BRIDGE)

- NEEDS GAS FEED
- ELECTRONS CONDUCTED INWARDS
  THROUGH PLASMA
- POTENTIALLY EFFICIENT

LIGHT ION EMITTER

- SIMILAR TO ION ENGINE, BUT
  LOW ACCELERATOR VOLTAGE
- NO NEUTRALIZER EITHER
- POTENTIALLY EFFICIENT
- EXISTING, NEEDS ADAPTATION
- NEARLY INDEPENDENT OF OUTSIDE PLASMA DENSITY (ONLY ONE)
- HIGH IONIZATION FRACTION

ANODES

gas
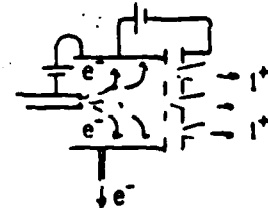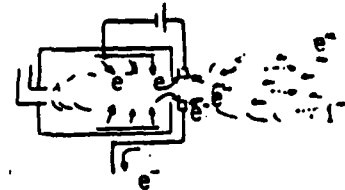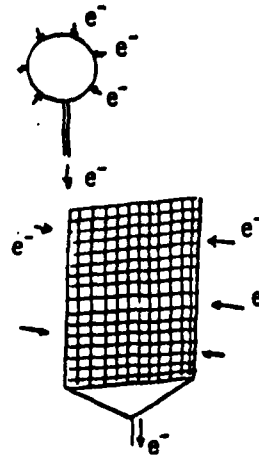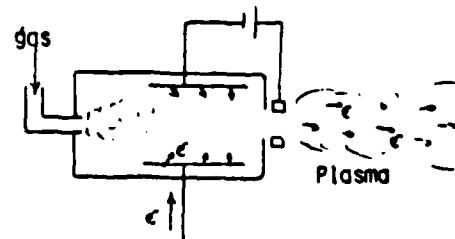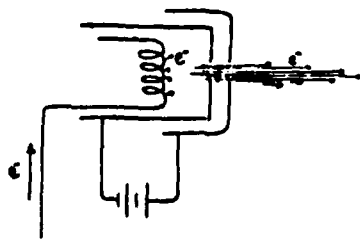
Plasma

E. GUN

- NO MASS FLOW
- ELECTRONS ACCELERATED TO
  1-5 KV
- EXISTING TECHNOLOGY
- INEFFICIENT (HIGH ΔV_C)

HOLLOW CATHODE

- NEEDS GAS FEED
- ELECTRONS CONDUCTED THROUGH
  PLASMA CLOUD
- LOW ΔV_C, EFFICIENT
- EXISTING, NEEDS DEVELOPMENT

FIGURE 3

Electron density vs. elapsed time   (300 Km orbit)
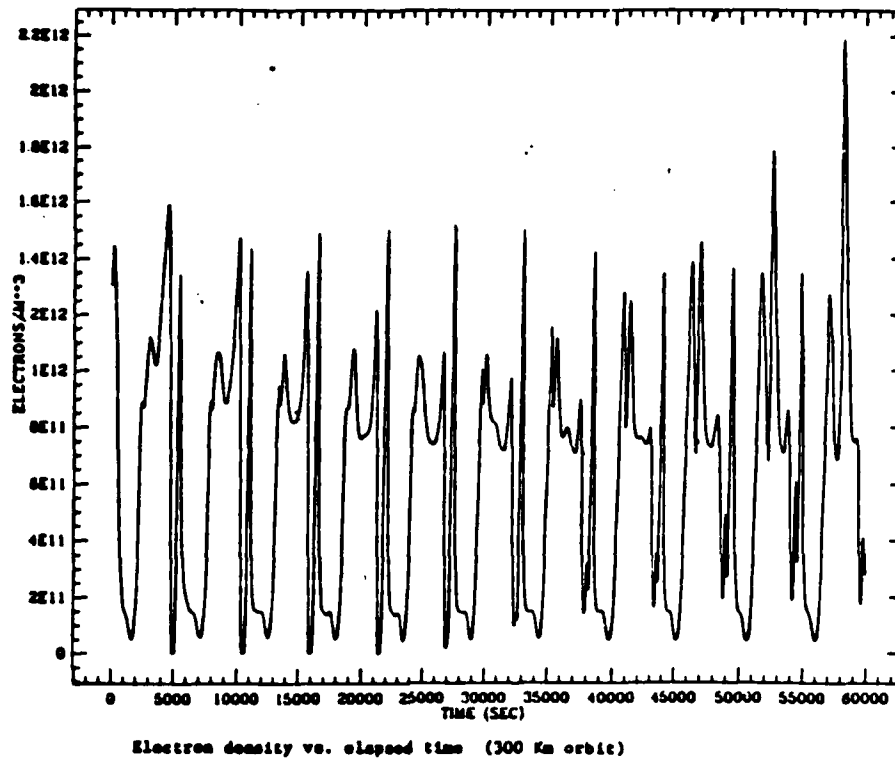
FIGURE 4

REVISED CIRCUIT

68

FIGURE 5A

INDUCED VOLTAGE
Dipole Model

FIGURE 5B

INDUCED VOLTAGE
Octopole Model

69

FIGURE 6

VOLTAGE VARIATIONS
Expanded Spherical Harmonics Model

70
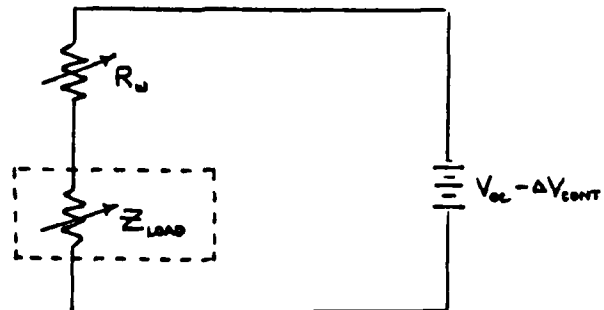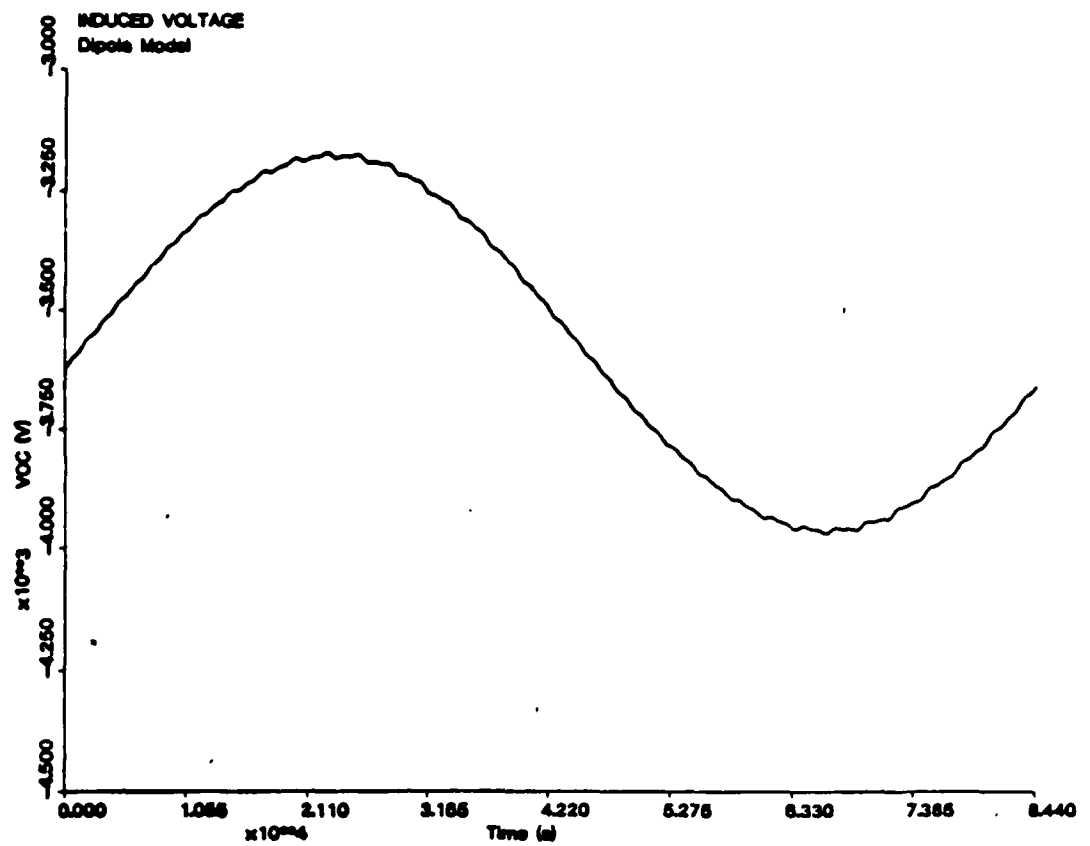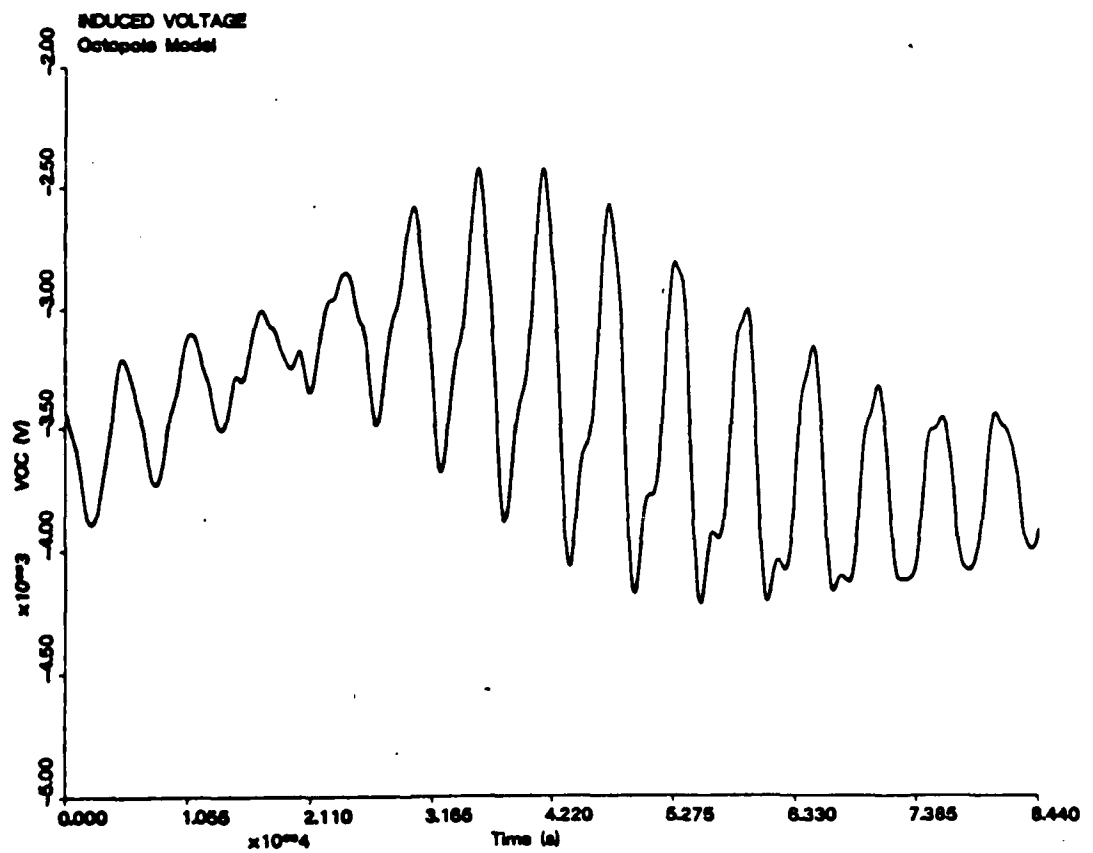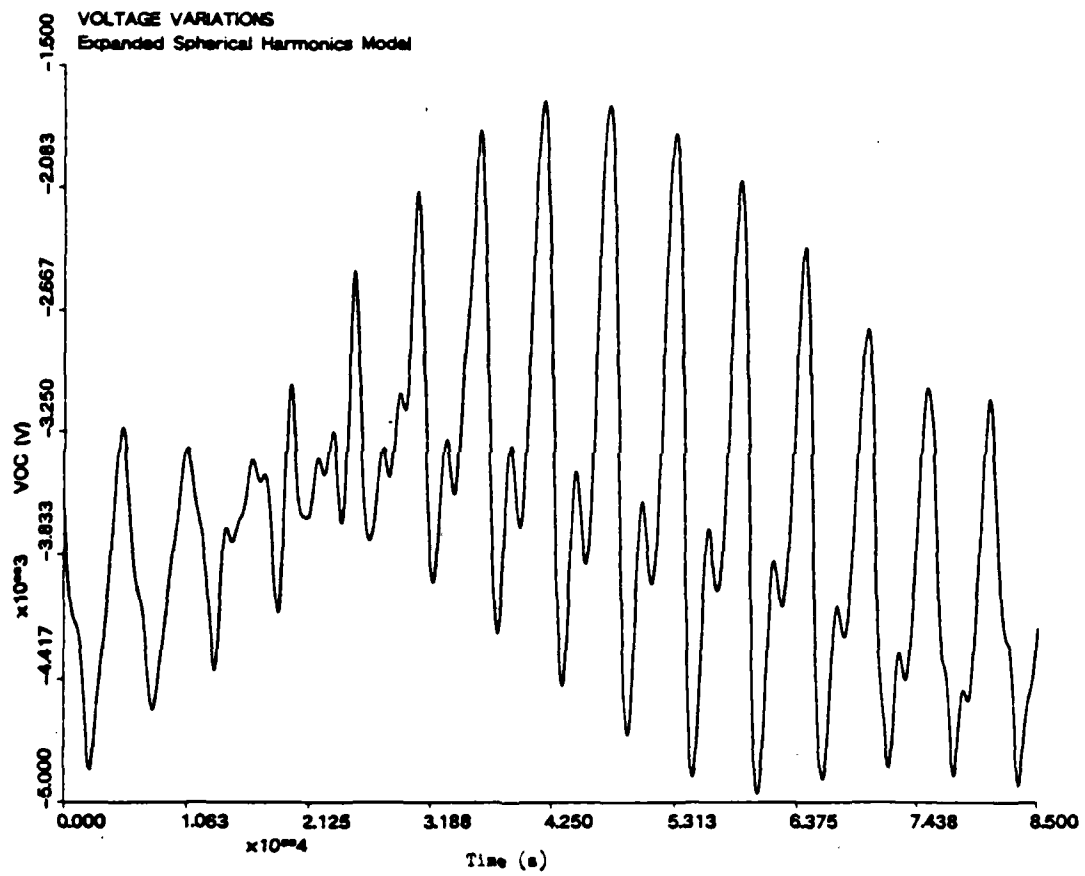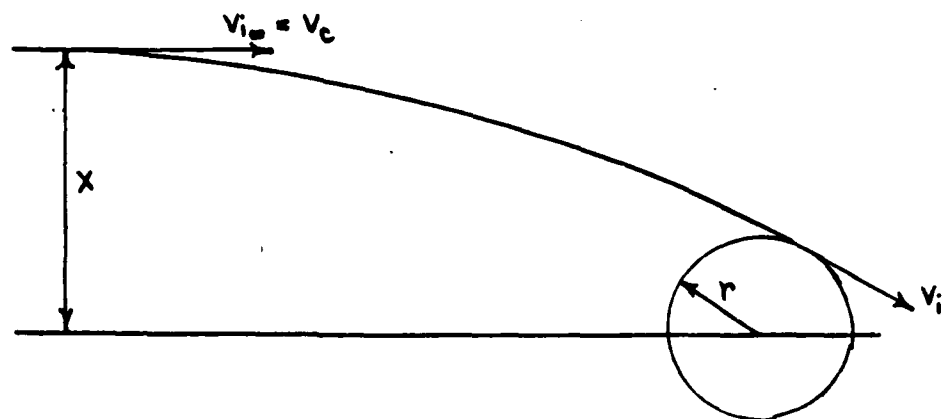
FIGURE 7

MOMENTUM BALANCE FOR
ION CAPTURE

FIGURE 8
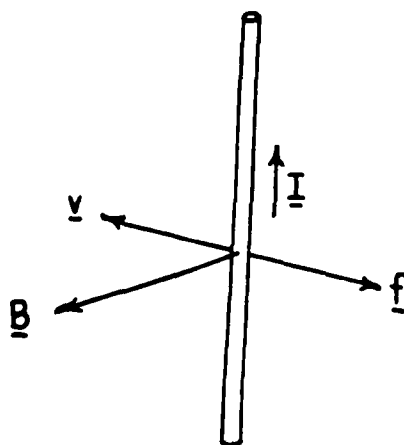
CURRENT DIRECTION IN
GENERATOR MODE
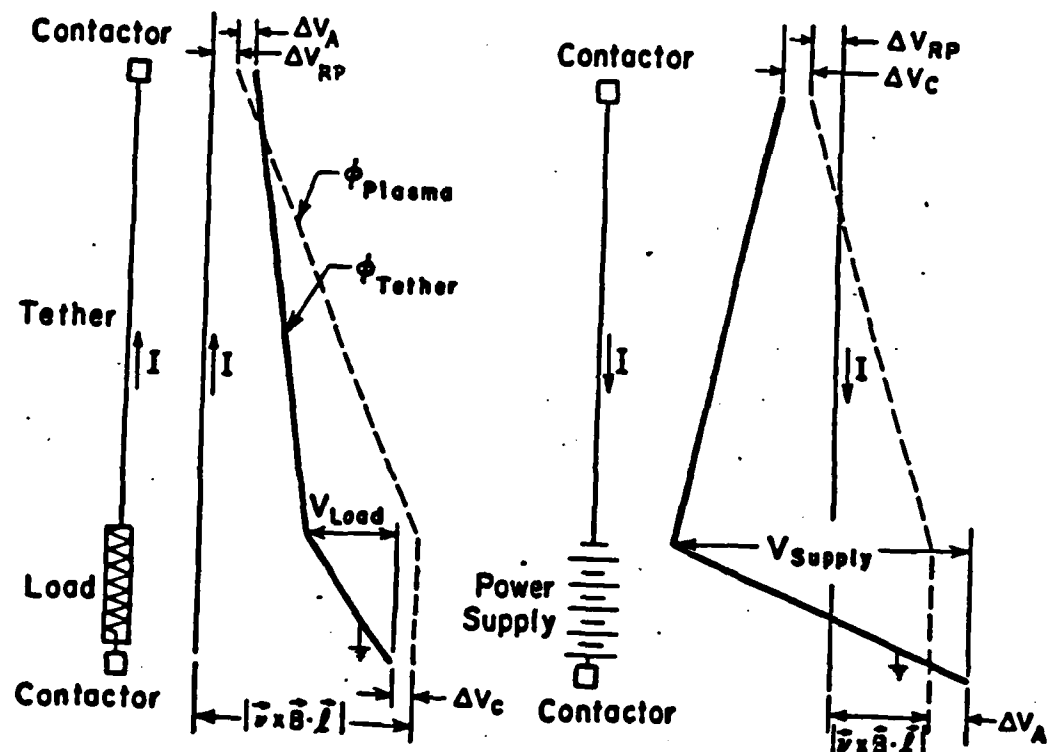
FIGURE 9

A   Potential diagram for
tether as a generator. Load at
bottom, tehter deployed upwards

B   Potential diagram for
tether as a thruster, with power
supply at bottom (tether deployed
upwards)

72
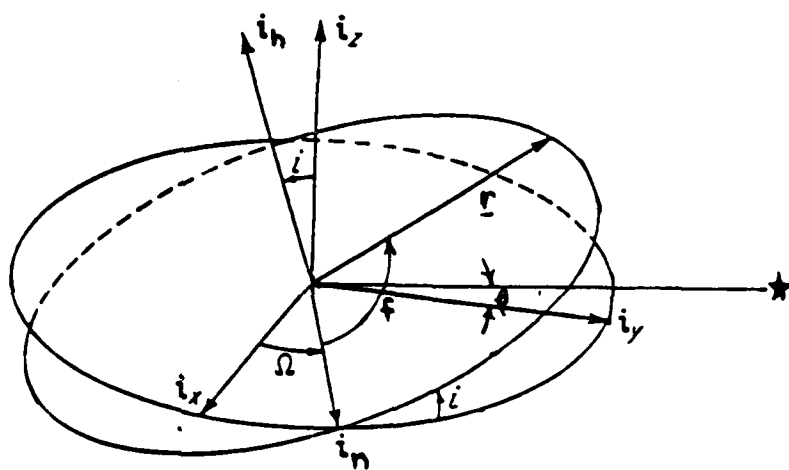
FIGURE 10

ROTATION ANGLES

FIGURE 11-3

CURRENT VARIATIONS
3.25mm Tether

FIGURE 11-4

FORCE VARIATIONS
3.25mm Tether

FIGURE 11-5

EFFICIENCY VARIATIONS
3.25mm Tether

FIGURE 12

CONDUCTANCE/MASS COMPARISON

76
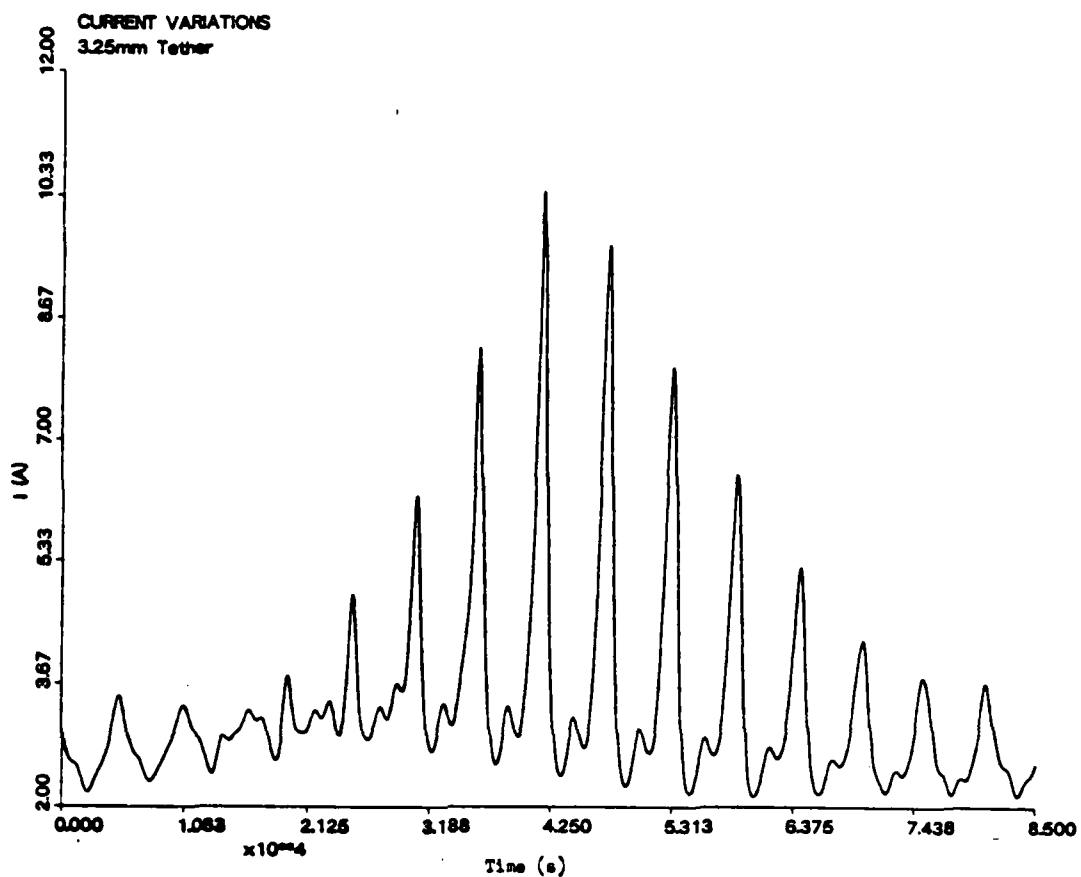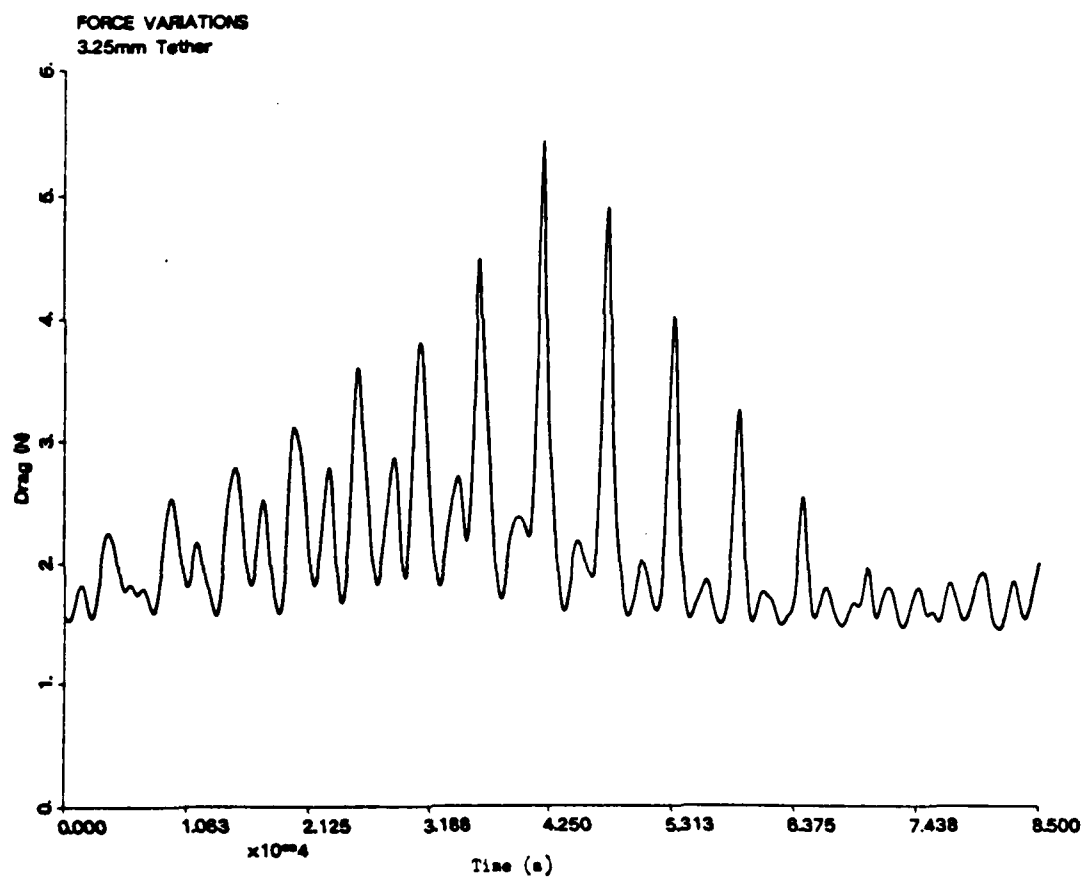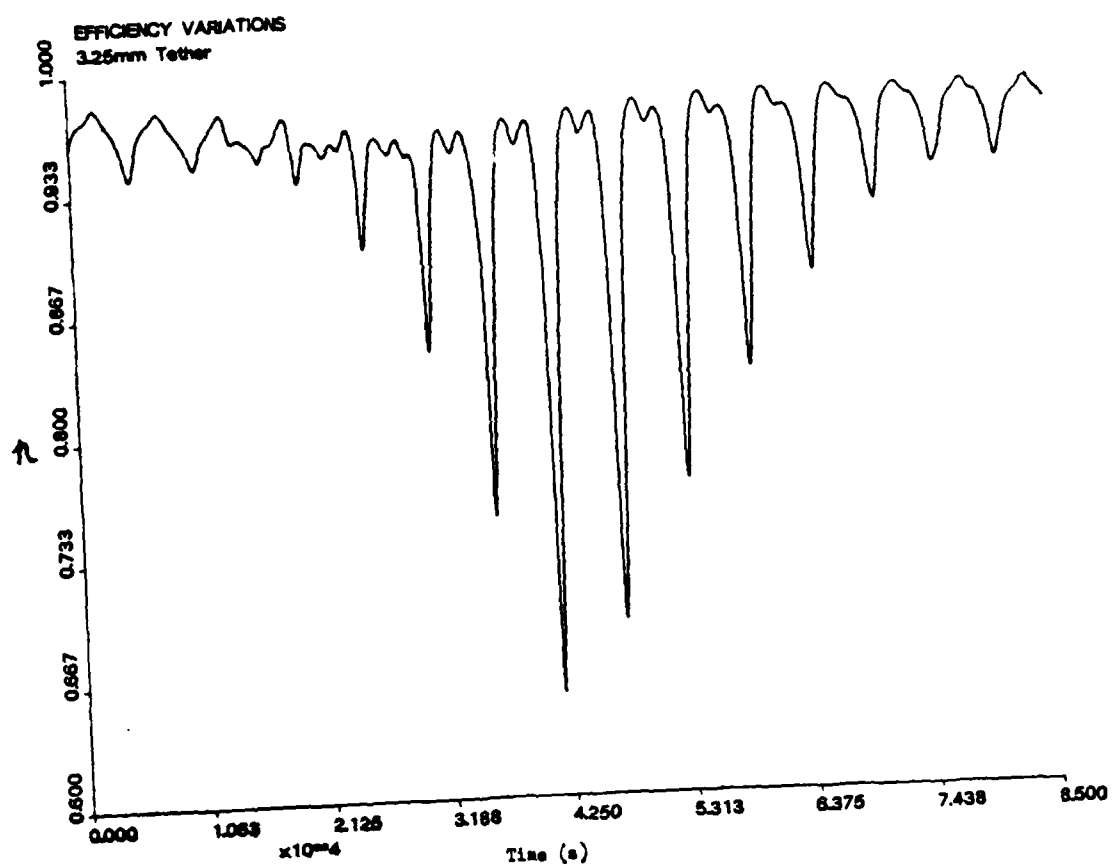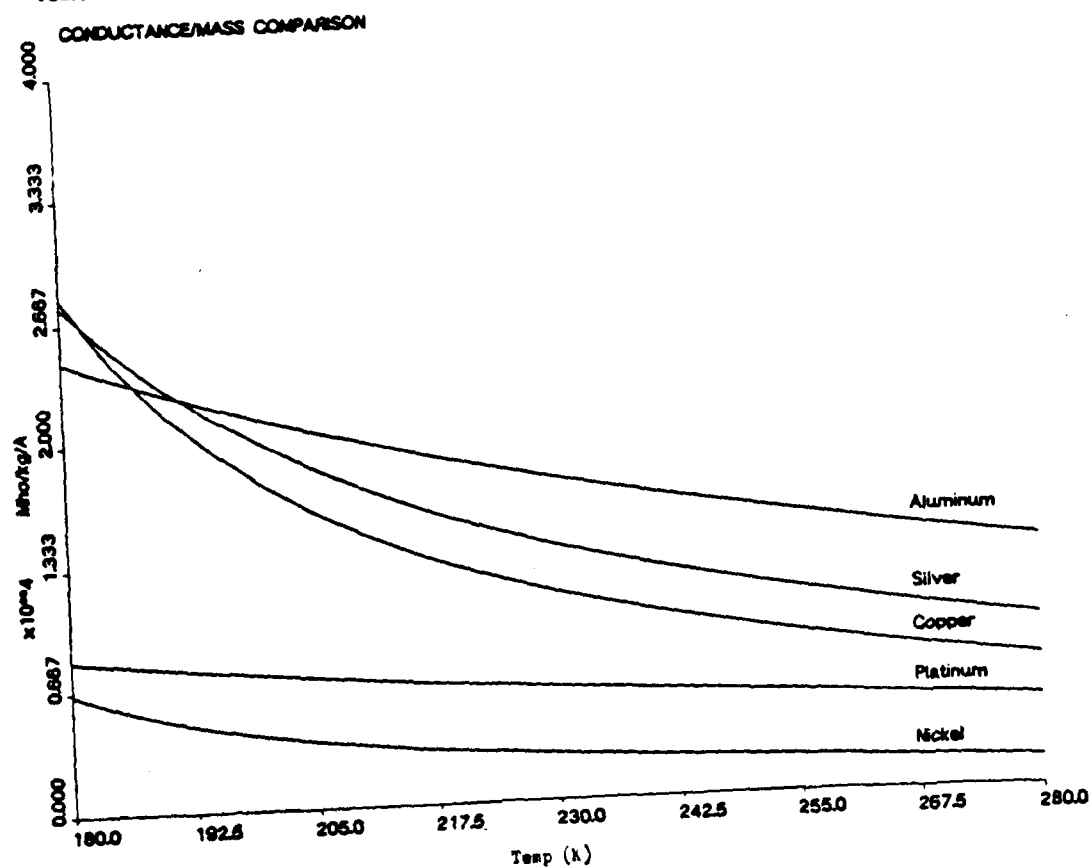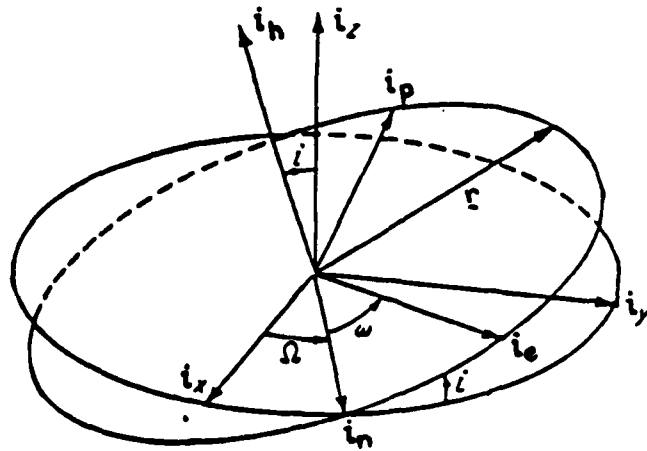
FIGURE 13

e, p, h COORDINATE SYSTEM

FIGURE 14
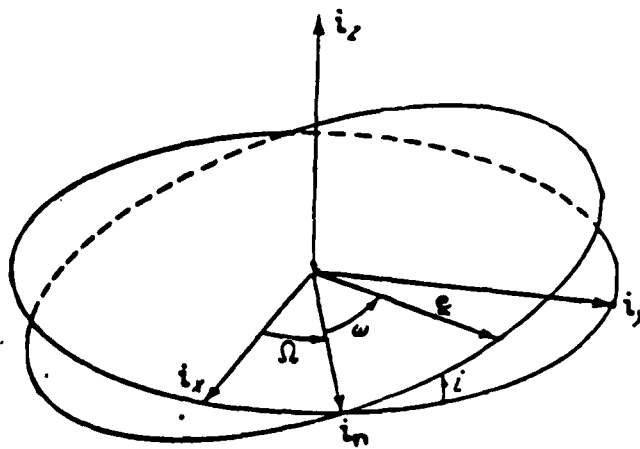
ECCENTRICITY VECTOR

FIGURE 15-1

TEMPERATURE VARIATIONS OVER 2 ORBITS
(3.5mm Tether @ Constant Power of 10 kW)

FIGURE 15-2

RESISTANCE VARIATIONS OVER 2 ORBITS
(3.5mm Tether @ Constant Power of 10 kW)

78
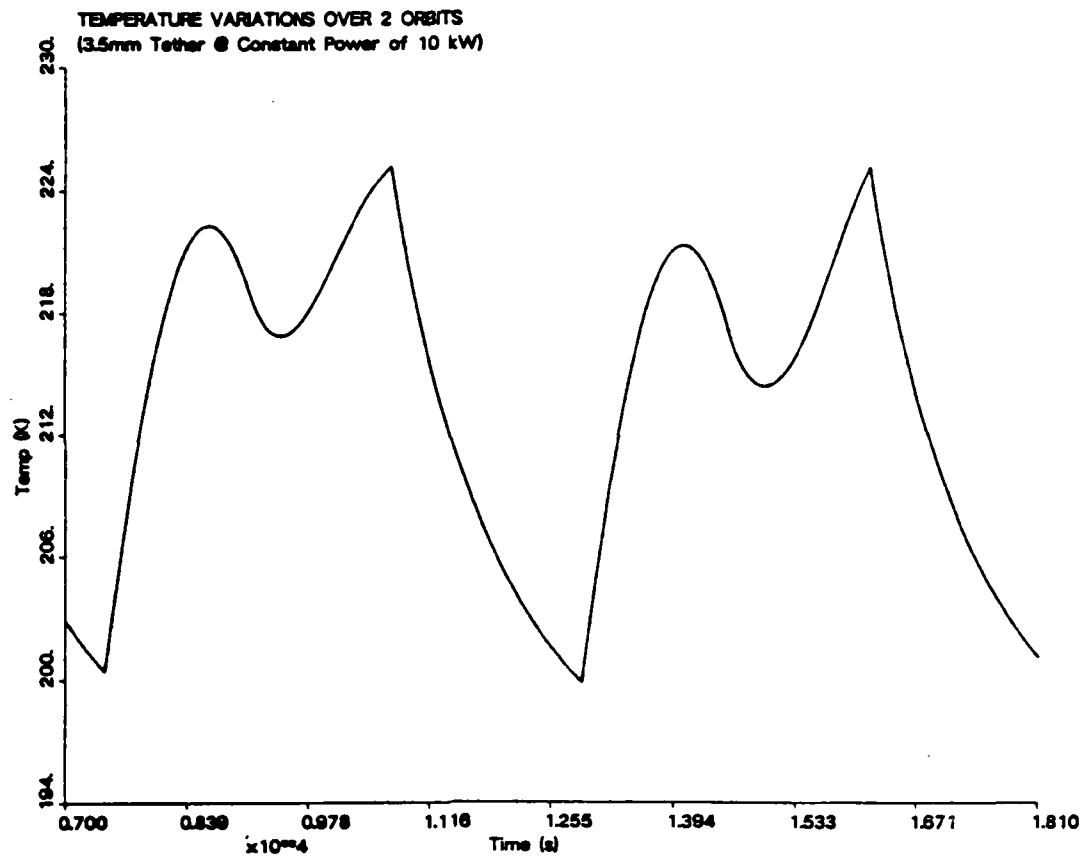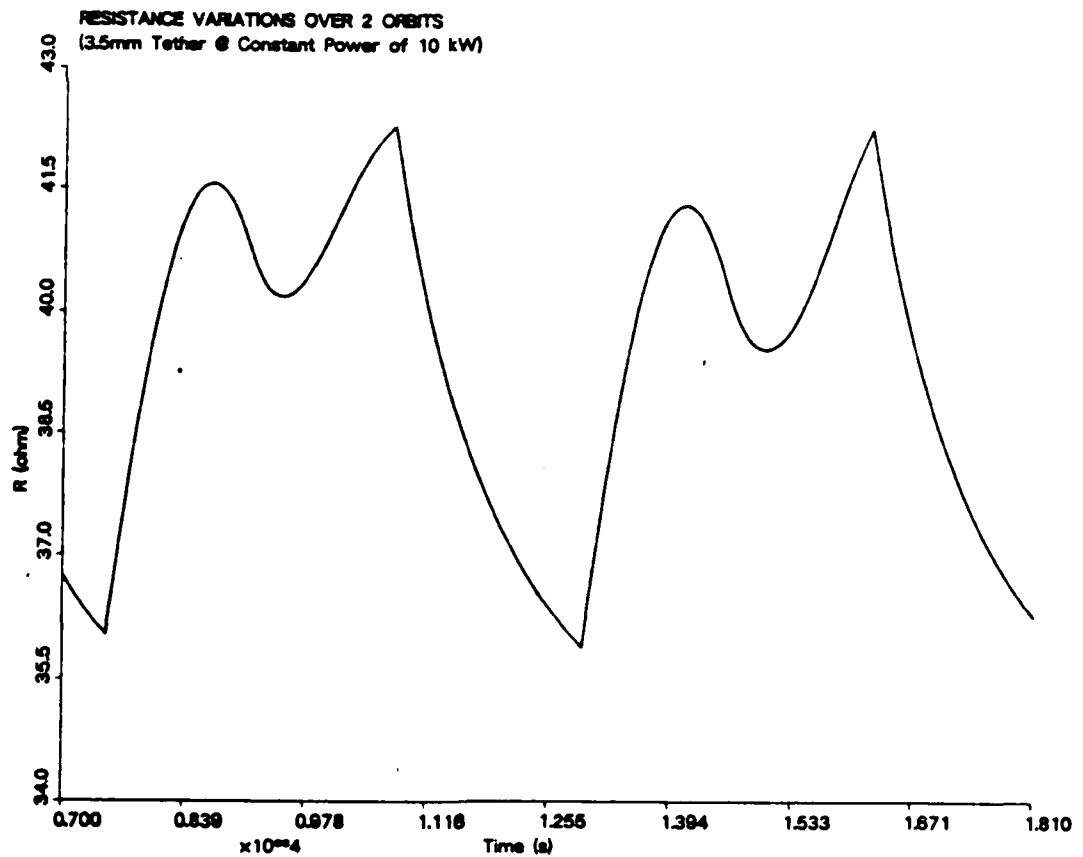
FIGURE 15-3

EFFICIENCY VARIATIONS OVER 2 ORBITS
(3.5mm Tether @ Constant Power of 10 kW)

79

FIGURE 16A

TETHER OPERATING TEMPERATURE
3.25mm Tether

FIGURE 16B

TETHER OPERATING TEMPERATURE
3.25mm Tether
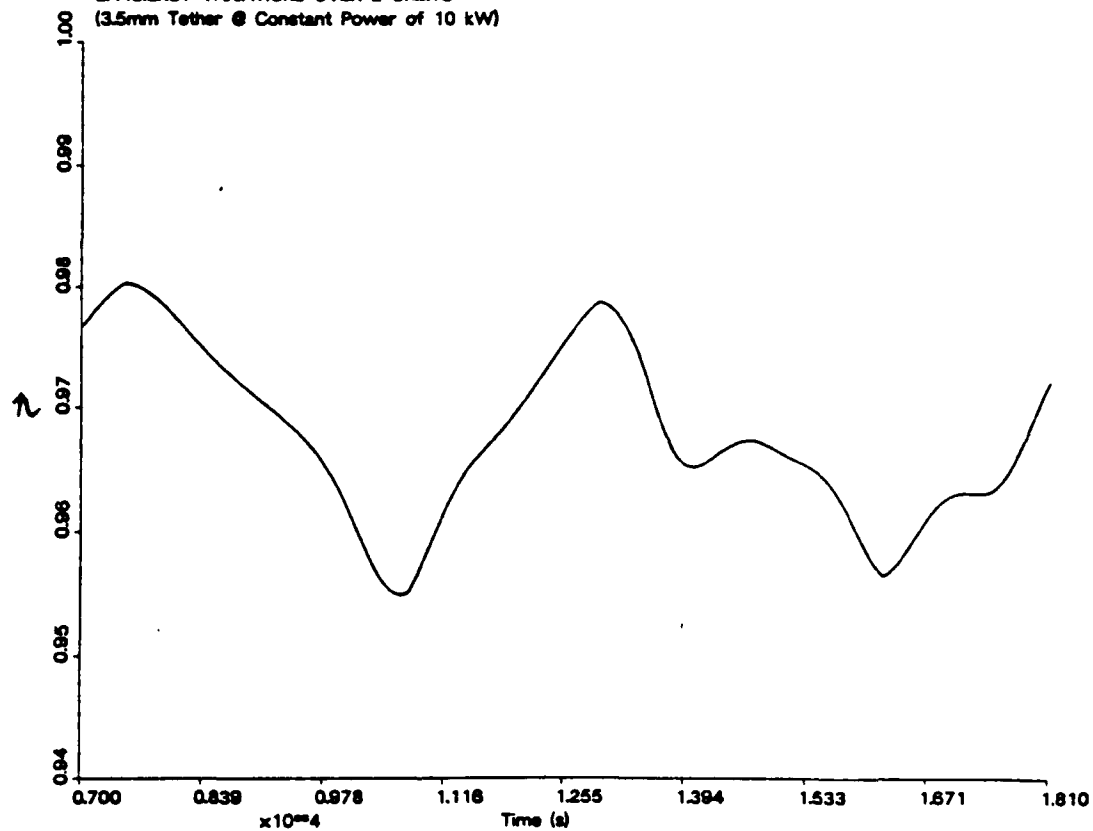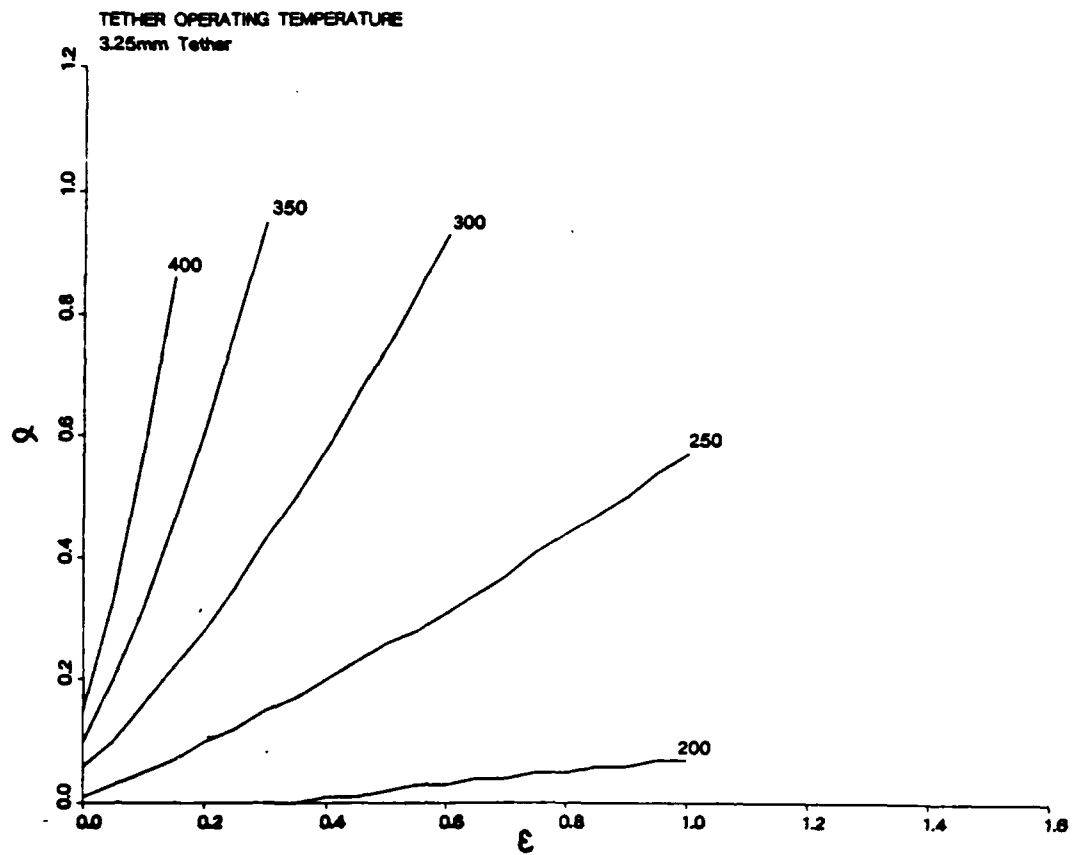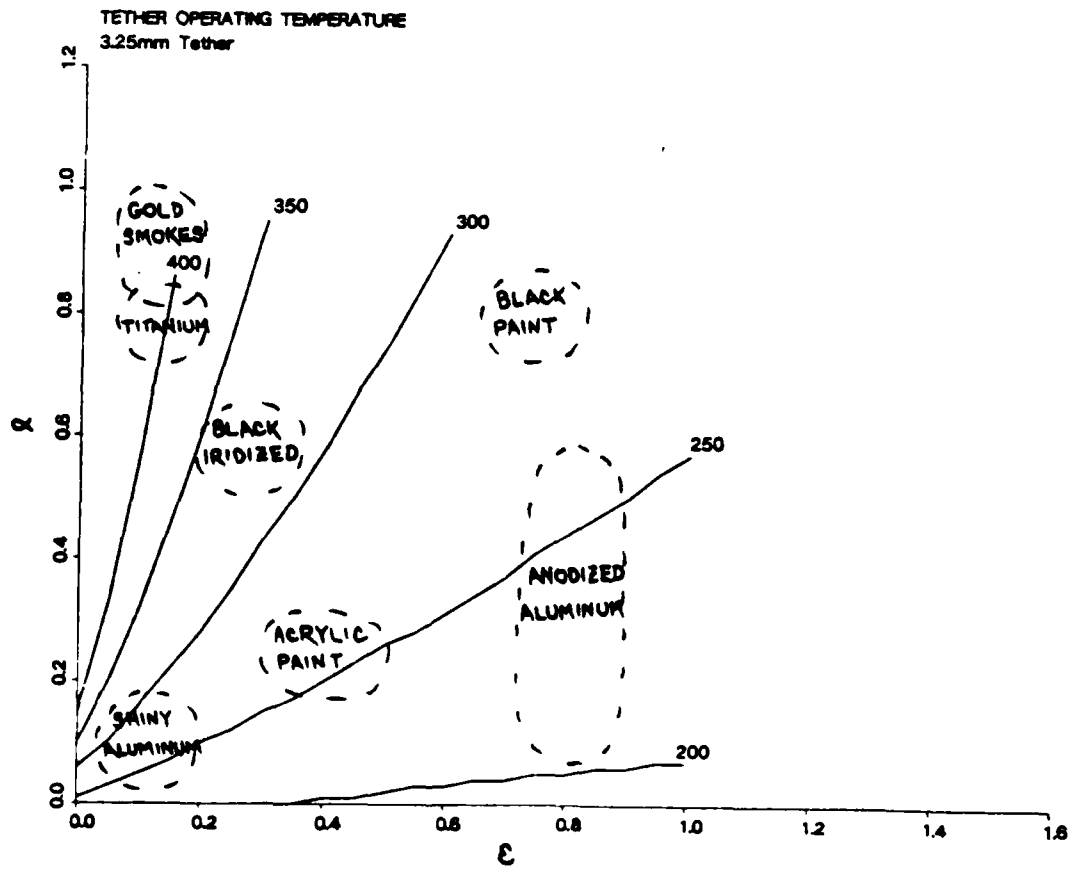
FIGURE 17

TEMPERATURE VARIATIONS FOR A COPPER TETHER
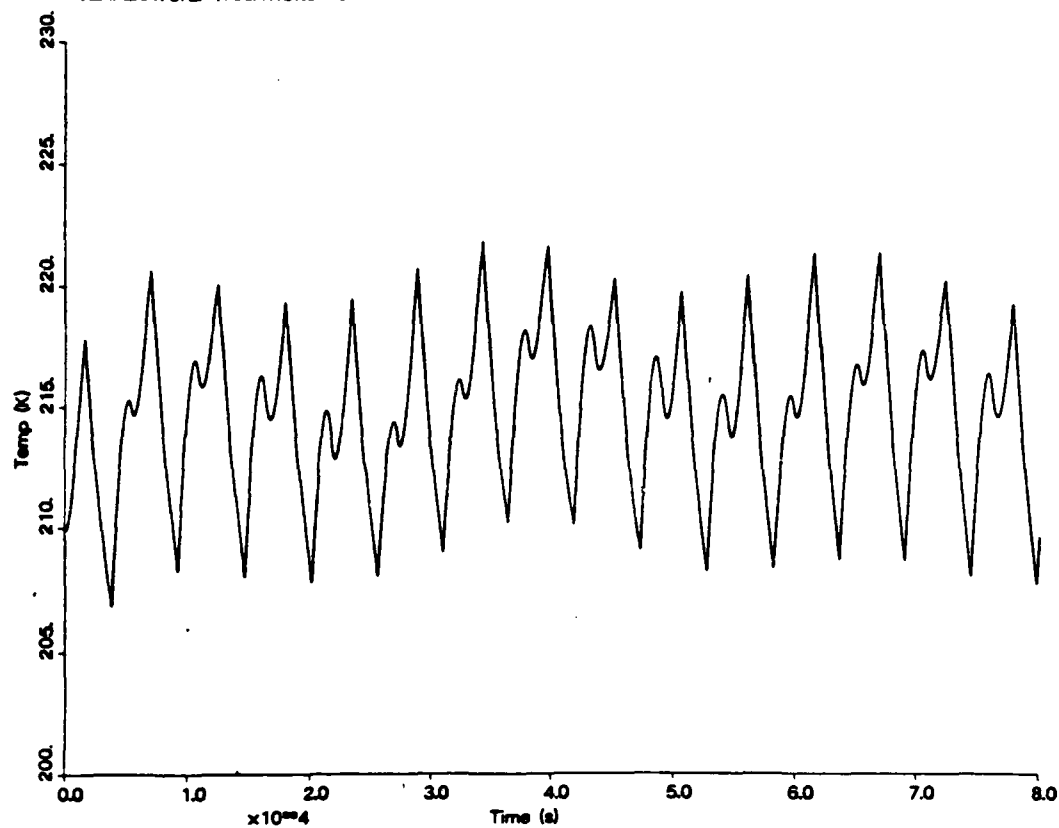
**VARIATION IN AVERAGE OPERATING TEMPERATURE
WITH DIAMETER AT 3 AMPS**
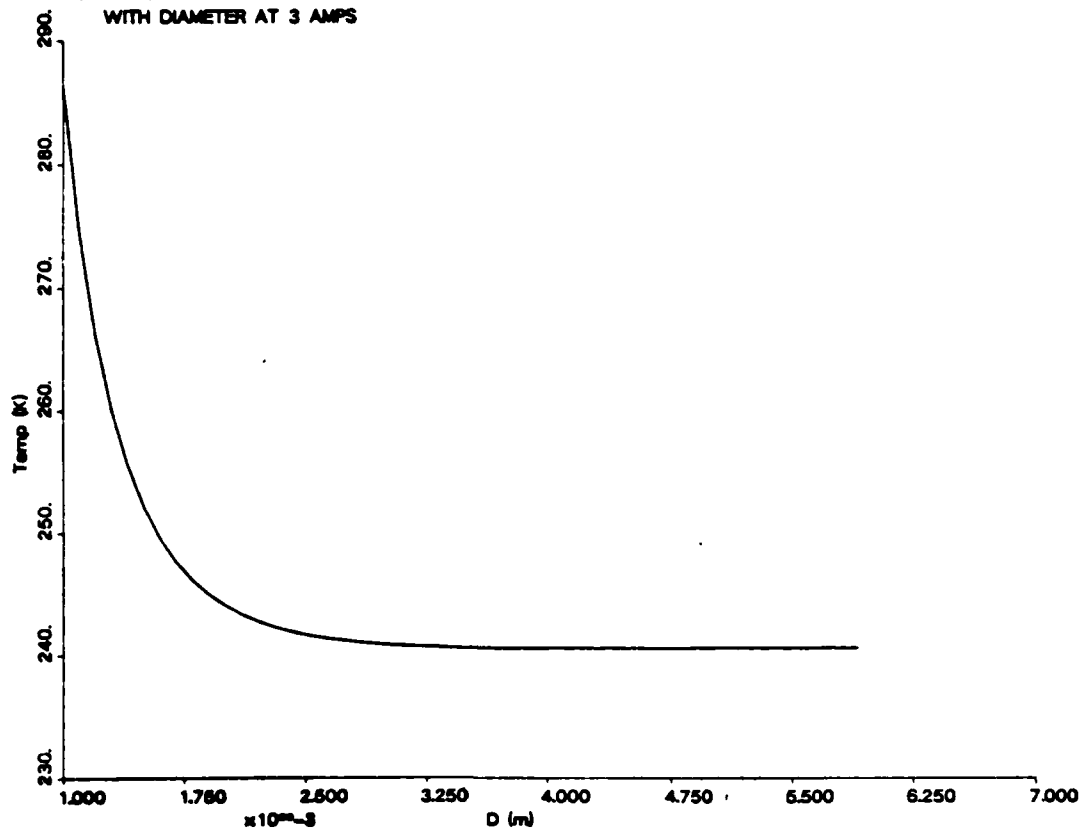
FIGURE 18B

**AVERAGE OPERATING TEMPERATURE VERSUS DIAMETER FOR
TETHER MAINTAINING CONSTANT LOAD POWER**

82
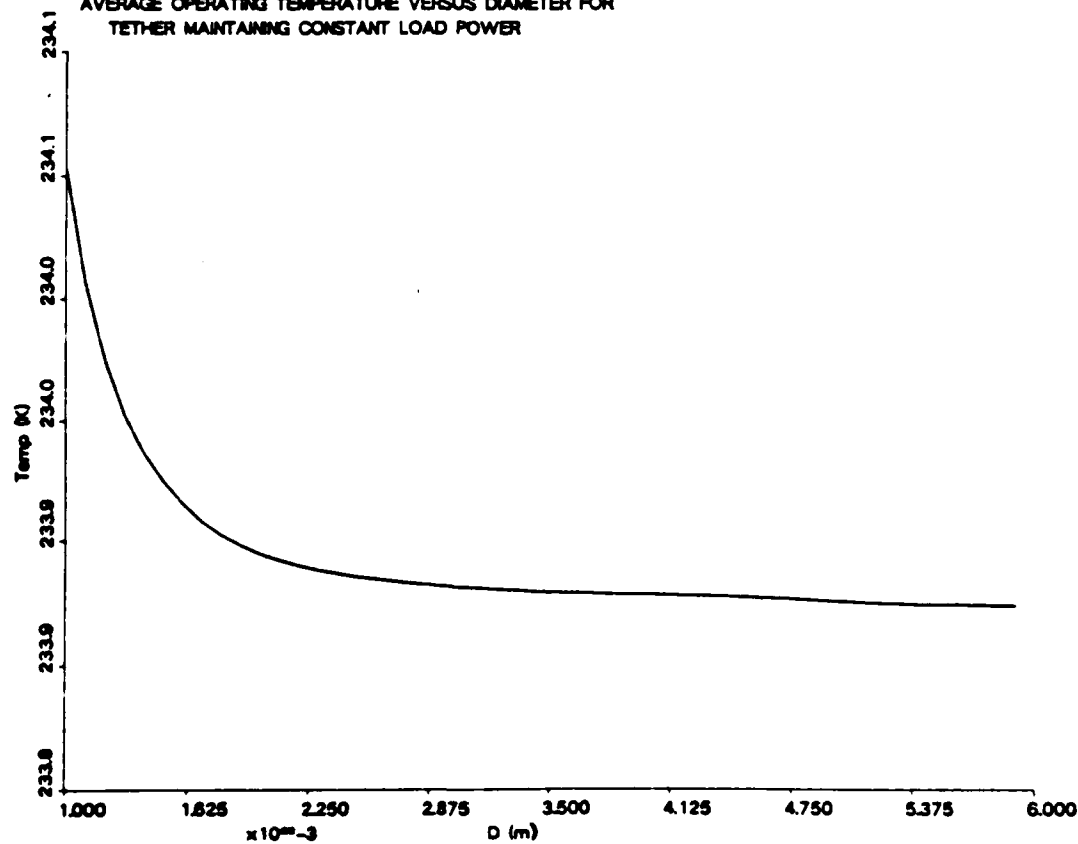
FIGURE 19

**VARIATION IN AVERAGE OPERATING TEMPERATURE
WITH LENGTH AT CONSTANT POWER**
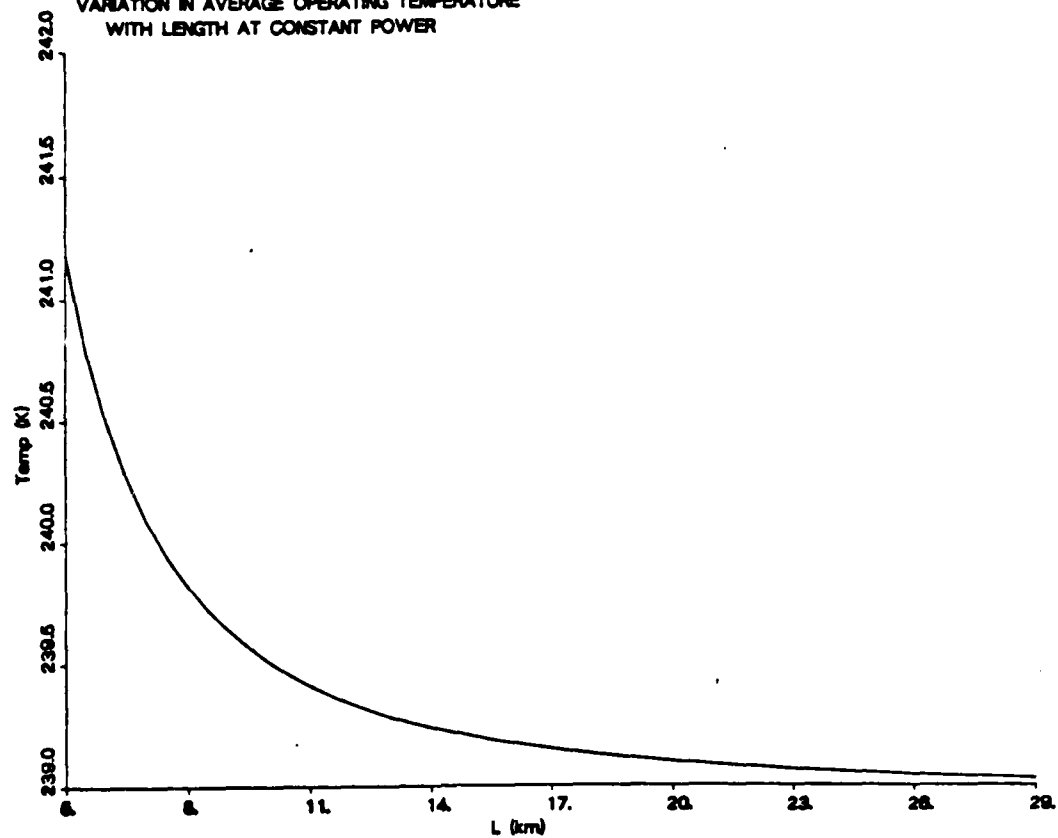
FIGURE 20

**VARIATION IN AVERAGE OPERATING TEMPERATURE
WITH ALTITUDE AT CONSTANT EFFICIENCY**

83

TEMPERATURE VARIATIONS
3.25mm Tether @ 10kW Load Power in Generator Mode

AUTUMNAL EQUINOX   0 deg

FIGURE 21B

TEMPERATURE VARIATIONS
3.25mm Tether @ 10kW Load Power in Generator Mode

AUTUMNAL EQUINOX   90 deg

84

FIGURE 22A

TEMPERATURE VARIATIONS
3.25mm Tether @ 10kW Load Power in Generator Mode

SUMMER SOLSTICE   0 DEG

FIGURE 22B

TEMPERATURE VARIATIONS
3.25mm Tether @ 10kW Load Power in Generator Mode

WINTER SOLSTICE   0 deg

85

FIGURE 22C

TEMPERATURE VARIATIONS

3.25mm Tether @ 10kW Load Power in Generator Mode

VERNAL EQUINOX   0 deg

86

FIGURE 23-1

ECCENTRICITY VARIATION
Open Circuit Mode
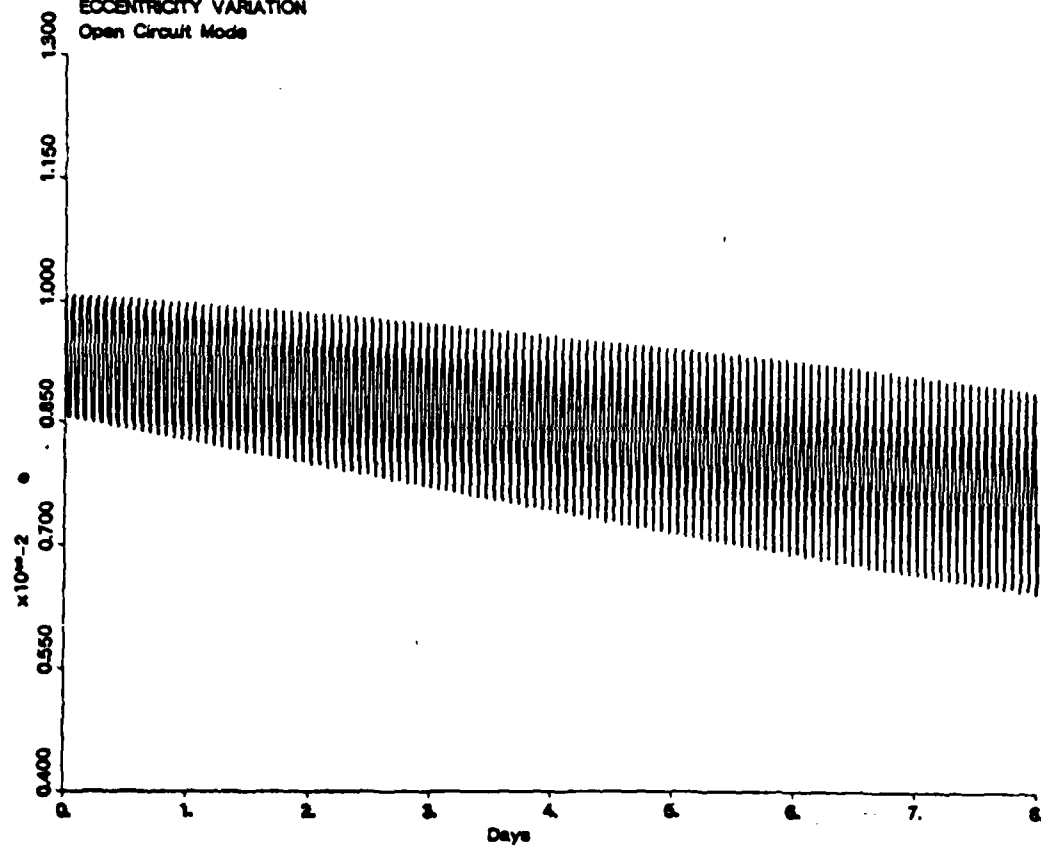
FIGURE 23-2

SEMI-MAJOR AXIS VARIATION
Open Circuit Mode

FIGURE 23-3

ORBITAL INCLINATION VARIATION
Open Circuit Mode

FIGURE 23-4

ARGUMENT OF PERIGEE VARIATION
Open Circuit Mode

88
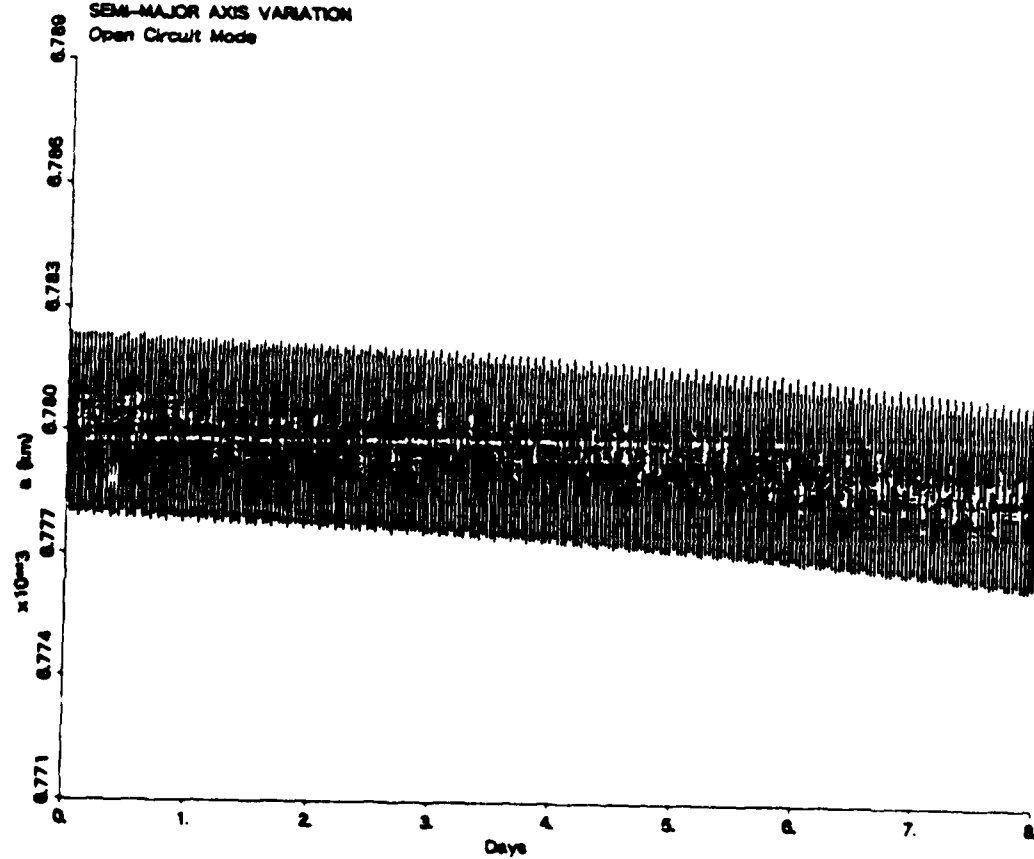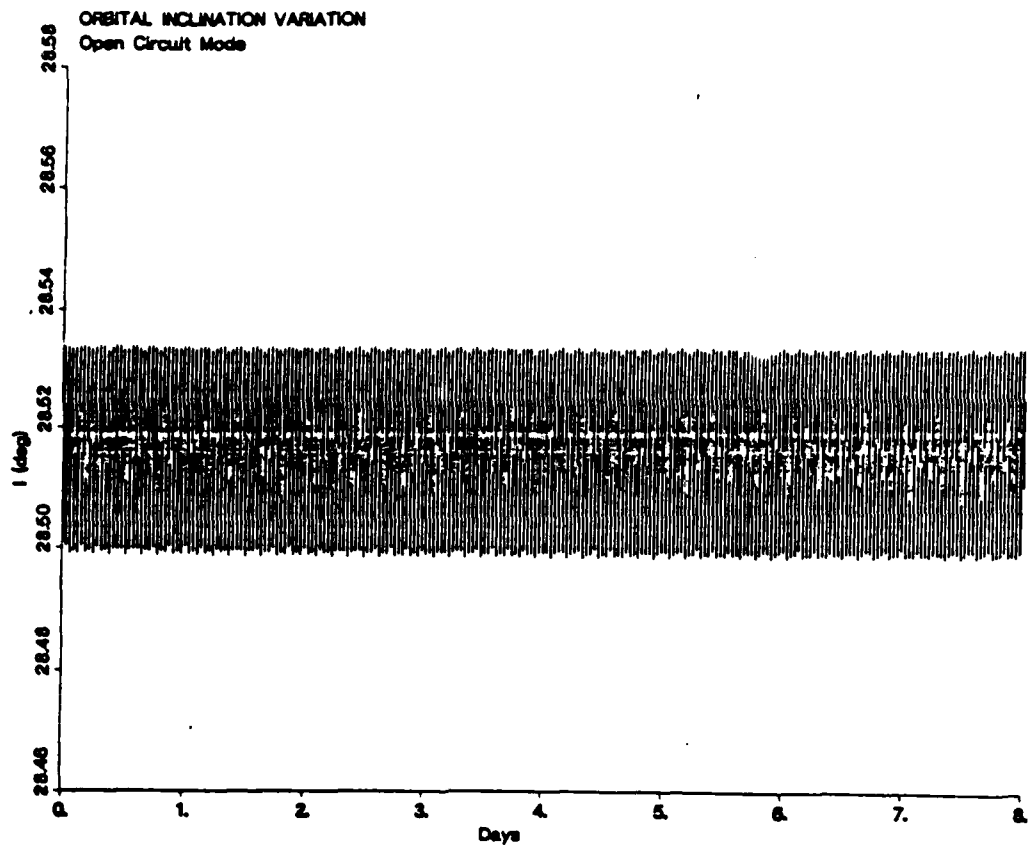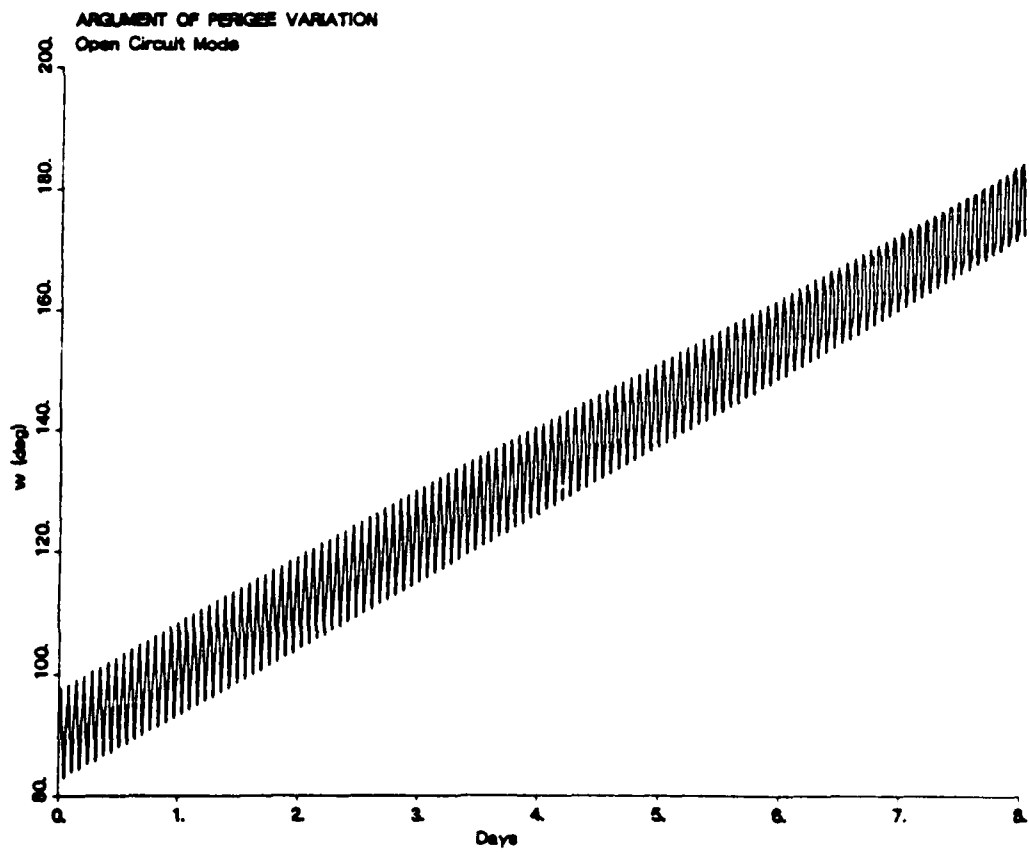
FIGURE 23-5

LINE OF NODES VARIATION
Open Circuit Mode

89

FIGURE 24-1

ECCENTRICITY VARIATION
Generator Mode

FIGURE 24-1

FIGURE 24-2

SEMI-MAJOR AXIS VARIATION
Generator Mode

FIGURE 24-2

FIGURE 24-3

ORBITAL INCLINATION VARIATION
Generator Mode

FIGURE 24-4

ARGUMENT OF PERIGEE VARIATION
Generator Mode
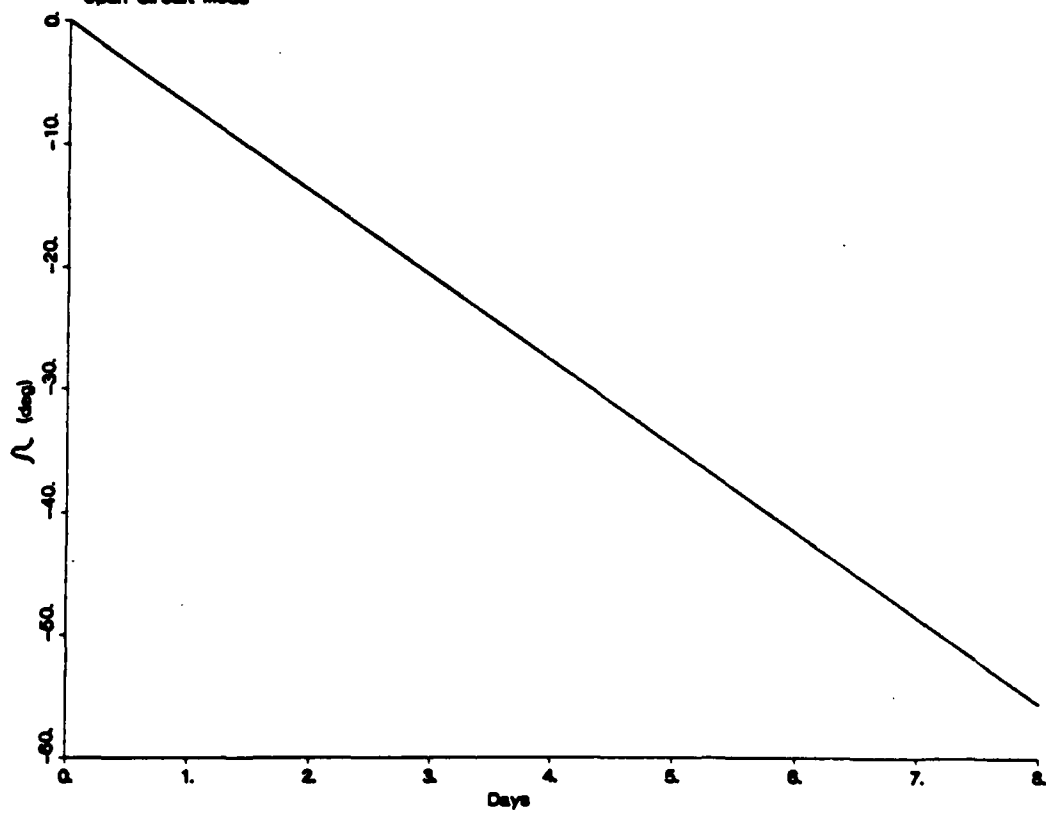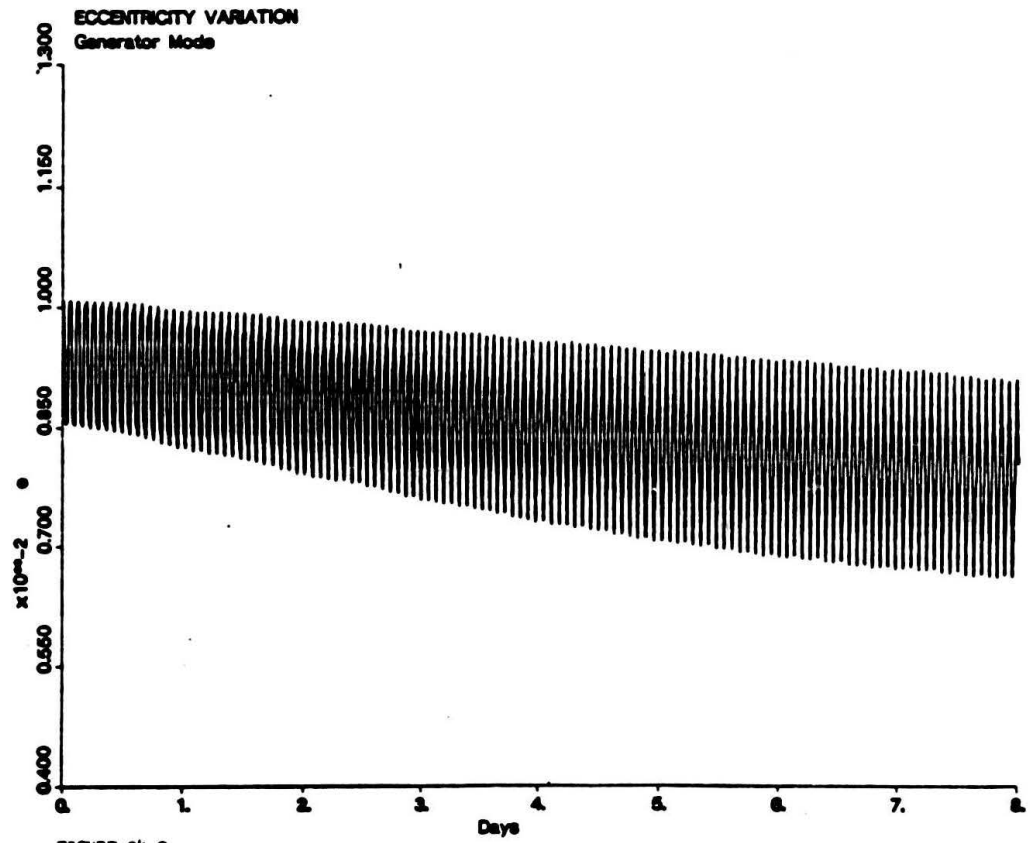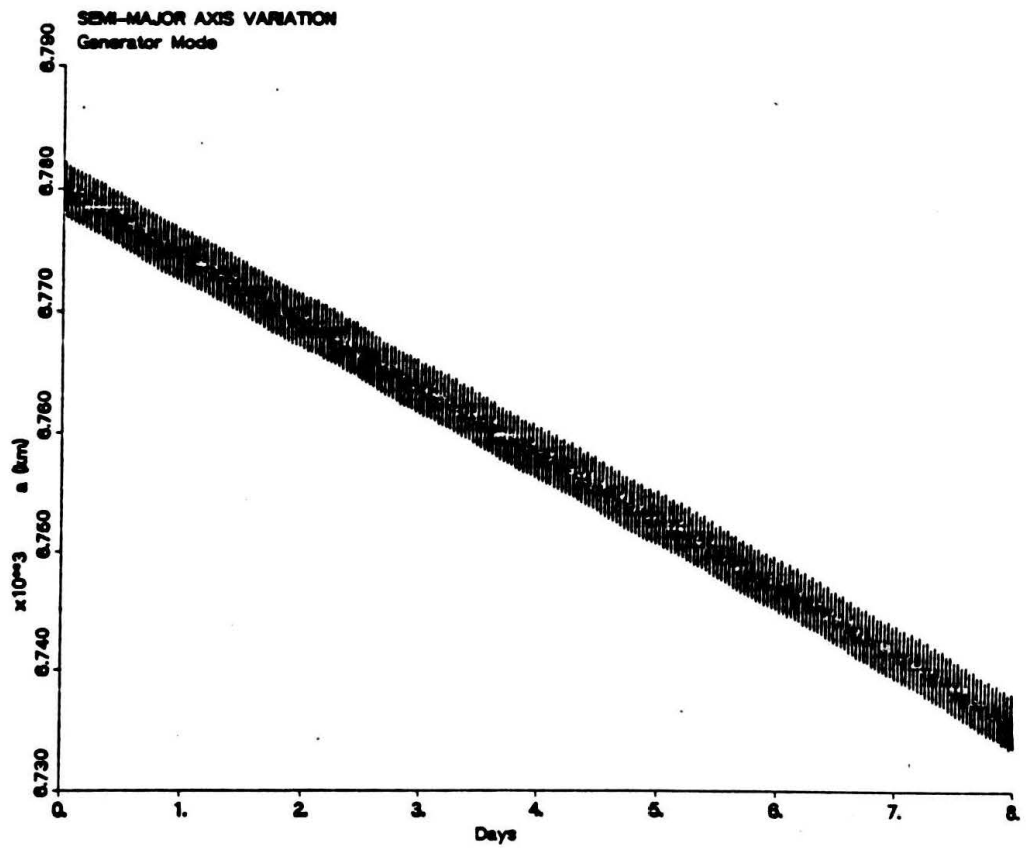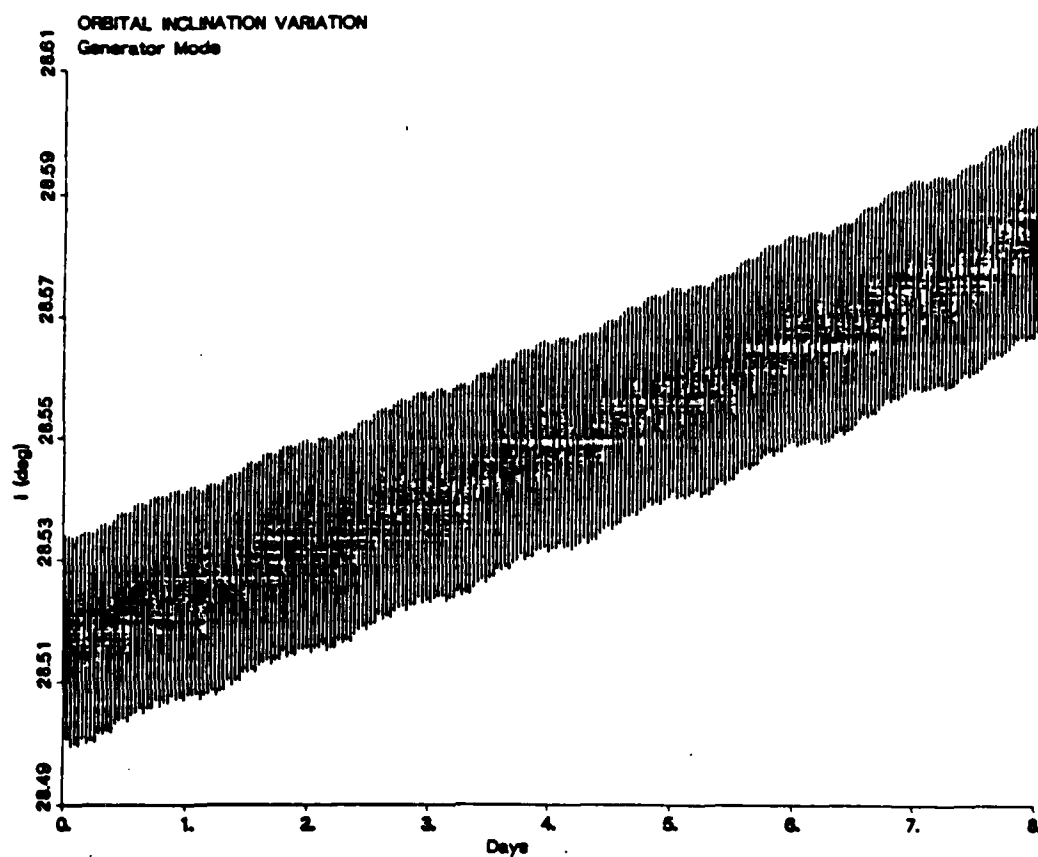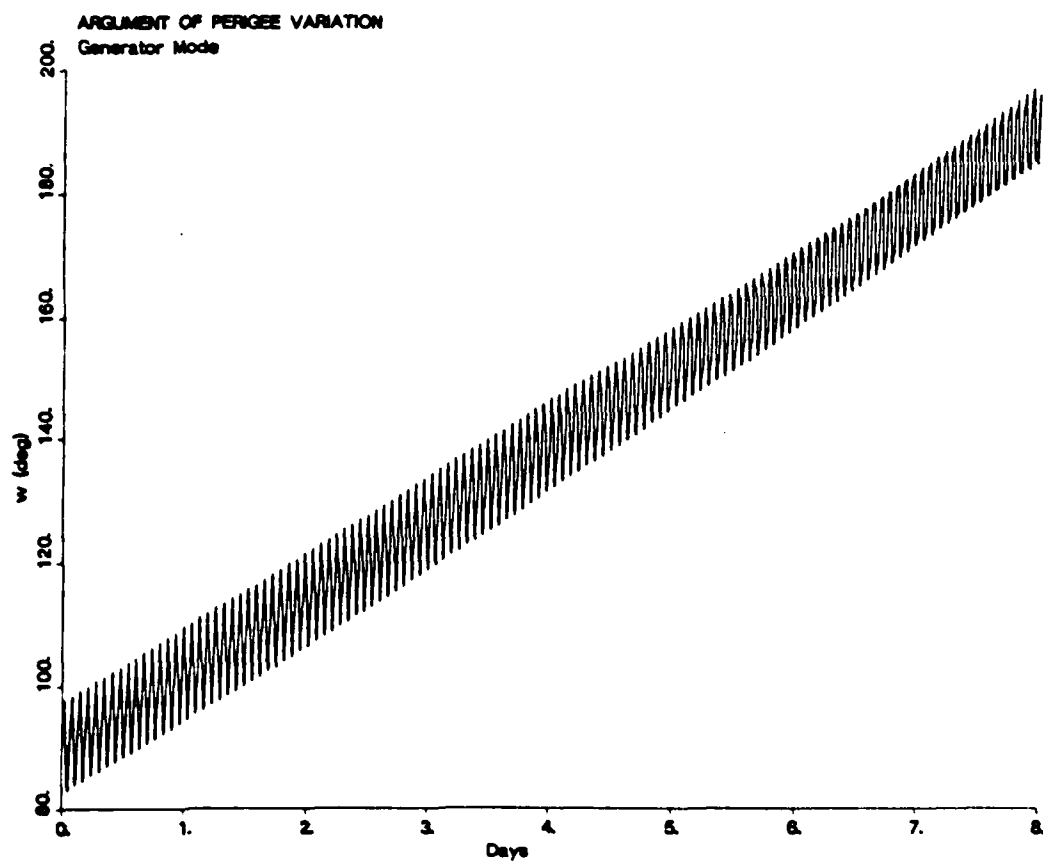
FIGURE 24-5

LINE OF NODES VARIATION
Generator Mode
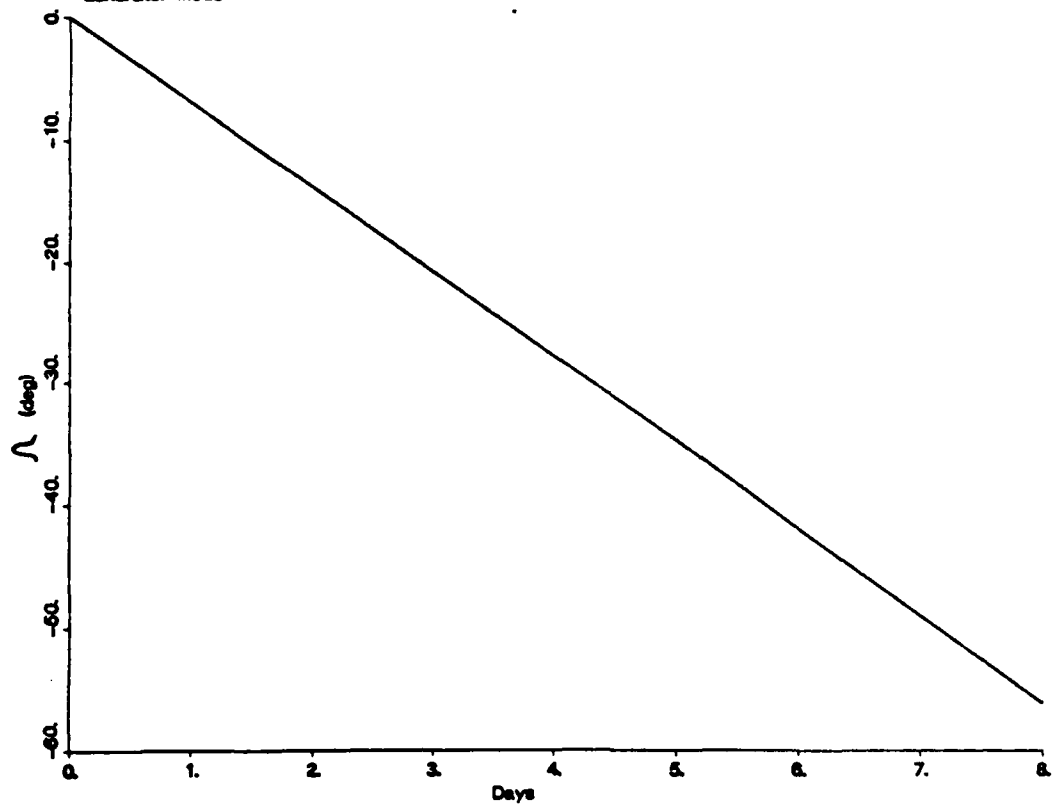
FIGURE 24-6

PERIGEE ALTITUDE VARIATION
Generator Mode

FIGURE 25-1

ECCENTRICITY VARIATION
Thruster Mode

FIGURE 25-2

SEMI-MAJOR AXIS VARIATION
Thruster Mode

93

ORBITAL INCLINATION VARIATION
Thruster Mode

ARGUMENT OF PERIGEE VARIATION
Thruster Mode
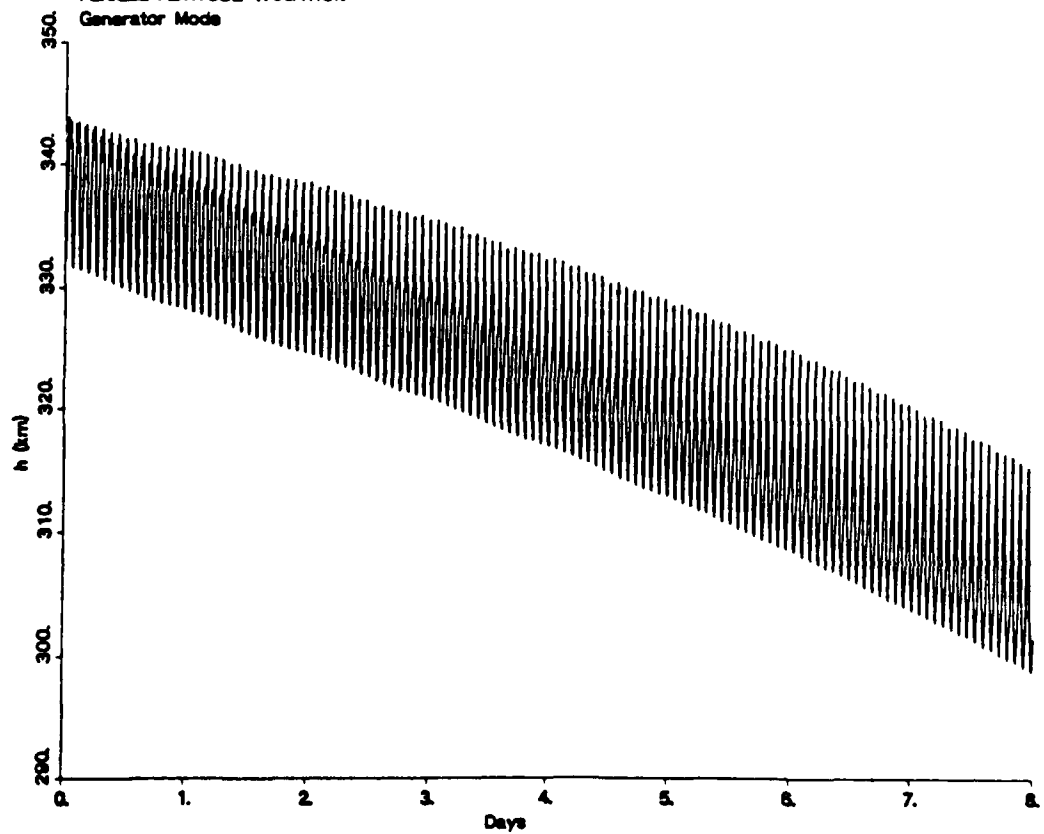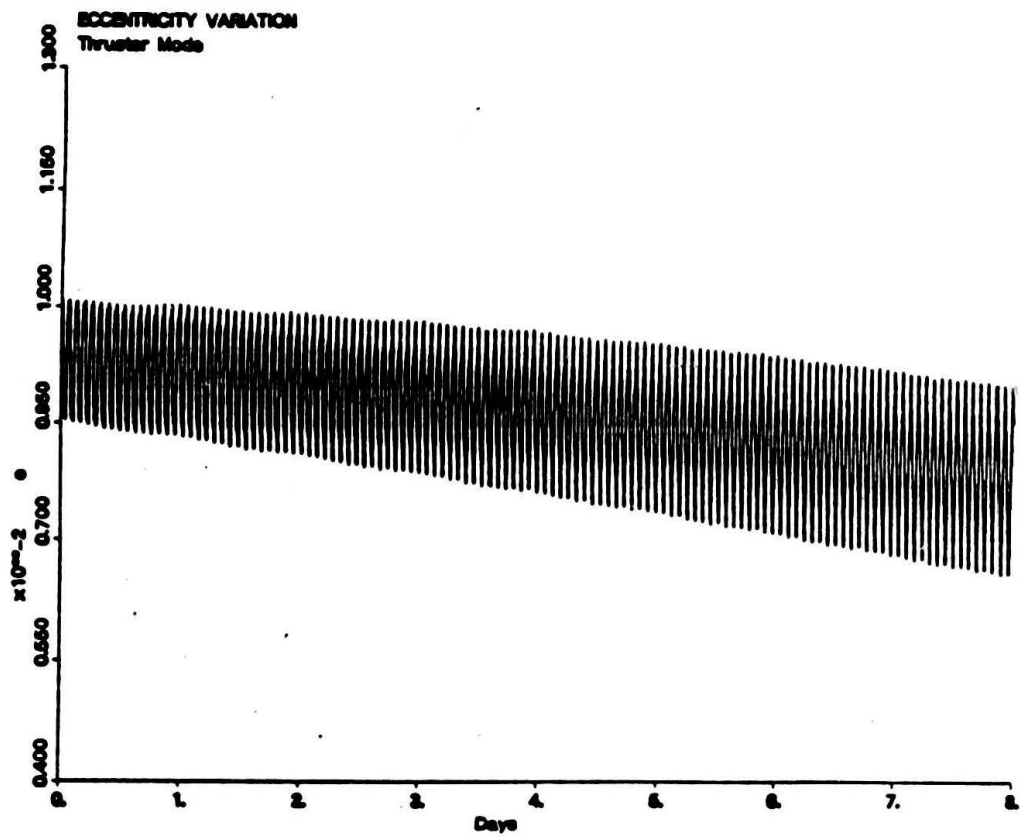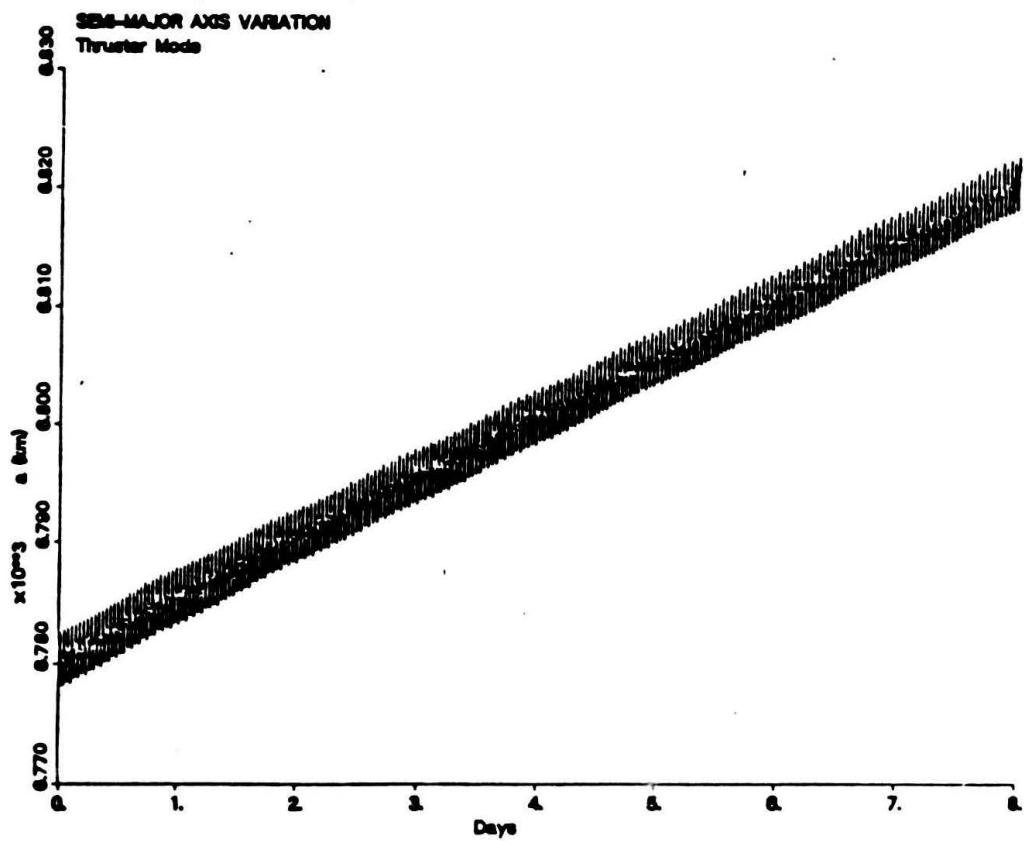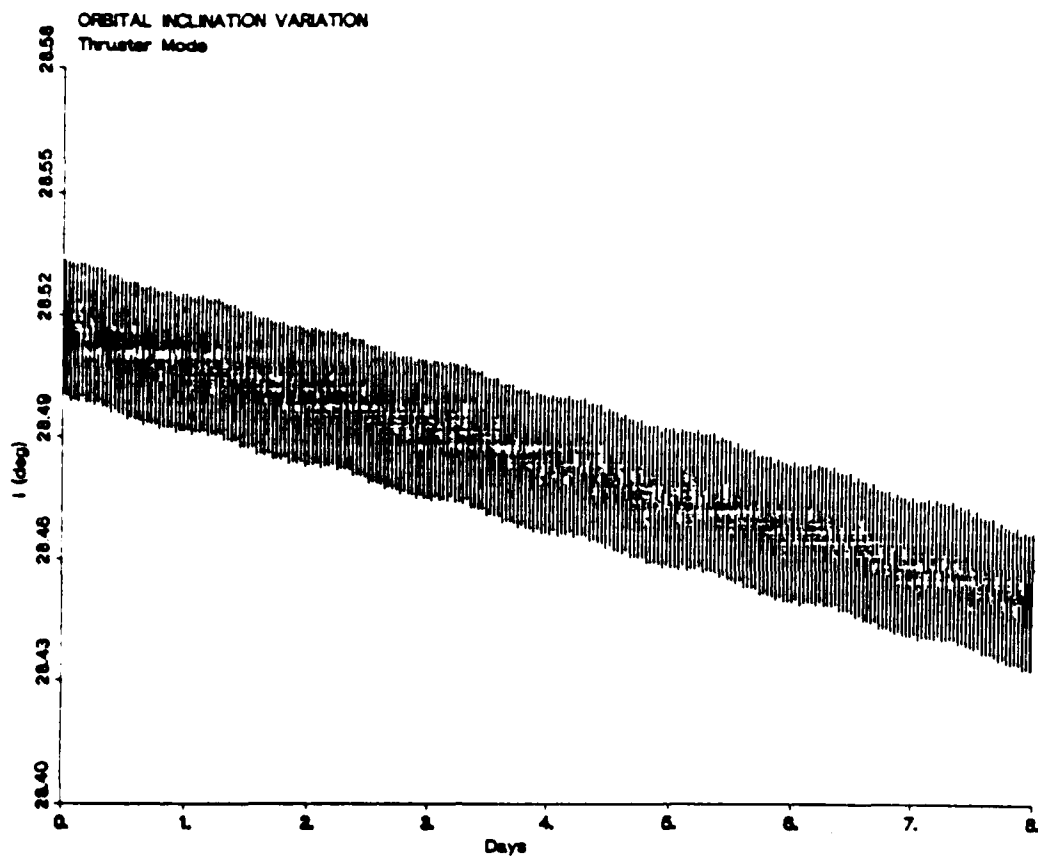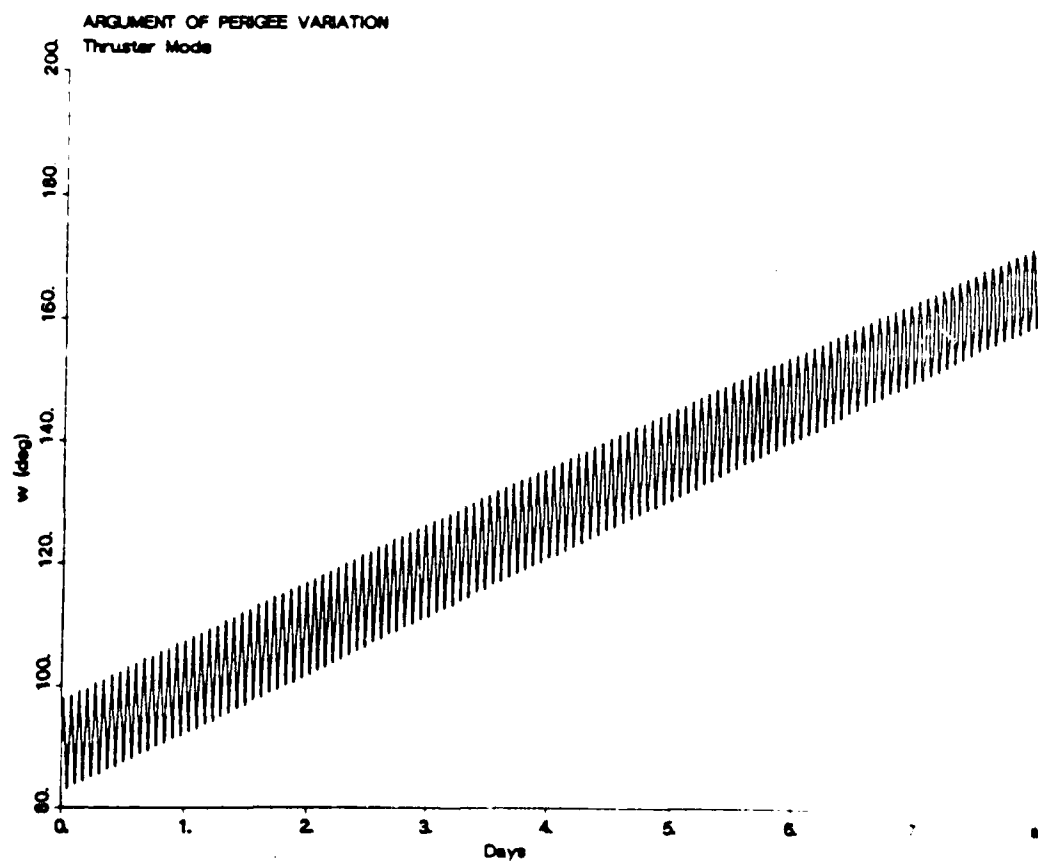
FIGURE 25-5

LINE OF NODES VARIATION
Thruster Mode
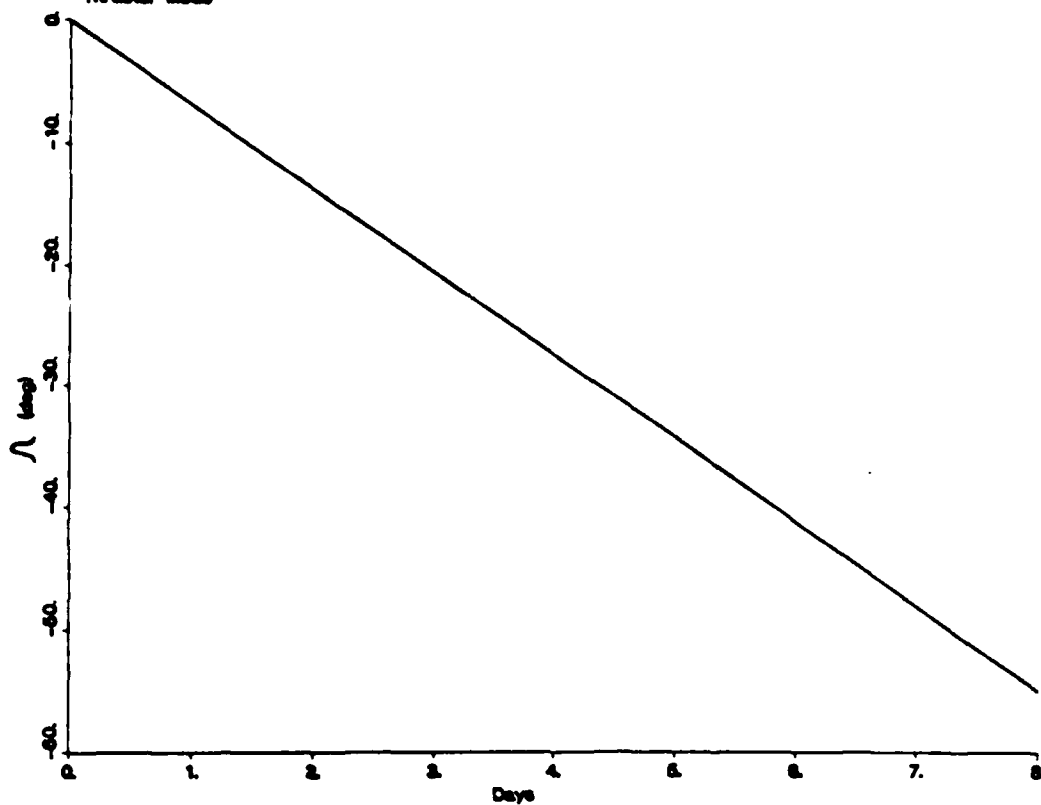
FIGURE 25-6

PERIGEE ALTITUDE VARIATION
Thruster Mode
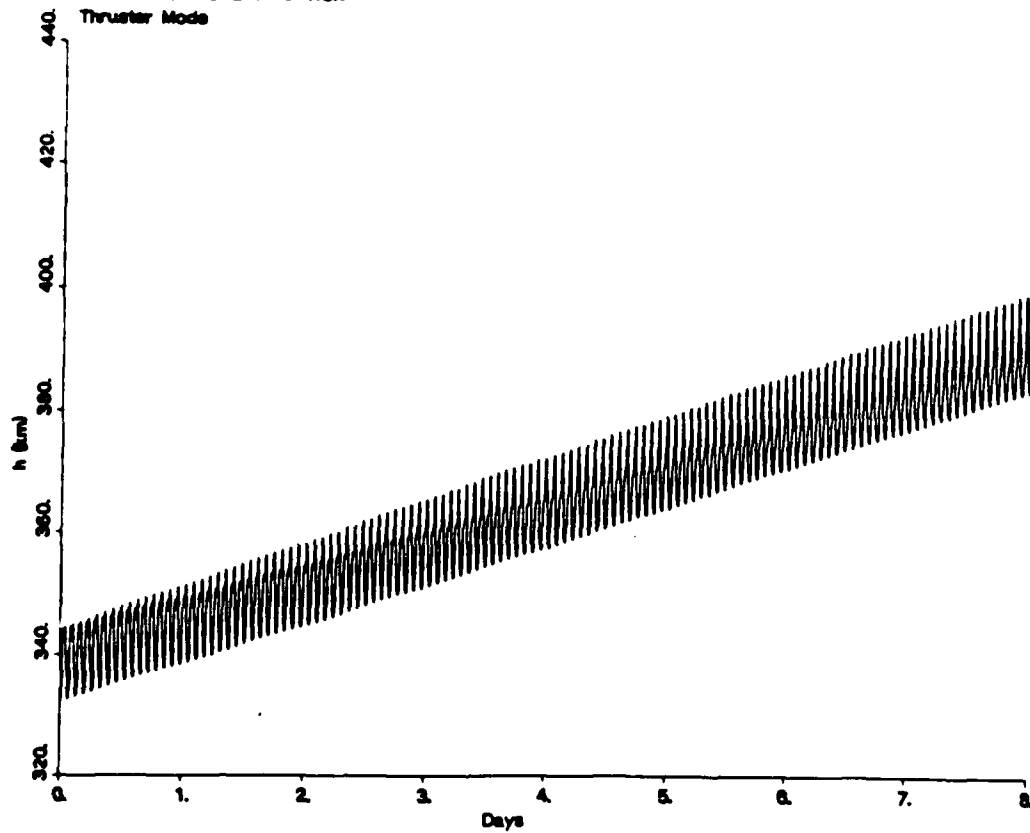
95

FIGURE 26-1

ECCENTRICITY VARIATION
Mixed Mode

FIGURE 26-2

SEMI-MAJOR AXIS VARIATION
Mixed Mode

FIGURE 26-3

ORBITAL INCLINATION VARIATION
Mixed Mode

FIGURE 26-4

ARGUMENT OF PERIGEE VARIATION
Mixed Mode

97

FIGURE 26-5

LINE OF NODES VARIATION
Mixed Mode

FIGURE 26-6

PERIGEE ALTITUDE VARIATION
Mixed Mode

98

FIGURE 27

ECCENTRICITY VARIATION
WITH INCREASING POWER-TO-MASS RATIO

P/M = 32.00

14.00

6.00

2.86

1.28

x10**-2

Days

99
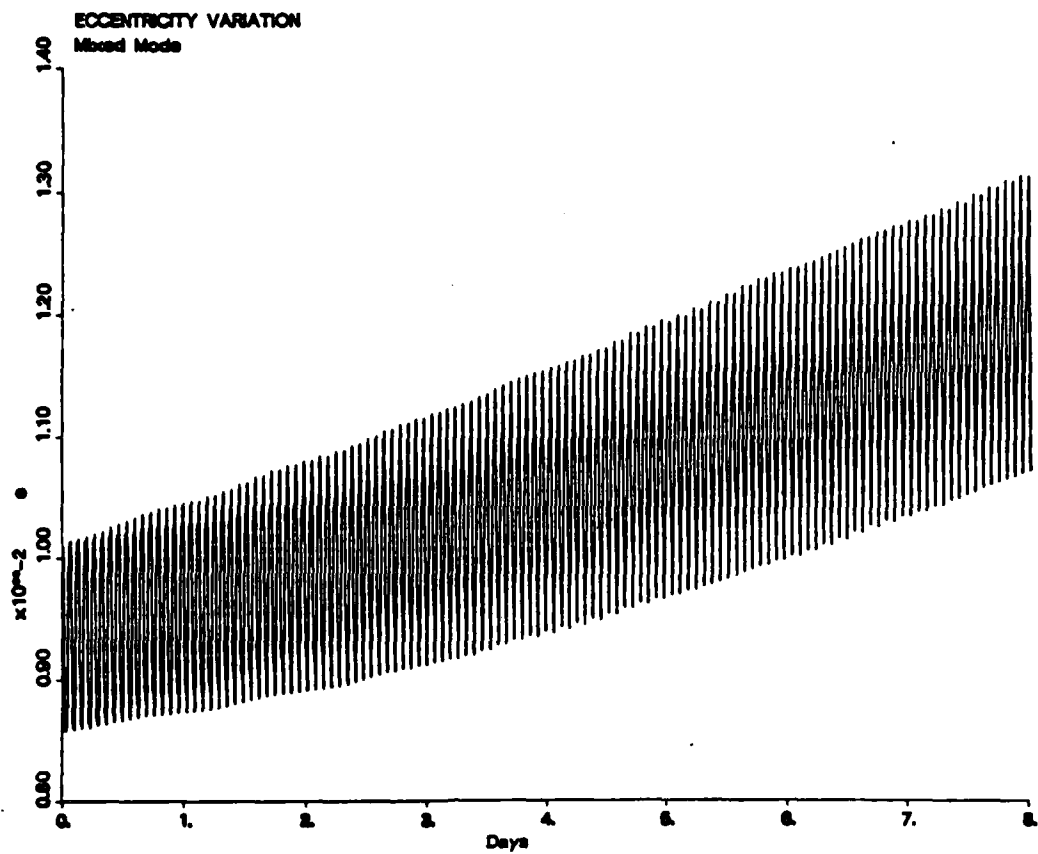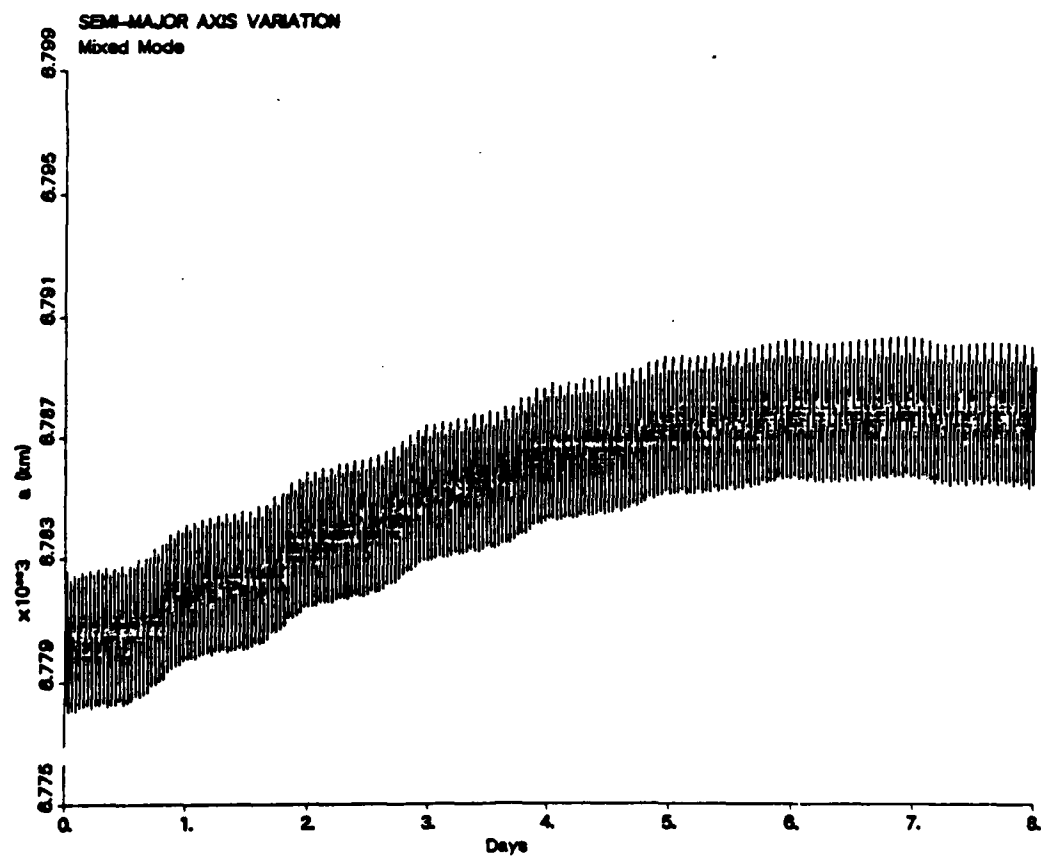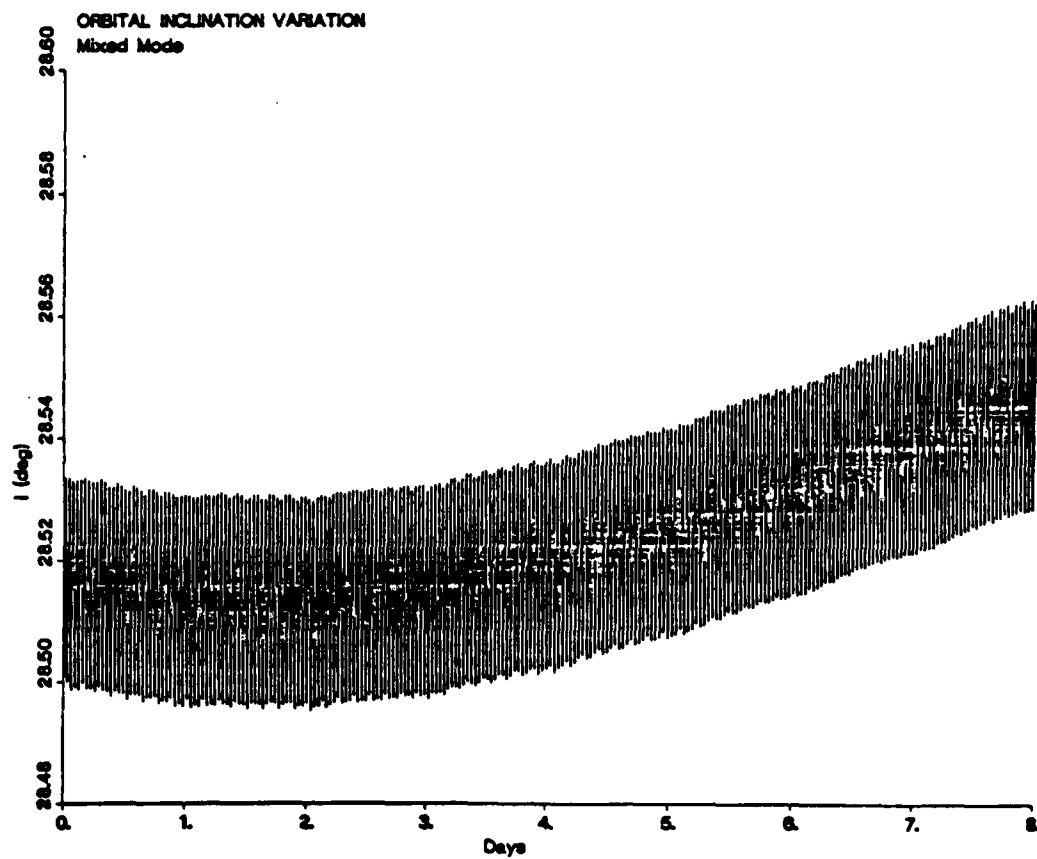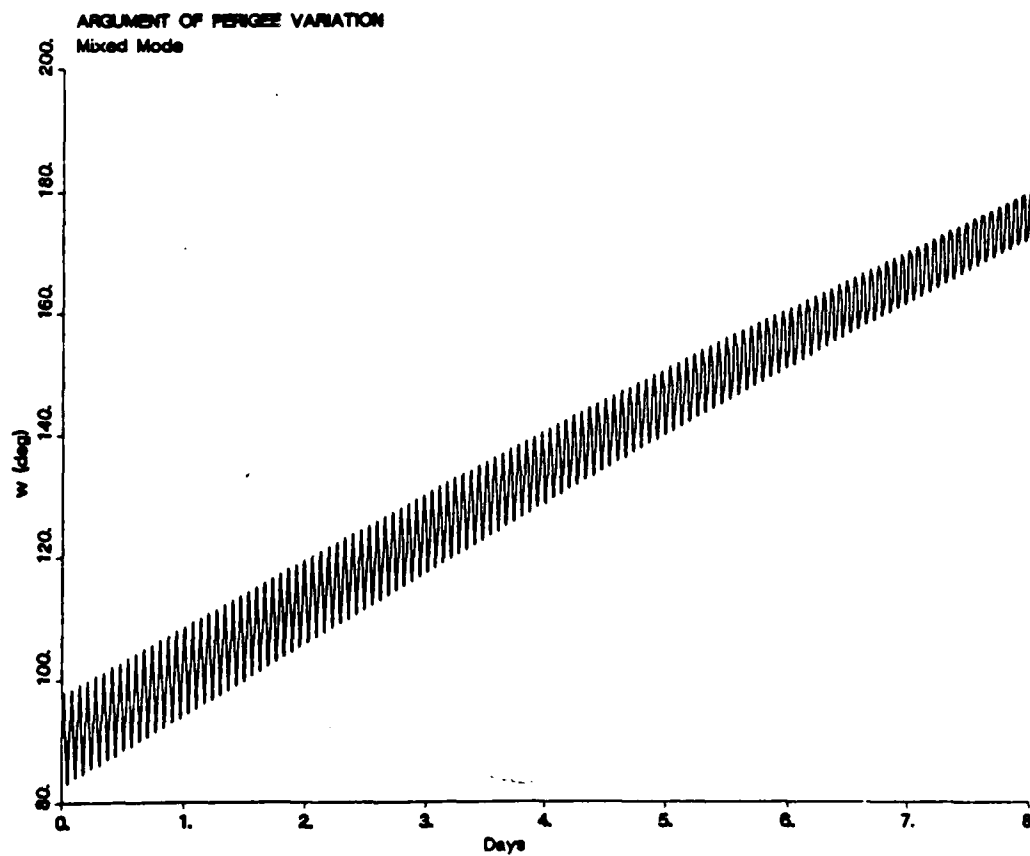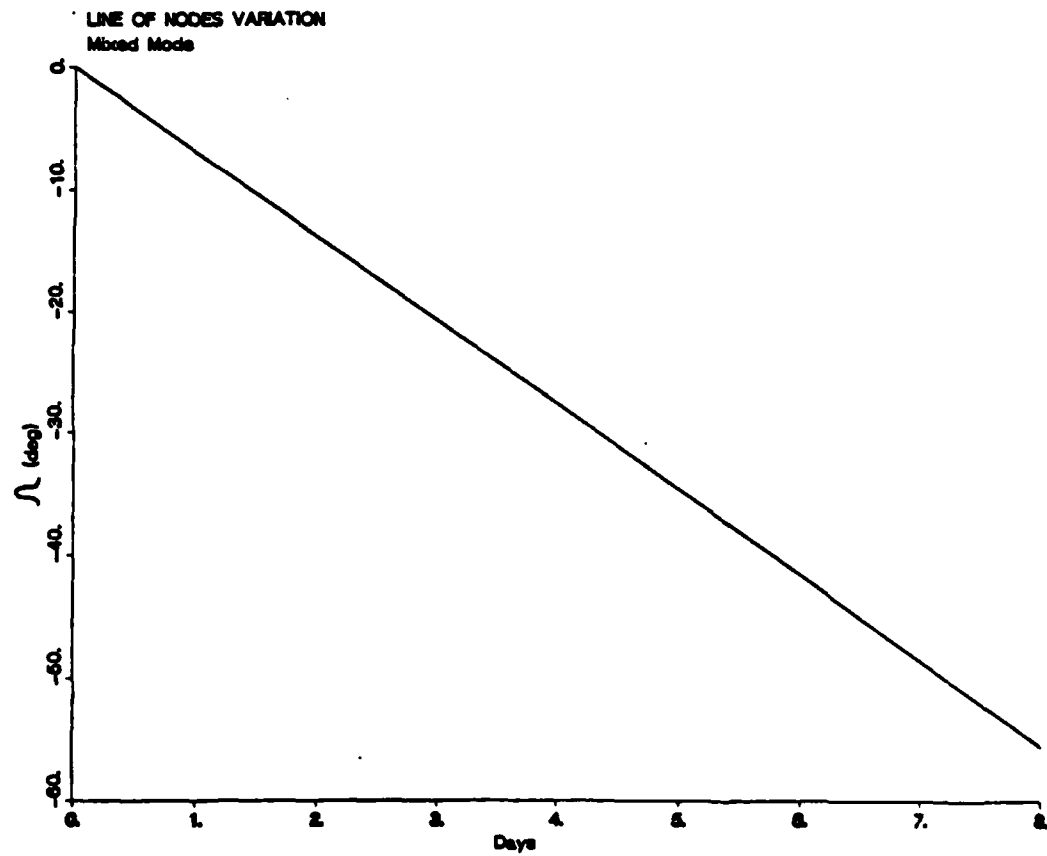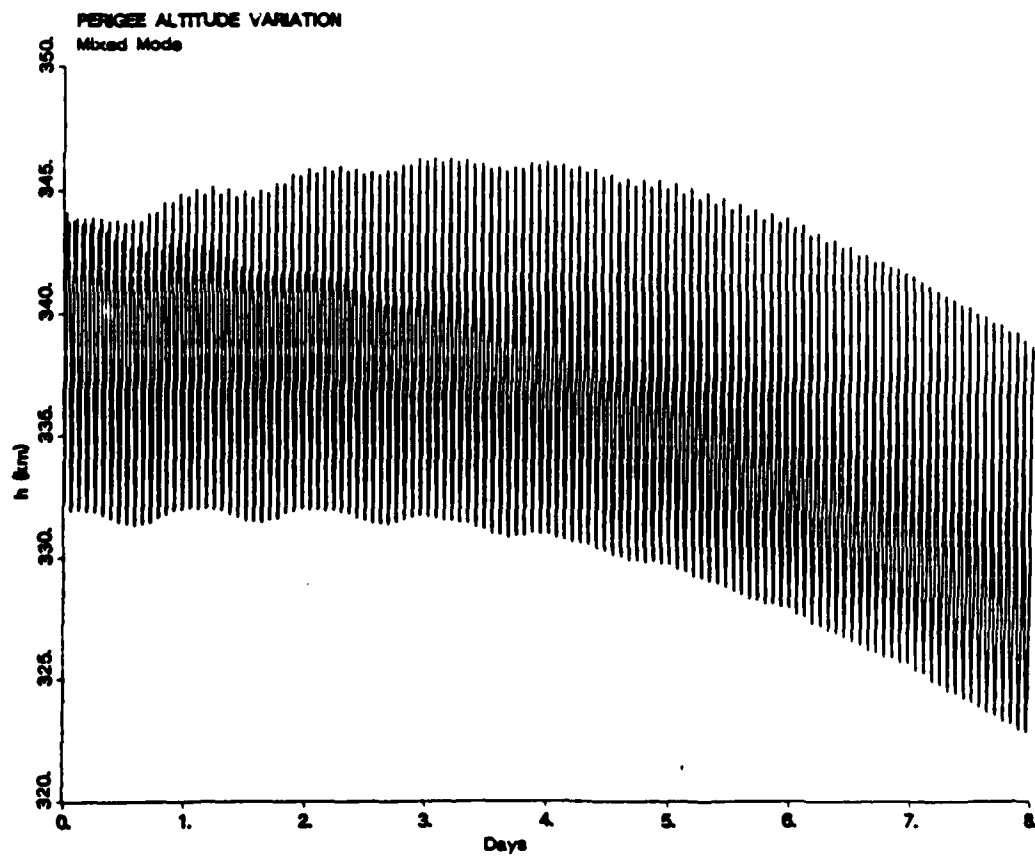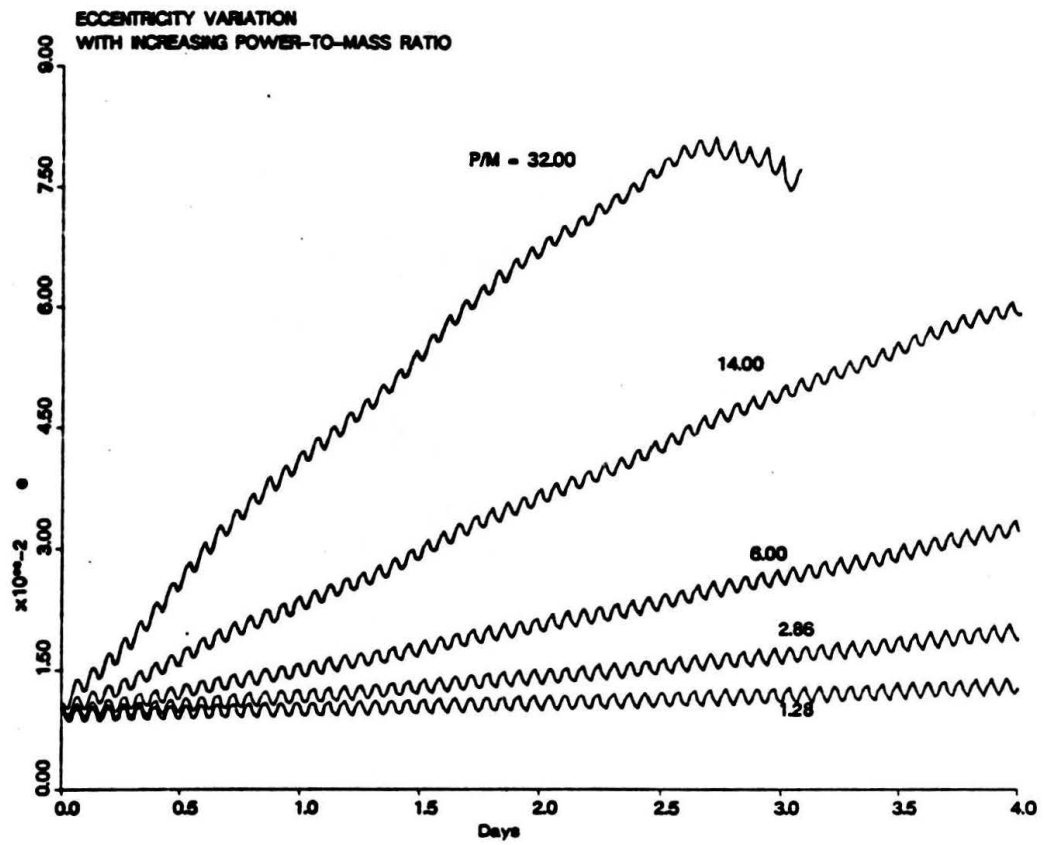
APPENDIX A

Computer Calculation of Thermal Variations

The thermal balance of the tether system, and the variations in the temperature, resistance, current level, and efficiency of the system, were evaluated with the mathematical model as discussed in Section 3.2. This appendix includes the computer program which implements this model. It employs an Euler forward code for the numerical integration of the temperature equation with a time step of 60 seconds. Although this is a relatively inaccurate integration method, the purpose of the analysis which this program implements is to show general trends in the variation of system values. Any numerical errors which develop over the course of the integration may be confidently ignored.

The values of the system parameters used in the program are tabulated below.

Physical Constants

Stefan-Boltzman Constant, σ_B	5.669×10^{-8} W/m^2/°K^4
Solar Constant, S	1368 W/m^2
Atmospheric Density at 400 km, ρ_a	1.49×10^{-11} kg/m^3
Earth Radiation	237 W/m^2
Earth Mean Radius, r_e	6378.1 km
Earth Gravitational Constant, μ	3.986×10^5 km^3/s^2

Material Properties of Aluminum

Specific Heat, C	878.4 J/kg/°K
Temperature Coefficient of Resistance, α_T	.00424 Ω/°K
Temperature Coefficient of Expansion, α_e	12.9 m/m/°K
Temperature Coefficient of Density, α_m	6.9118×10^{-5} kg/m^3/°k
Resistivity at 293.15°K	2.857×10^{-8} Ω
Density at 273.15°K	2710 kg/m^3

Design Parameters of Tether & Orbit

Tether Length, L	20 km
Velocity, v	7669 m/s
Longitude of Line of Nodes	0°
Sun Zenith Angle	0°
Orbital Inclination	28.5°
Earth View Factor, F	.31413
Absorptivity	.15
Emissivity	.85
Earth Albedo Factor	.28
Contactor Potential Drop	100 V
Orbital Altitude	300 km

The program presumes the tether to be in a circular orbit at the prescribed orbital altitude.

```
C      THIS PROGRAM COMPUTES THE VARIATION IN TEMPERATURE OF A
C           TETHER WHICH IS OPERATED IN MIXED MODE.  THE
C           THRUSTING PHASE MAY BE DONE WHILE MAINTAINING
C           EITHER CURRENT, VOLTAGE, OR FORCE CONSTANT.
C
C      PARAMETERS USED ARE FOR A 300 KM ORBIT.
C
C      DATA FILES ARE NUMBERED SEQUENTIALLY FOR TEMPERATURE,
C           RESISTANCE, CURRENT, FORCE & EFFICIENCY.
C
C      ******************************************
C
       REAL ITER,INC,L,MASS,LONG,LITE,LENGTH
       DIMENSION T(2000),VB(2000),VMAG(2000),DOT(2000)
C
C      ******************************************
C
C           SPECIFY SYSTEM PARAMETERS
C
C      ******************************************
C
       PARAMETER(PI=3.1415927,RHOR=2710.,AEXP=12.9D-6,LONG=0.)
       PARAMETER(ALFA=.00424,F=.31413,BOLT=5.669D-8,RATE=1.1569D-3)
       PARAMETER(C=878.4,RESTR=2.857D-8,DELT=60.,ERR=1.D5,BETA=0.)
       PARAMETER(V=7725.8,ITER=1727.,INC=28.5,CRHO=6.9118D-5)
       PARAMETER(VCONT=200.,RORB=6678.1,A=.15,EM=.85,SOL=1368.)
       PARAMETER(ALB=.28,ERAD=237.,RE=6378.1,LENGTH=2.D4)
C
C      ******************************************
C
C           READ INDUCED VOLTAGE FILE
C
C      (DATA FILE READ HERE IS THE ONE PRODUCED BY SAO
C      USING NEWMAG CODE)
C
C      ******************************************
C
       DO J=1,ITER
           READ(40,*,END=50)T(J),VB(J),VMAG(J)
           VB(J)=VB(J)-VCONT
       END DO
C
C      ...................................
C
C           ENTER RUN VARIABLES
C
C      ...................................
```

```
      WRITE(6,*) IS ITERATION FOR ENERGY BALANCE TO BE
     + INCLUDED?
C
C
C         ********************************************
C
C     THIS ITERATION SERVES TO DETERMINE THE APPROPRIATE
C     DIAMETER TETHER TO MAINTAIN A DESIRED LEVEL OF CURRENT,
C     VOLTAGE OR FORCE DEPENDING ON THRUSTER OPERATING MODE
C
C
C         ********************************************
C
      WRITE(6,*) (YES = 1; NO = 2)
      WRITE(6,*) CHOICE =
      READ '(I1)',KKK
C
C
C         ********************************************
C
C     ENTER SPECIFICS OF TETHER SYSTEM'S PHYSICAL SIZE, POWER,
C              LEVEL, AND INITIAL POSITION IN ORBIT
C
C
C         ********************************************
C
      WRITE(6,*)'ENTER TETHER DIAM (MM) AND PHASE ANGLE (RAD)'
      WRITE(6,*)'DIAMETER = '
      READ '(F12.6)',XD
      WRITE(6,*)'PHASE ANGLE = '
      READ '(F6.1)',THETAO
      WRITE(6,*)'ENTER LOAD POWER OF THE SYSTEM (KW)'
      READ '(F7.3)',P
.C
C
C         ********************************************
C
C             SPECIFY TYPE OF THRUSTER OPERATION
C
C
C         ********************************************
C
      WRITE(6,*)'IS THIS RUN FOR CONSTANT CURRENT, CONSTANT
     + VOLTAGE, OR CONSTANT THRUST?'
      WRITE(6,*)'(CURRENT = 1; VOLTAGE = 2; THRUST = 3)
      WRITE(6,*)'CHOICE =
      READ (I1) ,NN
C
C
C         ********************************************
C
C                   OPEN DATAFILES
C
C
C         ********************************************
C
```

```
        IF(NN.EQ.1)THEN
                OPEN(51,FILE='FOR051 ,STATUS= NEW )
                OPEN(52,FILE='FOR052 ,STATUS='NEW )
                OPEN(53,FILE=' FOR053 ,STATUS='NEW )
                OPEN(54,FILE= FOR054 ,STATUS='NEW )
                OPEN(55,FILE= FOR055 ,STATUS='NEW')
        END IF
        IF(NN.EQ.2)THEN
                OPEN(61,FILE= FOR061 ,STATUS= NEW )
                OPEN(62,FILE=' FOR062 ,STATUS='NEW )
                OPEN(63,FILE=' FOR063',STATUS='NEW )
                OPEN(64,FILE= FOR064 ,STATUS='NEW )
                OPEN(65,FILE= FOR065 ,STATUS='NEW )
        END IF
        IF(NN.EQ.3)THEN
                OPEN(71,FILE= FOR071 ,STATUS='NEW')
                OPEN(72,FILE= FOR072 ,STATUS= NEW )
                OPEN(73,FILE='FOR073',STATUS= NEW')
                OPEN(74,FILE=' FOR074',STATUS='NEW')
                OPEN(75,FILE='FOR075',STATUS='NEW')
        END IF
C
C
C                   *******************************************
C
C                          ENTER RUN VARIABLES
C
C       (MAY SPECIFY DESIRED LEVEL OF VOLTAGE, CURRENT OR FORCE
C       TO BE MAINTAINED AS A CONSTANT WHEN TETHER IS THRUSTING)
C
C                   *******************************************
C
60      IF(NN.EQ.2)THEN
                WRITE(6,*)'ENTER SOLAR ARRAY VOLTAGE (KW)'
                WRITE(6,*)'VOLTAGE = '
                READ '(F7.1)',VOC
                GO TO 80
        END IF
70      IF(NN.EQ.3)THEN
                WRITE(6,*)'ENTER CONSTANT THRUST (N)'
                WRITE(6,*) THRUST = '
                READ  (F8.3) ,THRUST
                GO TO 80
        END IF
        WRITE(6,*) ENTER NOMINAL CURRENT (AMPS)
        WRITE(6,*)'CURRENT =
        READ  (F6.2) ,XAMP
```

104

```
C
C
C        *****************************************
C
C               SPECIFY INITIAL CONDITIONS
C
C        *****************************************
C
 80      D=XD/1000.
         XINC=INC*PI/180.
         ZEN=BETA*PI/180.
         PREV=0.
         SHADOW=ACOS(SQRT(1.-(RE/RORB)**2.)/COS(ZEN))
 90      THETA=THETAO
         TEMP=205.
         TMAX=0.
         TMIN=400.
         ETAMAX=0.
         ETAMIN=1.
         RMIN=1000.
         RMAX=0.
         TTOT=0.
         ETAT=0.
         LITE=0.
         DARK=0.
         L=LENGTH
C
C        *****************************************
C
C               BEGIN ITERATIONS
C
C        *****************************************
C
         DO 500 N=1,ITER
             SUN1=SQRT((COS(THETA)*COS(LONG)-SIN(THETA)*COS(XINC)
     +  *SIN(LONG))**2.+(SIN(THETA)*SIN(XINC)*COS(ZEN)-(COS(THETA)
     +  *SIN(LONG)+SIN(THETA)*COS(XINC)*COS(LONG))*SIN(ZEN))**2.)
             SUN2=ABS(COS(THETA*PI/5.319))
             IF(THETA.GT.PI)SUN2=ABS(COS((2.*PI-THETA)*PI/5.319))
             REST=RESTR*(1.+ALFA*(TEMP-293.15))
             R=4.*REST*L/(PI*D**2.)
             IF(COS(THETA).GT.COS(PI-SHADOW))GO TO 130
             IF((VB(N)*L/LENGTH)**2..LT.4000.*P*R)GO TO 3000
             AMP=VB(N)*L/(2.*LENGTH*R)-.5*SQRT((VB(N)*L/(LENGTH*R))
     +  **2.-4000.*P/R)
             GO TO 150
 130         AMP=-XAMP
             IF(NN.EQ.2)THEN
                     AMP=-(VOC-VB(N)*L/LENGTH-VCONT)/P
```

105

```
                        IF(VB(N)*L/LENGTH.GT.VOC-VCONT)AMP=0.
                  END IF
                  IF(NN.EQ.3)AMP=-THRUST/(L*VMAB(N))
150               RHO=RHOR*(1.-CRHO(TEMP-273.15))
                  MASS=RHO*PI*(D**2.)*L/4.
                  FORCE=AMP*VB(N)*L/(LENGTH*V)
                  IF(NN.EQ.3.AND.COS(THETA).GT.COS(PI-SHADOW))
     +  FORCE=-THRUST
                  SOLAR=SOL*A*D*L*SUN1
                  EARTH=ERAD*EM*F*PI*D*L
                  ALBEDO=ALB*SOL*A*F*PI*D*L*SUN2
                  OHM=(AMP**2.)*R
                  VAIR=465.*(RORB/RE)*COS(XINC*COS(THETA))
                  VREL=SQRT(VAIR**2.+V**2.-2.*VAIR*V*COS(XINC*
     +  SIN(THETA)))
                  AIR=(3.113D-11)*D*L*VREL**3.
                  RAD=PI*D*L*BOLT*EM*(TEMP**4.)
                  OTEMP=TEMP
                  IF(COS(THETA).GT.COS(PI-SHADOW))GO TO 180
                  TEMP=TEMP+(EARTH+OHM+AIR-RAD)*DELT/(MASS*C)
                  DARK=DARK+DELT*AMP*VB(N)*L/LENGTH
                  GO TO 200
180               TEMP=TEMP+(EARTH+OHM+AIR+SOLAR+ALBEDO-RAD)*DELT
     +  /(MASS*C)
                  LITE=LITE+DELT*AMP*VB(N)*L/LENGTH
200               ETA=1.-LENGTH*ABS(AMP)*R/(VB(N)*L)
C
C
C           *****************************************
C
·C                    WRITE TO DATAFILES
C
C           *****************************************
C
                  IF(NN.EQ.1)THEN
                        WRITE(51,*)T(N),TEMP
                        WRITE(52,*)T(N),R
                        WRITE(53,*)T(N),AMP
                        WRITE(54,*)T(N),FORCE
                        WRITE(55,*)T(N),ETA
                  END IF
                  IF(NN.EQ.1)THEN
                        WRITE(61,*)T(N),TEMP
                        WRITE(62,*)T(N),R
                        WRITE(63,*)T(N),AMP
                        WRITE(64,*)T(N),FORCE
                        WRITE(65,*)T(N),ETA
                  END IF
                  IF(NN.EQ.1)THEN
```

```fortran
                        WRITE(71,*)T(N),TEMP
                        WRITE(72,*)T(N),R
                        WRITE(73,*)T(N),AMP
                        WRITE(74,*)T(N),FORCE
                        WRITE(75,*)T(N),ETA
                END IF
C
C       ********************************************
C
C       CALCULATE PARAMETER AVERAGES & VARIATIONS
C
C       ********************************************
C
                IF(R.LT.RMIN)RMIN=R
                IF(R.GT.RMAX)RMAX=R
                IF(TEMP.GT.TMAX)TMAX=TEMP
                IF(TEMP.LT.TMIN)TMIN=TEMP
                IF(ETA.GT.ETAMAX)ETAMAX=ETA
                IF(ETA.LT.ETAMIN)ETAMIN=ETA
                ETAT=ETAT+ETA
                TTOT=TTOT+TEMP
                THETA=THETA+RATE*DELT
                L=L*(1.+AEXP*(TEMP-OTEMP))
  500   CONTINUE
        TAVG=TTOT/ITER
        ETAVG=ETAT/ITER
C
C       ********************************************
C
C       MATCH ENERGY LEVELS OF GENERATION & THRUSTING
C
C       (ITERATION WILL MATCH ENERGY TAKEN FROM ORBIT WHILE
C       GENERATING POWER IN SHADOW WITH ENERGY INJECTED INTO
C               ORBIT WHILE THRUSTING IN SUNLIGHT)
C
C       ********************************************
C
        IF(KKK.EQ.2)GO TO 600
        IF(ABS(ABS(LITE)-DARK).LE.ERR)GO TO 600
        IF(ABS(LITE)-DARK.LT.0.)THEN
                IF(NN.EQ.1)THEN
                        IF(XAMP.EQ.PREV)GO TO 600
                        IF(DARK-ABS(LITE).GT.15.*ERR)XAMP=XAMP+..
                        IF(DARK-ABS(LITE).GT.5.*ERR.AND.DARK-
     + ABS(LITE).LE.15.*ERR)XAMP=XAMP+.01
                        IF(DARK-ABS(LITE).LE.5.*ERR)XAMP=XAMP+.00.
                END IF
                IF(NN.EQ.2)THEN
```

```fortran
                    IF(VOC.EQ.PREV)GO TO 600
                    IF(DARK-ABS(LITE).GT.15.*ERR)VOC=VOC+100.
                    IF(DARK-ABS(LITE).GT.5.*ERR.AND.DARK-
     + ABS(LITE).LE.15.*ERR)VOC=VOC+10.
                    IF(DARK-ABS(LITE).LE.5.*ERR)VOC=VOC+1.
            END IF
            IF(NN.EQ.3)THEN
                    IF(THRUST.EQ.PREV)GO TO 600
                    IF(DARK-ABS(LITE).GT.15.*ERR)THRUST=THRUST+.1
                    IF(DARK-ABS(LITE).GT.5.*ERR.AND.DARK-
     + ABS(LITE).LE.15.*ERR)THRUST=THRUST+.01
                    IF(DARK-ABS(LITE).LE.5.*ERR)THRUST=THRUST+.001
            END IF
            GO TO 90
      END IF
      IF(ABS(LITE)-DARK.GT.0.)THEN
            IF(NN.EQ.1)THEN
                    IF(XAMP.EQ.PREV)GO TO 600
                    PREV=XAMP
                    IF(ABS(LITE)-DARK.GT.15.*ERR)XAMP=XAMP-.1
                    IF(ABS(LITE)-DARK.GT.5.*ERR.AND.ABS(LITE)
     + -DARK.LE.15.*ERR)XAMP=XAMP-.01
                    IF(ABS(LITE)-DARK.LE.5.*ERR)XAMP=XAMP-.001
            END IF
            IF(NN.EQ.2)THEN
                    IF(VOC.EQ.PREV)GO TO 600
                    PREV=VOC
                    IF(ABS(LITE)-DARK.GT.15.*ERR)VOC=VOC-100.
                    IF(ABS(LITE)-DARK.GT.5.*ERR.AND.ABS(LITE)
     + -DARK.LE.15.*ERR)VOC=VOC-10.
                    IF(ABS(LITE)-DARK.LE.5.*ERR)VOC=VOC-1.
            END IF
            IF(NN.EQ.3)THEN
                    IF(THRUST.EQ.PREV)GO TO 600
                    PREV=THRUST
                    IF(ABS(LITE)-DARK.GT.15.*ERR)THRUST=THRUST-.1
                    IF(ABS(LITE)-DARK.GT.5.*ERR.AND.ABS(LITE)
     + -DARK.LE.15.*ERR)THRUST=THRUST-.01
                    IF(ABS(LITE)-DARK.LE.5.*ERR)THRUST=THRUST-.001
            END IF
            GO TO 90
      END IF
C
C
C     ******************************************
C
C                 PRINT RESULTS TO SCREEN
C
C     ******************************************
```

108

```
C
600    WRITE(6,*)  A / EM / AV T / MX T / MN T / AV EF / MX EF / MN
     +  EF
       WRITE(6,2)A,EM,TAVG,TMAX,TMIN,ETAVG,ETAMAX,ETAMIN
2      FORMAT(1X,F3.2,2X,F3.2,3F7.1,3F7.4)
       WRITE(6,3)  MAX RESISTANCE = ',RMAX,  OHMS
       WRITE(6,3)  MIN RESISTANCE = ',RMIN,  OHMS
3      FORMAT(A,F8.3,A)
       WRITE(6,3)  FINAL TETHER DIAMETER = ',1000.*D,  MM
       IF(NN.EQ.1)WRITE(6,3)  FINAL CURRENT = ',XAMP,  AMPS
       IF(NN.EQ.2)WRITE(6,3)  FINAL VOLTAGE = ',VOC,  VOLTS
       IF(NN.EQ.3)WRITE(6,3)  FINAL FORCE = ',THRUST,  NEWTONS
       WRITE(6,*)  ENERGY DIFFERENCE = ',ABS(LITE)-DARK
       GO TO 4000
3000   WRITE(6,*)  D IS TOO SMALL TO MAINTAIN CONSTANT P
       D=D+.0001
       GO TO 90
4000   END
```

APPENDIX B

Computer Calculation of Variation of Parameters

The variations in the parameters of the orbit of the tether system are evaluated as discussed in Section 3.3. The computer program which implements the mathematical model described there is included in this appendix. It employs a fourth order Runge-Kutta numerical integration code to compute the changes in the various orbital elements with a time step of 60 seconds.

All computations are referred to the e, p, h coordinate frame, although inertial coordinates (used to specify the terminator) in an earth-centered reference frame are also calculated at each iteration.

The equations used are as follow:

$$\frac{da}{dt} = \frac{2a^2}{\mu} \underline{v} \cdot \underline{a}_d$$

$$\frac{d\Omega}{dt} = \frac{r \sin \theta}{h \sin i} \underline{i}_h \cdot \underline{a}_d$$

$$\frac{de}{dt} = \frac{1}{\mu a e} \left[\left(\underline{r} \cdot \underline{v} \right)\left(\underline{r} \cdot \underline{a}_d \right) + \left(pa - r^2 \right)\left(\underline{v} \cdot \underline{a}_d \right) \right]$$

$$\frac{di}{dt} = \frac{r \cos \theta}{h} \underline{i}_h \cdot \underline{a}_d$$

$$\frac{d\omega}{dt} = \frac{-r}{h^2 e} \left[\left(\frac{h \left(\cos f + e \right)}{p} + \frac{h}{r} \right) \underline{r}^T - (p + r) \sin f \underline{v}^T \right] \underline{a}_d - \cos i \frac{d\Omega}{dt}$$

The sixth classical orbital element, of course, is time from perigee passage.

The components of the disturbing acceleration vector, with the exception of the force due to the earth's oblateness, are as described in Section 3.3.1 of the main body. The total acceleration due to gravity is determined as the gradient of the disturbing function associated with the earth's gravitational field as

$$\underline{a}_g = \left| \frac{\partial R}{\partial \underline{r}} \right|^T$$

$$= \frac{-\mu}{r^2} \left[\underline{i}_r - \sum_{k=2}^{\infty} J_K \left(\frac{r_e}{r} \right)^K \left[P'_{K+1}(\cos\phi)\underline{i}_r - P'_K(\cos\phi)\underline{i}_z \right] \right]$$

The disturbing acceleration due to oblateness is that portion of the total acceleration not associated with normal two-body motion, i.e., the infinite sum. Taking only the first three harmonics, as described in Section 3.3.1, the vector components of the disturbing acceleration due to oblateness, referred to e, p, h coordinates, are

$$a_{g,e} = \frac{\mu}{r^2} \left[\sum_{k=2}^{4} J_K \left(\frac{r_e}{r} \right)^K \left[P'_{K+1}(\cos\phi)\cos f - P'_K(\cos\phi)\sin i \sin \omega \right] \right]$$

$$a_{g,p} = \frac{\mu}{r^2} \left[\sum_{k=2}^{4} J_K \left(\frac{r_e}{r} \right)^K \left[P'_{K+1}(\cos\phi)\sin f - P'_K(\cos\phi)\sin i \cos \omega \right] \right]$$

$$a_{g,e} = \frac{-\mu}{r^2} \left[\sum_{k=2}^{4} J_K \left(\frac{r_e}{r} \right)^K \left[P'_K \ (\cos\phi)\cos i \right] \right]$$

These are the components used in the computation.

```
C              THIS PROGRAM COMPUTES THE VARIATION OF
C              INITIALLY SPECIFIED ORBITAL ELEMENTS FOR A
C              TETHER SYSTEM OPERATING IN A SPECIFIED MODE
C
C
C
C                      DIMENSION ARRAYS
C
C              ******************************************
C
      COMMON I,W(20000),INC(20000),LONG(20000),R(20000,3),
     + V(20000,3),F(20000,3),TF(20000),A(20000),H(20000),P,RD,X,
     + Y,Z,E(1),EC(20000),T(20000),DELT,ZZ,D(3),Q1,Q2,Q3
      REAL INC,MU,LONG
      INTEGER I
C
C              ******************************************
C
C                    DEFINE SYSTEM PARAMETERS
C
C              ******************************************
C
      PARAMETER(HEIGHT=400.D3,RE=6378.D3,MU=3.986D14)
      PARAMETER(PI=3.1415927)
C
C              ******************************************
C
C                    SPECIFY INITIAL CONDITIONS
C
C              ******************************************
C
      II=1
      DELT=60.
      ZZ=-1.
      A(1)=RE+HEIGHT
      T(1)=0.
      INC(1)=.4974
      LONG(1)=0.
      W(1)=PI/2.
      EC(1)=.01
      E(1)=EC(1)
      H(1)=SQPT(MU*A(1)*(1.-EC(1)**2.))
      TF(1)=0.
```

```
C
C
C          ******************************************
C
C                   OPEN DATAFILES
C
C          ******************************************
C
       OPEN(21,FILE='INC',STATUS='NEW')
       OPEN(22,FILE='ASC',STATUS='NEW')
       OPEN(23,FILE='AXIS',STATUS='NEW')
       OPEN(24,FILE='ECC',STATUS='NEW')
       OPEN(25,FILE='LONG',STATUS='NEW')
       OPEN(26,FILE='EXP',STATUS='NEW')
C
C          ******************************************
C
C          NUMERICALLY INTEGRATE VARIATIONAL EQUATIONS
C
C          ******************************************
C
       DO I=1,12000
C
C          ******************************************
C
C          COMPUTE INERTIAL COORDINATES OF TETHER
C
C          ******************************************
C
       P=(H(I)**2.)/MU
       RD=P/(1.+EC(I)*COS(TF(I)))
       IF(RD.LE.RE)GO TO 500
       X=COS(TF(I)+W(I))*COS(LONG(I))-SIN(TF(I)+W(I))
     + *COS(INC(I))*SIN(LONG(I))
       Y=SIN(TF(I)+W(I))*COS(INC(I))*COS(LONG(I))+
     + COS(TF(I)+W(I))*SIN(LONG(I))
       Z=SIN(TF(I)+W(I))*SIN(INC(I))
C
C          ******************************************
C
C                 CALCULATE ORBITAL ELEMENTS
C
C       INITIALLY DEFINE STATE (POSITION & VELOCITY) VECTOR
C
C          ******************************************
C
       CALL STATE(TF(I),EC(I))
C
```

113

```
C       ********************************************
C
C               ECCENTRICITY
C
C       ********************************************

        CALL RANTE(I),EC(I))
        EC(I+1)=EC(I)

C
C       ********************************************
C
C               REDEFINE STATE VECTOR
C
C       ********************************************

        CALL STATE(TF(I),EC(I))

C
C       ********************************************
C
CALCULATE DISTURBING ACCELERATION AT TIME INSTANT
C
C       ********************************************

        CALL ACC(TF(I),EC(I))
        T(I+1)=T(I)+DELT

C
C       ********************************************
C
C               LONGITUDE OF LINE OF NODES
C
C       ********************************************

        LONG(I+1)=LONG(I)+RD*DELT*SIN(W(I)+TF(I))*F(I,3)
     *  (H(I)*SIN(INC(I)))

C
C       ********************************************
C
C               SEMI MAJOR AXIS
C
C       ********************************************

        A(I+1)=A(I)+(1.+E(I)**2.)*DELT*(V(I,1)*F(I,1)
     *  ........*..... M
```

```
C
C
C         *****************************************
C
C                  ANGULAR MOMENTUM
C
C         *****************************************
C
          H(I+1)=H(I)+DELT*(R(I,1)*F(I,2)-R(I,2)*F(I,1))
C
C         *****************************************
C
C                    TRUE ANOMALY
C
C         *****************************************
C
          CALL TRUE(DELT,EC(I),TF(I+1))
C
C         *****************************************
C
C                 ORBITAL INCLINATION
C
C         *****************************************
C
          INC(I+1)=INC(I)+DELT*RD*COS(W(I)+TF(I))*F(I,3)
        + /H(I)
C
C         *****************************************
C
C                 ARGUMENT OF PERIGEE
C
C         *****************************************
C
          W(I+1)=W(I)-(P*COS(TF(I))*(R(I,1)*F(I,1)+R(I,2)
        + (F(I,2))-(P+RD)*SIN(TF(I))*(R(I,1)*F(I,2)-R(I,2)*F(I,1)))
        - *DELT/(RD*EC(I)*H(I))-COS(INC(I))*(LONG(I+1)-LONG(I))
C
C         *****************************************
C
C                 DETERMINE CURRENT DIRECTION
C
C             AS A FUNCTION OF MIXED RULE OPERATION
C
C         .........................................
```

```fortran
              IF(RD*SQRT(1.+E**2.).LE.PE AND.Y.LT.0.)THEN
                    Z...=4
              ELSE
                    Z...
              END IF
C
C             ***************************************
C
C             COMPUTE VARIATION IN ORBITAL ALTITUDES
C
C             ***************************************
C
              PERIGEE=(A(I)*(1.-EC(I))-RE) 1000.
              APOGEE=(A(I)*(1.+EC(I))-RE) 1000.
              GO TO 600
   500        WRITE(6,*)I, 'RADIUS BELOW SURFACE OF EARTH
              GO TO 6000
C
C             ***************************************
C
C             WRITE TO DATAFILES
C
C             ***************************************
C
   600        IF(II.EQ.5)THEN
                    WRITE(21,*)T(I)/86400.,INC(I)*180./PI
                    WRITE(22,*)T(I)/86400.,W(I)*180./PI
                    WRITE(23,*)T(I)/86400.,A(I)/1000.
                    WRITE(24,*)T(I)/86400.,EC(I)
                    WRITE(25,*)T(I)/86400.,LONG(I)*180./PI
                    WRITE(26,*)T(I)/86400.,PERIGEE
                    GO TO 5000
              ELSE
                    GO TO 5000
              END IF
  5000        II=II+1
              IF(II.GT.5)I.=.
         END DO
  6000   END
C
C
C         ***********************************************
```

```fortran
C                AT THE INSTANTANEOUS POINT IN THE OSCULATING ORBIT
C
C       ******************************************
C
        SUBROUTINE AGN(TRF,ECC)

        COMMON I,W(20000),INC(20000),LONG(20000),R(20000,3),
     +  V(20000,3),F(20000,3),TF(20000),A(20000),H(20000),P,RD,X,
     +  Y,L,E(1),EC(20000),T(20000),DELT,ZZ,D(3),G1,G2,G3
        REAL INC,MU,LONG,LIB,LAT,MASS,L,LIBMAG
        INTEGER I
        DIMENSION B(3),CURR(3),VREL(3),AIR(20000,3),SOLAR(20000,3)
        DIMENSION LIB(20000,3),EMF(20000,3),GRAV(20000,3)
        PARAMETER(L=2.D4,AMP=3.,TEMP=1100.,MASS=25.D3,RE=6378.D3)
        PARAMETER(COEFF=1.25,FLUX=4.4D-6,PI=3.1415927,DRAG=2.2)
        PARAMETER(MU=3.986D14,DIAM=.003)
C
C       *********************************************
C
C               COMPUTE MAGNETIC FIELD STRENGTH
C
C       *********************************************
C
        CALL MAG(TRF)
        BQ=D(1)*COS(LONG(I))+D(2)*SIN(LONG(I))
        BR=-D(1)*SIN(LONG(I))+D(2)*COS(LONG(I))
        B(1)=BQ*COS(W(I))+(BR*COS(INC(I))+D(3)*SIN(INC(I)))*SIN(W(I))
        B(2)=-BQ*SIN(W(I))+(BR*COS(INC(I))+D(3)*SIN(INC(I)))
     +  *COS(W(I))
        B(3)=-BR*SIN(INC(I))+D(3)*COS(INC(I))
C
C       *********************************************
C
C               COMPUTE CURRENT VECTOR
C
C       *********************************************
C
        ALFA=ECC*SIN(TRF)
        CURR(1)=AMP*(COS(ALFA)*COS(TRF)+SIN(ALFA)*SIN(TRF)
        CURR(2)=AMP*(COS(ALFA)*SIN(TRF)-SIN(ALFA)*
        CURR(3)=0.

C       ...............................
C
C       CALCULATE INDUCED ELECTROMAGNETIC
C
C       ...............................
```

```
      EMF(1,1)=II*L*B(3)*CURR(1)/MASS
      EMF(1,2)=II*L*B(3)*CURR(1)/MASS
      EMF(1,3)=II*L*(B(2)*CURR(1)-B(1)*CURR(2))/MASS


C     **********************************************
C
C     COMPUTE RELATIVE AIR VELOCITY
C
C     **********************************************
C

      LAT=ASIN(Z/SQRT(X**2.+Y**2.))
      PSI=LONG(I)+ACOS(X/SQRT(X**2.+Y**2.))
      VERMAG=4650.*COS(LAT)*RD/RE
      IF(I.EQ1)THEN
              VREL(1)=-VERMAG*((-SIN(PSI)*COS(LONG(I))+COS(PSI)
     +  *SIN(LONG(I)))*COS(W(I))+(COS(PSI)*COS(LONG(I))-SIN(PSI)
     +  *SIN(LONG(I)))*COS(INC(I))*SIN(W(I)))
              VREL(2)=SQRT(MU/A(1))-VERMAG*((SIN(PSI)*COS(LONG
     +  (I))-COS(PSI)*SIN(LONG(I)))*SIN(W(I))+(COS(PSI)*COS
     +  (LONG(I))-SIN(PSI)*SIN(LONG(I)))*COS(W(I))*COS(INC(I)))
      ELSE
              VREL(1)=V(I,1)-VERMAG*((-SIN(PSI)*COS(LONG(I))+
     +  COS(PSI)*SIN(LONG(I)))*COS(W(I))+(COS(PSI)*COS(LONG(I))-
     +  SIN(PSI)*SIN(LONG(I)))*COS(INC(I))*SIN(W(I)))
              VREL(2)=V(I,2)-VERMAG*((SIN(PSI)*COS(LONG(I))-
     +  COS(PSI)*SIN(LONG(I)))*SIN(W(I))+(COS(PSI)*COS(LONG(I))-
     +  SIN(PSI)*SIN(LONG(I)))*COS(W(I))*COS(INC(I)))
      END IF
      VREL(3)=-VERMAG*(SIN(PSI)*SIN(LONG(I))-COS(PSI)*COS(LONG(I)))
     +  *SIN(INC(I))
      REL=SQRT(VREL(1)**2.+VREL(2)**2.+VREL(3)**2.)
C
C     **********************************************
C
C     COMPUTE AIR DENSITY
C
C     **********************************************
C

      ALT=(RL-RE)/1000.
      TEM=TEMP*(....*T*...**.+..+..*..)
      IF(ALT.LE.....AND.ALT.....+.DENS....+....+..)
      IF(ALT.GE.....AND.ALT....+.DENS.....+....+..)
      IF(ALT.GE.....)DENS..... .+....*TE*....+....+...+..
      ..(ALT....... ...)**.
```

IIV

```fortran
C
C     *********************************************
C
C        CALCULATE AERODYNAMIC ACCELERATION VECTOR
C
C     *********************************************
C
C        AIR(I,J)=-.5*DRAG*DIAM*L*COS(ALFA)*DENS*REL*VREL(J)
C
C
C
C     *********************************************
C
C            COMPUTE TETHER NORMAL AREA
C
C     *********************************************
C
      PERP=SQRT((COS(ALFA)*COS(W(I)+TRF)*COS(LONG(I))-SIN(ALFA)*
     + SIN(W(I)+TRF)*COS(LONG(I))-COS(ALFA)*SIN(W(I)+TRF)*
     + COS(INC(I))*SIN(LONG(I))-SIN(ALFA)*COS(W(I)+TRF)*COS(INC(I))*
     + SIN(LONG(I)))**2.+(COS(ALFA)*SIN(W(I)+TRF)*SIN(INC(I))+
     + SIN(ALFA)*COS(W(I)+TRF)*SIN(INC(I)))**2.)
C
C     *********************************************
C
C        CALCULATE SOLAR RADIATION ACCELERATION VECTOR
C
C     *********************************************
C
      IF(RD*SQRT(X**2.+Z**2.).LE.RE.AND.Y.LT.0.)THEN
          DO J=1,3
                SOLAR(I,J)=0.
          END DO
      ELSE
          SOLAR(I,1)=-(COEFF*DIAM*L*PERP*SIN(INC(I))*
     + COS(LONG(I))*FLUX/MASS)*(SIN(LONG(I))*COS(W(I))-COS(INC(I)+
     + COS(INC(I))*SIN(W(I)))
          SOLAR(I,2)=-(COEFF*DIAM*L*PERP*SIN(INC
     + SIN(LONG(I))*FLUX/MASS)*(COS(LONG(I))*COS(INC
     +
          SOLAR(I,3)=-(COEFF*DIAM*L*PERP*SIN(INC
     +
     +
```

```
C
C       **********************************
C
C       CALCULATE EARTH OBLATENESS ACCELERATION VECTOR
C
C       **********************************
C
        CAL EARTH(TPF)
        GRAV(I,1)=G1
        GRAV(I,2)=G2
        GRA(I,3)=G3

C       **********************************
C
C       CALCULATE TETHER LIBRATION ACCELERATION VECTOR
C
C       **********************************
C
        LIBMAG=3.*MU*(L**2.)/(2.*PD**4.)
        LIB(I,1)=-LIBMAG*(COS(TRF)+ALFA*SIN(TRF))
        LIB(I,2)=-LIBMAG*(SIN(TRF)-ALFA*COS(TPF))
        LIB(I,3)=0.

C
C       **********************************
C
C       CALCULATE TOTAL DISTURBING ACCELERATION VECTOR
C
C       **********************************
C
        DO J=1,3
            F(I,J)=AIP(I,J)+GRAV(I,J)+LIB(I,J)+SOLAP(I,J)+EMF(I,J)
        END DO
        RETURN
        END
```

```
      SUBROUTINE TRUE(DT,ECCC,TRF)

      COMMON I,W(20000),INC(20000),LONG(20000),R(20000,3),
     + V(20000,3),F(20000,3),TF(20000),A(20000),H(20000),P,RD,X,
     + Y,Z,E(1),EC(20000),T(20000),DELT,ZZ,D(3),Q1,Q2,Q3
      REAL INC,MU,LONG
      INTEGER I
      PARAMETER(MU=3.986D14,PI=3.1415927)
      TRF=TF(I)+DT*(H(I)/RD**2.+(P*COS(TF(I))*(R(I,1)*F(I,1)+
     + R(I,2)*F(I,2)-(P+RD)*SIN(TF(I))*(R(I,1)*F(I,2)-R(I,2)*
     + F(I,1)))/(RD*ECCC*H(I)))
      RETURN
      END
C
C
C
C
C
C ****************************************************************
C
C     COMPUTE TETHER POSITION & VELOCITY VECTORS
C
C         ******************************************
C
      SUBROUTINE STATE(TRF,ECCC)

      COMMON I,W(20000),INC(20000),LONG(20000),R(20000,3),
     + V(20000,3),F(20000,3),TF(20000),A(20000),H(20000),P,RD,X,
     + Y,Z,E(1),EC(20000),T(20000),DELT,ZZ,D(3),Q1,Q2,Q3
      REAL INC,MU,LONG
      INTEGER I
      PARAMETER(MU=3.986D14)
      R(I,1)=RD*COS(TRF)
      R(I,2)=RD*SIN(TRF)
      R(I,3)=0.
      VR=MU*ECCC*SIN(TPF)/H(I)
      VT=MU*(1.+ECCC*COS(TPF))/H(I)
      V(I,1)=VP*COS(TPF)-VT*SIN(TPF)
      V(I,2)=VP*SIN(TPF)+VT*COS(TPF)
      V(I,3)=0.
      RETURN
      END
C
C
C
C
```

```
C    ********************************************************************
C
C    THIS SUBROUTINE CALCULATES THE FIELD STRENGTH  B   OF EARTH'S
C    MAGNETIC FIELD (MODELLED AS AN OCTOPOLE) AT THE  INSTANTANEOUS
C               POINT ON THE OSCULATING ORBIT
C
C    ********************************************************
C

      SUBROUTINE MAG(IPF)

      COMMON I,W(20000),INC(20000),LONG(         ),F(20000),V(
    + V(20000,3),F(20000,3),TF(20000),A(20000),R(20000),P(     ,
    + Y,Z,E(1),EC(20000),T(20000),DELT,LL,D(3),G1,G2,G3
      DIMENSION PP(4,4),PS(4,4),A(4,4),S(4,4),B(4,4),HM(4,4)
      DIMENSION BB(3),GG(4,4),hm(4,4)
      REAL INC,MU,LONG,M,N,MC,MLONG
      INTEGER I
      PARAMETER(RE=6378.D3,ROTRATE=7.312D-5,PI=3.1415927,ORDER=4.)
      DO K=1,ORDER
            DO J=1,ORDER
                  G(K,J)=0.
                  HM(K,J)=0.
            END DO
      END DO
      G(2,1)=-30186.D-9
      G(2,2)=-2036.D-9
      G(3,1)=-1898.D-9
      G(3,2)=2997.D-9
      G(3,3)=1551.D-9
      G(4,1)=1299.D-9
      G(4,2)=-2144.D-9
      G(4,3)=1296.D-9
      G(4,4)=805.D-9
      HM(2,2)=5735.D-9
      HM(3,2)=-2124.D-9
      HM(3,3)=-37.D-9
      HM(4,2)=-361.D-9
      HM(4,3)=249.D-9
      HM(4,4)=
      PP(1,1)=
```

```fortran
              END DO
      END DO
      S(1,1)=1.
      DO N=2,ORDER
              S(N,1)=S(N-1.,1)*((2.*(N-1.)-1.)/(N-1.))
              DO M=2,ORDER
                    IF(M.EG.2.)THEN
                            DEL=1.
                    ELSE
                            DEL=0.
                    END IF
                    S(N,M)=S(N,M-1.)*SQRT(ABS((N-M+1.)*(DEL+1.)
   + (N+M-2.))
              END DO
      END DO
      DO J=1,3
              BB(J)=0.
      END DO
      ANG=TRF+W(I)
      THETA=ACOS(SIN(ANG)*SIN(INC(I)))
      IF(ANG.EG.PI/2..OR.ANG.EO.3.*PI/2.)THEN
              ALFA=ANG
      ELSE
              ALFA=ATAN(COS(INC(I))*TAN(ANG))
      END IF
      IF(ANG.GT.PI/2..AND.ANG.LT.3.*PI/2.)ALFA=ALFA+PI
      IF(ANG.GT.3.*PI/2..AND.ANG.LT.2.*PI)ALFA=ALFA+2.*PI
      MLONG=ALFA+LONG(I)-T(I)*ROTRATE
      DO N=2,ORDER
              DO M=1,ORDER
                    IF(N.EQ.M)THEN
                            PS(N,M)=SIN(THETA)*PS(N-1.,N-1.)
                    ELSE
                            PS(N,M)=COS(THETA)*PS(N-1.,M)-
   + KC(N,M)*PS(N-2.,M)
                    END IF
              END DO
      END DO
      PP(1,1)=0.
      DO N=1,ORDER
              DO M=1,ORDER
                    IF(N.EQ.M)THEN
                            PP(N,M)=SIN(THETA)*PP(N-1.,N-1.)-
   +                    *PP(N-1,N-1.)
                    ELSE
                            PP(N,M)=COS(THETA)*PP(N-1.,M)-SIN(THETA)
   +                    *PS(N-1.,M)+KC(N,M)*PP(N-2.,M)
                    END IF
```

```
                END DO
        END DO
        DO N=2,ORDER
                DO M=1,ORDER
                        GG(N,M)=S(N,M)*G(N,M)
                        HH(N,M)=S(N,M)*HM(N,M)
                END DO
        END DO
        DO N=2,ORDER
                SUM1=0.
                SUM2=0.
                SUM3=0.
                DO M=1,N
                        SUM1=SUM1+(GG(N,M)*COS((M-1.)*MLONG)+HH(N,M)*
     +  SIN((M-1.)*MLONG))*PS(N,M)
                        SUM2=SUM2+(GG(N,M)*COS((M-1.)*MLONG)+HH(N,M)*
     +  SIN((M-1.)*MLONG))*PP(N,M)
                        SUM3=SUM3+(M-1.)*(-GG(N,M)*SIN((M-1.)*MLONG)+
     +  HH(N,M)*COS((M-1.)*MLONG)*PS(N,M)
                END DO
                BB(1)=BB(1)+((RE/RD)**(N+1.))*N*SUM1
                BB(2)=BB(2)+((RE/RD)**(N+1.))*SUM2
                BB(3)=BB(3)+((RE/RD)**(N+1.))*SUM3
        END DO
        BB(2)=-BB(2)
        BB(3)=-BB(3)/SIN(THETA)
        D(1)=(BB(1)*COS(PI/2.-THETA)+BB(2)*SIN(PI/2.-THETA))*
     +  COS(ALFA)-BB(3)*SIN(ALFA)
        D(2)=(BB(1)*COS(PI/2.-THETA)+BB(2)*SIN(PI/2.-THETA))*
     +  SIN(ALFA)+BB(3)*COS(ALFA)
        D(3)=BB(1)*SIN(PI/2.-THETA)-BB(2)*COS(PI/2.-THETA)
        RETURN
        END
C
C
C
C
C
C
C      ********************************************      ..................
C
C
C      THIS SUBROUTINE COMPUTES THE GRADIENT ... ...
C                    MODIFIED WITH ... ...
C
C      ********************************************      ........
C
```

```fortran
      SUBROUTINE EARTH(TRF)

      COMMON I,W(20000),INC(20000),LONG(20000),R(20000,3),
     + V(20000,3),F(20000,3),TF(20000),A(20000),H(20000),P,RD,X,
     + Y,Z,E(1),EC(20000),T(20000),DELT,ZZ,D(3),G1,G2,G3
      DIMENSION ZZZ(3),JJ(4),LP(5),LPP(6),GRAV(3)
      REAL INC,MU,LONG,LP,LPP,JJ
      INTEGER I
      PARAMETER(MU=3.986D14,RE=6378.D3)
      JJ(1)=0.
      JJ(2)=1.08263D-3
      JJ(3)=-2.54D-6
      JJ(4)=-1.61D-6
      ZZZ(1)=SIN(INC(I))*SIN(W(I))
      ZZZ(2)=SIN(INC(I))*COS(W(I))
      ZZZ(3)=COS(INC(I))
      XI=SIN(W(I)+TRF)*SIN(INC(I))
      LP(1)=1.
      LP(2)=XI
      LP(3)=.5*(3.*XI**2.-1.)
      IF(XI.LT.0.)THEN
            LP(4)=.5*(-5.*(ABS(XI))**3.-3.*XI)
      ELSE
            LP(4)=.5*(5.*XI**3.-3.*XI)
      LP(5)=(35.*(ABS(XI))**4.-30.*XI**2.+3.)/8.
      LPP(1)=0.
      DO XK=2,6
            LPP(XK)=XI*LPP(XK-1.)+(XK-1.)*LP(XK-1.)
      END DO
      DO J=1,3
            SUM=0.
            DO XK=2,4
                  SUM=SUM+JJ(XK)*((RE/RD)**XK)*(LPP(XK+2.)
     + *R(I,J)/RD-LPP(XK+1.)*ZZZ(J))
            END DO
            GRAV(J)=(MU/RD**2.)*SUM
      END DO
      G1=GRAV(1)
      G2=GRAV(2)
      G3=GRAV(3)
      RETURN
      END
```

```
C     ****************************************************************
C
C              CALCULATE CHANGE IN ECCENTRICITY
C
C     ******************************************
C

      SUBROUTINE DERIV(DE)

      COMMON I,W(20000),INC(20000),LONG(20000),P(20000,3),
     + V(20000,3),F(20000,3),TF(20000),A(20000),H(20000),P,RD,X,
     + Y,Z,E(1),EC(20000),T(20000),DELT,EE,B(3),G1,G2,G3
      REAL INC,MU,LONG
      INTEGER I
      PARAMETER(MU=3.986D14)
      DE=((P*A(I)-RD**2.)*(V(I,1)*F(I,1)+V(I,2)*F(I,2)+(R(I,1)*
     + V(I,1)+R(I,2)*V(I,2))*(R(I,1)*F(I,1)+R(I,2)*F(I,2)))/(MU*
     + A(I)*EC(I))
      RETURN
      END

C
C
C
C
C
C     ****************************************************************
C
C              RUNGE-KUTTA INTEGRATION
C
C     ******************************************
C

      SUBROUTINE RK(TRF,ECC)

      COMMON I,W(20000),INC(20000),LONG(20000),R(20000,3),
     + V(20000,3),F(20000,3),TF(20000),A(20000),H(20000),P,RD,X,
     + Y,Z,E(1),EC(20000),T(20000),DELT,EE,B(3),G1,G2,G3
      REAL INC,LONG,K1,K2,K3,K4
      INTEGER I
      CALL ACC(TRF,ECC)
      CALL DERIV(D)
      K1=DELT*DE
      EC(I+1)=EC(I)+..
      B(EE)=B(I)+K1
      CALL TRF(..     ..TRF.
      CALL STAFF(..  ..)
      CALL A(..)=...  ..
      CALL DERIV..
      K.=DELT*..
      EC(I+1)=..
      T(..)=DELT*..
```

126

```
CALL ACC(TPF,STEP2)
CALL DERIV(DE)
K3=DELT*DE
STEP=DELT
CALL TRUE(STEP,ECC,TPF2)
STEP2=E(1)+K3
CALL STATE(TPF2,STEP2)
CALL ACC(TPF,STEP2)
CALL DERIV(DE)
K4=DELT*DE
E(1)=E(1)+(K1+K4)/6.+(K2+K3)/3.
RETURN
END
```

APPENDIX C

Development of the Variation of Parameters

To evaluate the effects of an external force on the orbit of a satellite it is useful to write Newton's second law as

$$\frac{d^2\underline{r}}{dt^2} + \frac{\mu}{r^3}\underline{r} = \sum_{j=3}^{n} \left|\frac{\partial R_j}{\partial\underline{r}}\right|^T = \underline{a}_d$$

where $\underline{a}_d$ is the vector representation of the total disturbing acceleration due to all forces except the primary acceleration associated with the gravitational field of the main body, and R_j is the scalar disturbing function associated with the disturbing body m_j.

Lagrange fully developed the method of the variation of parameters to study the problem of perturbations of comets moving in elliptical orbits. Expressing the disturbing acceleration as the gradient of the disturbing function, the result of his analysis is the equation

$$\underline{L}\frac{d\underline{\alpha}}{dt} = \left|\frac{\partial R}{\partial\underline{\alpha}}\right|^T \tag{1}$$

where $\underline{\alpha}$ is a six dimensional vector composed of the orbital elements, and $\underline{L}$, the Lagrange matrix, is six-dimensional and skew-symmetric and equal to

$$\left|\frac{\partial\underline{r}}{\partial\underline{\alpha}}\right|^T \frac{\partial\underline{v}}{\partial\underline{\alpha}} - \left|\frac{\partial\underline{v}}{\partial\underline{\alpha}}\right|^T \frac{\partial\underline{r}}{\partial\underline{\alpha}}$$

If $\underline{\alpha}$ is expressed in terms of the classical orbital elements as

$$\underline{\alpha}^T = |\Omega \ i \ \omega \ a \ e \ \lambda|$$

where Ω, i, and ω are the three Euler angles as shown in Figure 13, a is the semi-major axis, e is the orbital eccentricity and $\lambda = -n\tau$ the time of pericenter passage, then the elements of $\underline{L}$ may be determined as detailed in Reference 32, and the derivatives of the orbital elements solved for to produce Lagrange's planetary equations, as follow:

128

$$\frac{d\Omega}{dt} = \frac{1}{nab \sin i} \frac{\partial R}{\partial i}$$

$$\frac{di}{dt} = \frac{-1}{nab \sin i} \frac{\partial R}{\partial \Omega} + \frac{\cos i}{nab \sin i} \frac{\partial R}{\partial \omega}$$

$$\frac{d\omega}{dt} = \frac{-\cos i}{nab \sin i} \frac{\partial R}{\partial i} + \frac{b}{na^3 e} \frac{\partial R}{\partial e}$$

$$\frac{da}{dt} = \frac{2}{na} \frac{\partial R}{\partial \lambda}$$

$$\frac{de}{dt} = \frac{-b}{na^3 e} \frac{\partial R}{\partial \omega} + \frac{b^2}{na^4 e} \frac{\partial R}{\partial \lambda}$$

$$\frac{d\lambda}{dt} = \frac{-2}{na} \frac{\partial R}{\partial a} - \frac{b^2}{na^4 e} \frac{\partial R}{\partial e}$$

Obviously, $\underline{L}$ is non-singular if e is neither zero nor one (since $b^2 = |a^2(1-e^2)|$), and i is not zero.

Gauss eliminated the restriction of the representation of the disturbing acceleration as the gradient of the disturbing function by expressing Equation 1 as

$$\underline{L} \frac{d\underline{\alpha}}{dt} = \left|\frac{\partial \underline{r}}{\partial \underline{\alpha}}\right|^T \underline{a}_d \qquad (2)$$

Gauss then computed the matrix coefficients of $\underline{a}_d$ to obtain the appropriate variational equations. The results of this analysis, again detailed in Reference 32, are Gauss' planetary equations

$$\frac{d\Omega}{dt} = \frac{r \sin \theta}{h \sin i} a_{dh}$$

$$\frac{di}{dt} = \frac{r \sin \theta}{h} a_{dh}$$

$$\frac{d\omega}{dt} = \frac{1}{eh} \left[- p \cos f \, a_{dr} + (p + r) \sin f \, a_{dt} \right] - \frac{r \sin \theta}{h \tan i} a_{dh}$$

$$\frac{da}{dt} = \frac{2a^2}{h} \left[e \sin f \, a_{dr} + \frac{p}{r} a_{dt} \right]$$

$$\frac{de}{dt} = \frac{1}{h} \left[p \sin f \, a_{dr} + \left((p + r) \cos f + re\right) a_{dt} \right]$$

$$\frac{dM}{dt} = n + \left(\frac{b}{aeh}\right) \left[(p \cos f - 2 \, re) a_{dr} - (p + r) \sin f \, a_{dt} \right]$$

129

Obviously, there are again difficulties if the orbital eccentricity is small or if the inclination of the orbit is near zero. Of course, this is not a surprise as the line of nodes does not exist for an orbit of zero inclination, and the line of apsides is meaningless for an orbit of zero eccentricity. A means to avoid these singularities occurs if orbital elements are defined from combinations of the six classical ones listed above which do not depend on either the line of nodes or the line of apsides. For this analysis, we will stick with the classical elements and artificially avoid the singularities which occur when a particular element becomes undefined.

Vectorial forms of the variational equations may be obtained by rewriting Equation 2 as

$$\frac{d\underline{\alpha}}{dt} = \underline{P}^T \left|\frac{\partial \underline{r}}{\partial \underline{\alpha}}\right|^T \underline{a}_d$$

where $\underline{P}$ is called the Poisson matrix defined as

$$\underline{P} = -\underline{L}^{-1}$$

Following substitution, this yields

$$\frac{d\underline{\alpha}}{dt} = \frac{\partial \underline{\alpha}}{\partial \underline{v}} \underline{a}_d$$

which may be used to directly produce variational equations of vector orbital elements which are independent of the coordinate system in which the components of $\underline{a}_d$ are expressed. With $\underline{\alpha}$ composed of the classical orbital elements as described above, the variational equations for these orbital elements become

$$\frac{da}{dt} = \frac{2a^2}{\mu} \underline{v} \cdot \underline{a}_d$$

$$\frac{d\Omega}{dt} = \frac{r \sin\theta}{h \sin i} \underline{i}_h \cdot \underline{a}_d$$

$$\frac{di}{dt} = \frac{r \cos\theta}{h} \underline{i}_h \cdot \underline{a}_d$$

$$\frac{d\omega}{dt} = -\frac{\partial f}{\partial \underline{v}} \underline{a}_d - \cos i \frac{d\Omega}{dt}$$

130

$$\frac{df}{dt} = \frac{h}{r^2} + \frac{\partial f}{\partial \underline{v}} \, \underline{a}d$$

$$\frac{de}{dt} = \frac{1}{\mu} \left[2(\underline{v} \cdot \underline{a}_d) \, \underline{r} - (\underline{r} \cdot \underline{a}_d)\underline{v} - (\underline{r} \cdot \underline{v}) \, \underline{a}_d \right]$$

where the perturbative derivative of the true anomaly is

$$\frac{\partial f}{\partial \underline{v}} = \frac{r}{eh^2} \left[\left(\frac{h \, (\cos f + e)}{p} + \frac{h}{r} \right) \underline{r}^T - (p + r) \sin f \, \underline{v}^T \right]$$

and the scalar derivative of the eccentricity is

$$\frac{de}{dt} = \frac{1}{\mu ae} \left[(\underline{r} \cdot \underline{v})(\underline{r} \cdot \underline{a}_d) + (pa - r^2)(\underline{v} \cdot \underline{a}_d) \right]$$

These are the equations which may be used to evaluate the changes in the satellite's orbit caused by the presence of accelerations other than the primary one.

REFERENCES

1   Ionospheres & Radio Physics 1958-1964
    NASA SP-95
    Washington DC: US Government Printing Office 1966

2   Tethers in Space Handbook
    Washington DC: NASA, Office of Space Flight, Advanced Program
    August 86

3   Alfven, H & CG Falthammer
    Cosmical Electrodynamics: Fundamental Principles
    New York: Oxford University Press 1963

4   Barnett, A. & S. Olbert
    "Radiation of Plasma Waves by a Conducting Body Moving Through a
    Magnetized Plasma"
    Journal of Geophysical Research 91, 10117 1986

5   Battin, Richard H.
    An Introduction to the Mathematics and Methods of Astrodynamics
    Cambridge MA: Charles Stark Draper Lab, Inc 1986

6   Battin, Richard H.
    Astronautical Guidance
    New York: McGraw-Hill Book Company 1964

7   Booker, HG
    Comments on Spaceborne ELF Systems
    Rand Corporation December 1981

8   Booker, HG
    Guidance and Beaming of Alfven Waves
    Rand Corporation August 1983

9   Candidi, M
    Computation of Tethered Satellite Potential, Current and Ambient
    Magnetic Field
    Rome IT: CNR August 1985

10 Carroll, Joseph A.
    Guidebook for Analysis of Tether Applications
    Final Report on Contract RH4-394049 with Martin Marietta
    Corporation March 1985

11 Cobine, James D.
    Gaseous Conductors
    New York: McGraw-Hill Book Co., Inc. 1941

REFERENCES

12 Dobrowolny, M
    Electrodynamic Interactions
    Venice IT: October 1985

13 Dobrowolny, M
    Spontaneous Radiation Emitted by Moving Tethers
    Venice IT: October 1985

14 Duckett, RJ & CS Gilliland
    Variable Anodic Thermal Control Coating on Aluminum
    AIAA #83-1492 June 1983

15 Estes, Robert D.
    Alfven Waves from an Electrodynamic Tethered Satellite System
    Cambridge MA: Harvard-Smithsonian Center for Astrophysics 1966

16 Estes, Robert D. & David A. Arnold, Mario D. Grossi, Gordon E.
    Gullahorn
    Investigation of Electrodynamic Tether as a Generator of Electric
    Power
    Cambridge MA: SAO for MIT January 1987

17 Garrett, Henry B. & Charles P. Pike, editors
    Space Systems & Their Interactions with Earth's Space Environment
    New York: American Institute of Aeronautics & Astronautics 1980

18 Grossi, Mario D. & David A. Arnold
    Engineering Study of the Electrodynamic Power
    Cambridge MA: Smithsonian Institution Astrophysical Observatory
    June 1984

19 Grossi, M.D.
    Historical Background Leading to the Tethered Satellite System
    (TSS)
    Cambridge MA: SAO January 1986

20 Hall, John B., Jr., compiler
    Earth Radiation Science Seminars
    NASA CP-2239 1982

21 Hastings, Daniel E.
    The Theory of Plasma Contactors Used in the Ionosphere
    Cambridge MA: MIT

22 Hastings, D.E. & J. Wang
    The Radiation Impedance of an Electrodynamic Tether with End
    Connectors
    Cambridge MA: MIT 1986

REFERENCES

23 Heller, Gerhard B., editor
    Thermophysics & Temperature Control of Spacecraft & Entry Vehicles
    New York: Academic Press 1966

24 Holman, J.P.
    Heat Transfer
    New York: McGraw-Hill Book Company 1976

25 Jones, W.B. & F.G. Steward
    "A Numerical Method for Global Mapping of Plasma Frequency"
    Radio Science, Volume 5, #5 1970

26 Kaplan, Marshall H.
    Modern Spacecraft Dynamics & Control
    New York: John Wiley & Sons, Inc. 1976

27 LaBonte B.J. et al, editors
    Solar Irradiance Variations in Active Region Time Scales
    NASA CP-2310 1984

28 Martinez-Sanchez, Manuel
    Conceptual Design of a 100 KW Electrodynamic Tether System
    Cambridge MA: MIT April 10, 1985

29 Martinez-Sanchez, Manuel & Daniel E. Hastings
    A Systems Study of a 100 KW Electrodynamic Tether
    Cambridge MA: MIT July 1986

30 Martinez-Sanchez, Manuel & Sarah A. Gavit
    Orbital Modifications Using Forced Tether Length Variations
    Cambridge MA: MIT

31 McCoy, J.
    Electrodynamic Interactions
    Venice IT: October 1985

32 Nobles, William
    Electrodynamic Tethers for Energy Conversion

33 Parks, D.E. & I. Katy
    Theory of Plasma Contactors for Electrodynamic Tethered Satellite
    Systems
    S-Cubed October 1985

34 Powers, Walter L., Barbara F. Adams, George T. Inouye
    "Electron Penetration of Spacecraft Thermal Insulation"
    Spacecraft Charging Technology: 1980
    NASA CP-2182 Washington DC: US Government Printing Office 1981

REFERENCES

35 Sofia, S., editor
    Variations of the Solar Constant
    NASA CP-2191 1981

36 Souders, Sue W.
    Relative Geometries of the Earth, Sun, and Mars for the Year 1973
    to the Year 2000
    NASA SP-3053 1970

37 Thomas, John D. & M.J. Rycroft, L. Coliln
    Electron Densities & Scale Heights in the Topside Ionsphere:
    Alouette I Observations in Mid-Latitudes
    Washington DC: US Government Printing Office 1966

38 Vignoli, M., W. Miller & M. Matteoni
    Power Generation with Electrodynamic Tethers
    Arlington VA: NASA September 1986

39 Von Engel, A.
    Ionized Gases
    New York: Oxford University Press 1965

40 Von Tiesenhausen, Georg
    Tethers in Space: Birth and Growth of a New Avenue to Space
    Utilization
    NASA Marshall Space Flight Center February 1984

41 Wertz, James R. editor
    Spacecraft Attitude Determination and Control
    Boston: D. Reidel Publishing Company 1985

42 Williamson, P. Roger
    High Voltage Characteristics of the Electrodyanmic Tether and the
    Generation of Power & Propulsion
    Stanford CA: Stanford University, Department of Electrical
    Engineering January 23, 1986